PLASTIC SHEAR IN A MODEL AMORPHOUS SOLID

BY

NTHOBANE CABLE MOJI

A DISSERTATION SUBMITTED IN PARTIAL FULFILMENT OF THE

REQUIREMENTS FOR THE DEGREE OF

MASTER OF SCIENCE

IN THE

DEPARTMENT OF PHYSICS

UNIVERSITY OF NATAL

PIETERMARITZBURG

1 9 9 2

PREFACE

THE EXPERIMENTAL WORK DESCRIBED IN THIS THESIS WAS CARRIED OUT IN THE PHYSICS DEPARTMENT OF THE QWA-QWA BRANCH OF THE UNIVERSITY OF THE NORTH, AND IN THE PHYSICS DEPARTMENT OF THE UNIVERSITY OF NATAL, PIETERMARITZBURG FROM JANUARY 1989 TO JUNE 1990.

THE WORK REPRESENTS ORIGINAL RESEARCH BY THE AUTHOR AND HAS NOT BEEN SUBMITTED IN ANY FORM FOR EXAMINATION AT ANOTHER UNIVERSITY. WHERE USE WAS MADE OF THE WORK OF OTHERS, IT HAS BEEN DULY ACKNOWLEDGED IN THE TEXT.

ACKNOWLEDGEMENTS

The author extends his thanks and appreciation to the following people and organizations:

The Mothiane brothers who work at the Namahali Bridge Agricultural Project, on whose site the river sand was obtained for the research.

The Uniqwa Physics Department for the premises where the materials and apparatus used in the experiments, were prepared, as well as the space where this research work presented in this thesis, was done.

Prof. P.J. Jackson, of the Department of Physics at the University of Natal, Pietermaritzburg, who promoted this dissertation. His assistance and advices are greatly appreciated.

Mrs S. Diederichs for her untiring assistance in computer instruction and word processing, as well as facilitating most communications to the promoter.

Prof. W. De Haas for his encouragements during difficult times of research when materials were not easy to construct, and his comments on results obtained.

Prof. F.R.N. Nabarro for his comment about the perspex model of the surface constructed from the data accumulated.

The F.R.D. for financing this project, without whose generous financial assistance, this research would not have have been possible.

Bongiwe, Rufus and Farouk for their preparedness to carry thesis material to Pietermaritzburg and back.

Vindi and the boys who patiently bore with me through the hard abscences of studies, and many other supportive people who shouted courage when studies, family and work were too demanding to bear.

ABSTRACT

The plastic deformation of crystalline materials, in particular metals, has been a subject of intensive investigation. It has been established that in these materials the carriers of displacement during plastic deformation are crystal line defects called dislocations. Such line defects are subject to certain well understood constraints as they move.

Plastic shear in amorphous materials is, however, less well understood. An important example of such shear is the large scale deformation of the earth's crust along fault lines, as studied in geology and plate tectonics.

In this thesis an experimental study of shear in a model amorphous solid, namely sand, is reported, after introducing the mechanisms of plastic deformation in metals.

When glide surfaces are formed in crystals, and a gliding dislocation encounters an obstacle, a screw section of the dislocation may cross-slip (see chapter 2) into another glide plane, while the edge section of the same dislocation continues to glide on the original glide plane. In this way cross-slip can divide the glide plane into two segments, i.e. bifurcate the glide plane. Dislocation cross-slip can also corrugate the glide plane. The work described in this thesis is an investigation of the following:

1. What kind of fault surface will develop when an amorphous solid is plastically deformed by shear?

2. What similarities are there between fault surfaces in amorphous solids and fault surfaces in crustal or geological deformation? It is hoped that studies of these similarities could lead to better understanding of geological processes like earthquakes.

To carry out the investigations, a rectangular wooden box cut into two halves that could slide relative to each other on shearing was constructed. The box was filled with damp compacted river sand that was divided into sections separated by distemper lamellae, ready to be sheared. After shearing the marker lamellae appeared stepped on the surface of the sand. The distances of the steps from the center line were measured at regular levels in the sand body after removing successive layers of sand. The measurements were used as data to construct perspex and computer models. The examination of the fault surface on these two models led to the following conclusions:

1. A well defined fault surface develops when sand is sheared. This material can therefore provide a model for shear on a larger scale. e.g. fault formation.

2. The fault surface is corrugated and bifurcated.

3. The fault surface is also very complex. Further work will be necessary to establish clearly the details of similarities between shear in sand and shear on a geological scale.

LIST OF CONTENTS.

CHAPTER 4.

CHAPTER 5.

LIST OF FIGURES

CHAPTER 1

INTRODUCTION

When crystalline solids are subjected to stress, they deform either elastically or, if the stresses are large enough, plastically. Elastic deformation obeys Hooke's law, namely that the stress is proportional to strain. Hooke's law is obeyed until the so-called proportionality limit. Beyond this limit plastic deformation sets in. At low homologous temperature the mechanism of plastic deformation in crystals is shear across planes of high atomic density. These planes are called slip planes. Shear occurs in directions parallel to the lines of closest atomic packing. Such directions are called slip directions. The displacement associated with slip spreads across a glide plane and the boundary between slipped and unslipped regions marks the position of one or more dislocations. Large displacements may be produced when groups of dislocations move across a slip plane. The slip plane (or slip surface) is also known as a glide surface (or shear surface) in crystalline solids. In geology, where crustal materials are slipped relative to each other, it is called a fault surface.

If a dislocation or a slip front encounters a finite obstacle while gliding on its glide plane, the dislocation bends around the obstacle and segments of different characters develop. A segment parallel to the slip direction is called a screw dislocation segment. This segment may move onto a new glide plane to avoid the the obstacle. Such transfers from one glide plane to another are called cross-slip. The glide planes involved must share a common direction, namely the slip direction. Other segments, not parallel

to the slip direction, called edge or mixed segments, are unable to deviate from the original glide plane. They continue to spread on the original surface. The dislocation thus divides into segments moving on different planes. The glide surface is then said to be bifurcated (28,31). If a screw segment cross-slips more than once, the result may be either the formation of a stepped glide surface as it moves from one glide plane to another, or the formation of glide surface with curved corrugations parallel to the slip direction. Screw dislocations that cross-slip more than once are said to undergo multiple cross-slip (31,41).

It has previously been suggested that the geological analogue of dislocation cross-slip corrugates and bifurcates fault surfaces in a direction parallel to the shear during crustal deformation (28,31). The work reported in this thesis is an investigation of the validity of this suggestion. Fault surfaces produced by crustal deformation cannot be directly observed because they lie deep in the earth's crust, but useful information can be obtained using a model of crustal material. One characteristic of crustal deformation is that on a geological scale, the atomic crystallinity of the deforming rocks can be ignored. Crustal material which is deforming on a large scale then behaves like an amorphous solid.

In the work to be described here, a convenient and inexpensive model amorphous solid, namely sand, was used to model deformation. A moist sample of river sand was poured and compacted into a rectangular wooden experimental box with an open top. The box was cut into two halves kept together by cloth strips pasted across the cut at both ends of the box. The two halves were free to slide against each other along the long axis of

the box. Sand in the box could therefore be sheared without the box itself falling apart during the process. The line marking the cut along the bottom of the box lay along the center line. Shearing of the box then created a glide surface inside the sand. Such glide surfaces were examined in the present work. A similar shear in crustal deformation, where two parts of the earth slide against each other in a horizontal direction, on a vertical plane, is called a strike-slip fault (36,45).

The method developed for studying glide surfaces in compacted sand was as follows: contrasting colour distemper lamellae were introduced vertically at right angles to the center line so as to indicate any displacement due to the fault surface. We shall refer to displacements parallel to the shear direction as offsets. The distance of offsets seen on the sand surface from the center line is the distance of the glide surface from the center line. These distances were determined for every distemper lamella at various depths below the original surfaces. Measurements were accumulated and used to construct a three-dimensional model of the fault surface generated by shear (42,47).

Two models were constructed from the data accumulated above. One was made of perspex as described below (section 4.4.1). The other model could be displayed by computer graphics. Examining these two models aided in assessing the suggestion made that the analogue of dislocation cross-slip bifurcates and corrugates the glide surfaces in amorphous solids.

CHAPTER 2

PLASTICITY IN CRYSTALS AND AMORPHOUS SOLIDS

2.1. INTRODUCTION

The solids considered here are those classified according to their structures as either crystalline or amorphous (1,2). The deformation on both kinds of solids are described with emphasis on the similarities and differences. In crystalline solids it is well known that deformation is due to motion of dislocations. In amorphous solids dislocations are difficult to define. However slip often propagates on well defined surfaces, with well defined boundaries between slipped and unslipped regions. These boundaries or lines resemble crystal dislocations in many respects. For example, when describing geological faults, such boundaries are called tip lines. In order to apply dislocation concepts to deformation of amorphous solids, it is necessary to discuss briefly dislocations in crystalline solids. To do this, some important aspects of crystallographic nomenclature are described below (1,2,3,4).

2.2 CRYSTALLOGRAPHIC NOMENCLATURE

Crystalline solids consist of atoms arrayed in regular patterns. A common pattern in ductile metals (discussed below) is based on close packing of spheres. For example, the face-centered cubic structure (f.c.c.) is made up of close-packed spheres stacked upon each other. The basic building block of this structure is a cubic unit cell: the close packed planes are

stacked along the cube diagonal in such a way as to extend the close packing to three dimensions. Two other crystal structures are common in ductile materials: the simple cubic structure (e.g. NaCl) and the body centered cubic (b.c.c.) structure (e.g. Fe). These structures are illustrated in Fig 2.1. When discussing ductility and dislocation movement it is useful to be able to refer to particular crystal planes by using so-called Miller indices (5,6,7).

The orientation of crystal planes and crystal directions are specified by these indices. Crystal planes are labelled as follows: the Miller indices of a plane are the smallest set of integers bearing the same ratio to each other as the reciprocal of the intercepts of the plane with the crystal axes. The intercepts are measured in units of the basis vectors of the structure. The examples of crystal plane nomenclature are shown in Fig 2.2. The Miller indices for crystal directions are the smallest set of integers bearing the same ratio to each other as the components of the unit vector along that direction. A few simple examples are shown in Fig 2.3 (8,9,11,12).

The experimental study of the mechanical properties of solids involves examining the response of the solid to forces applied to it. The force applied per unit area is termed stress. To define a state of stress at a point in a solid one must define the six components (σ_x, σ_y, σ_z and τ_{xy}, τ_{xz}, τ_{yz}) of a (symmetric) second-rank tensor, the stress tensor. The components σ_x, σ_y and σ_z are stresses perpendicular to surfaces across which they act, that is, normal to x, y, and z respectively. These are called normal stresses. The off-diagonal components τ_{xy}, τ_{yz}, τ_{xz} are

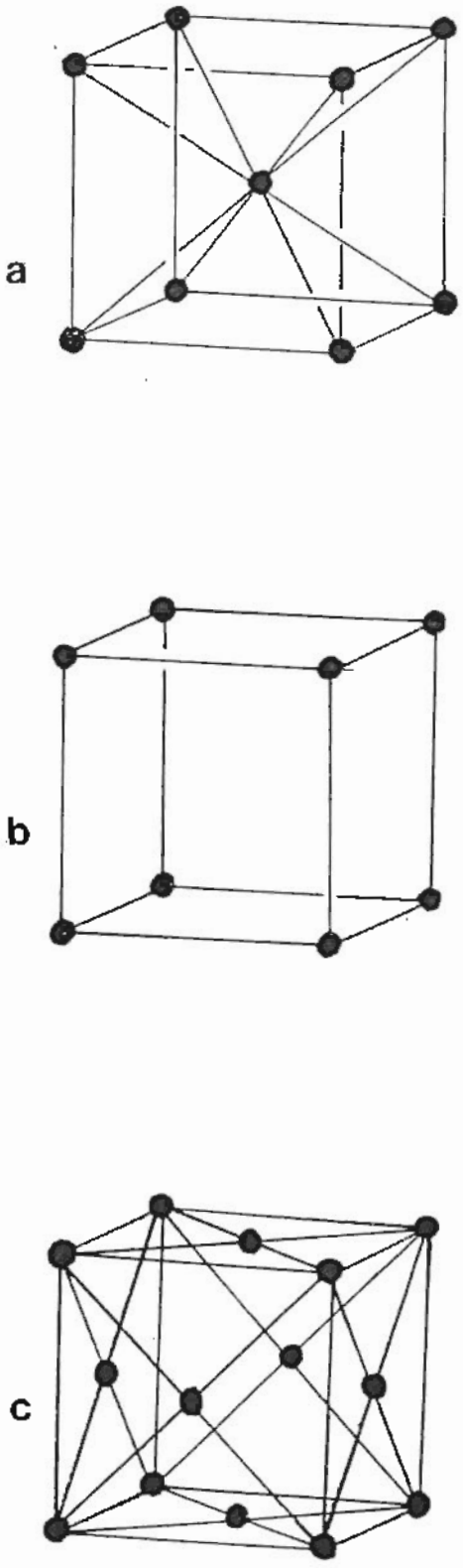

Fig 2.1: Structures of cubic crystals: (a) body centered cubic (b) simple cubic (c) face centered cubic (fcc).

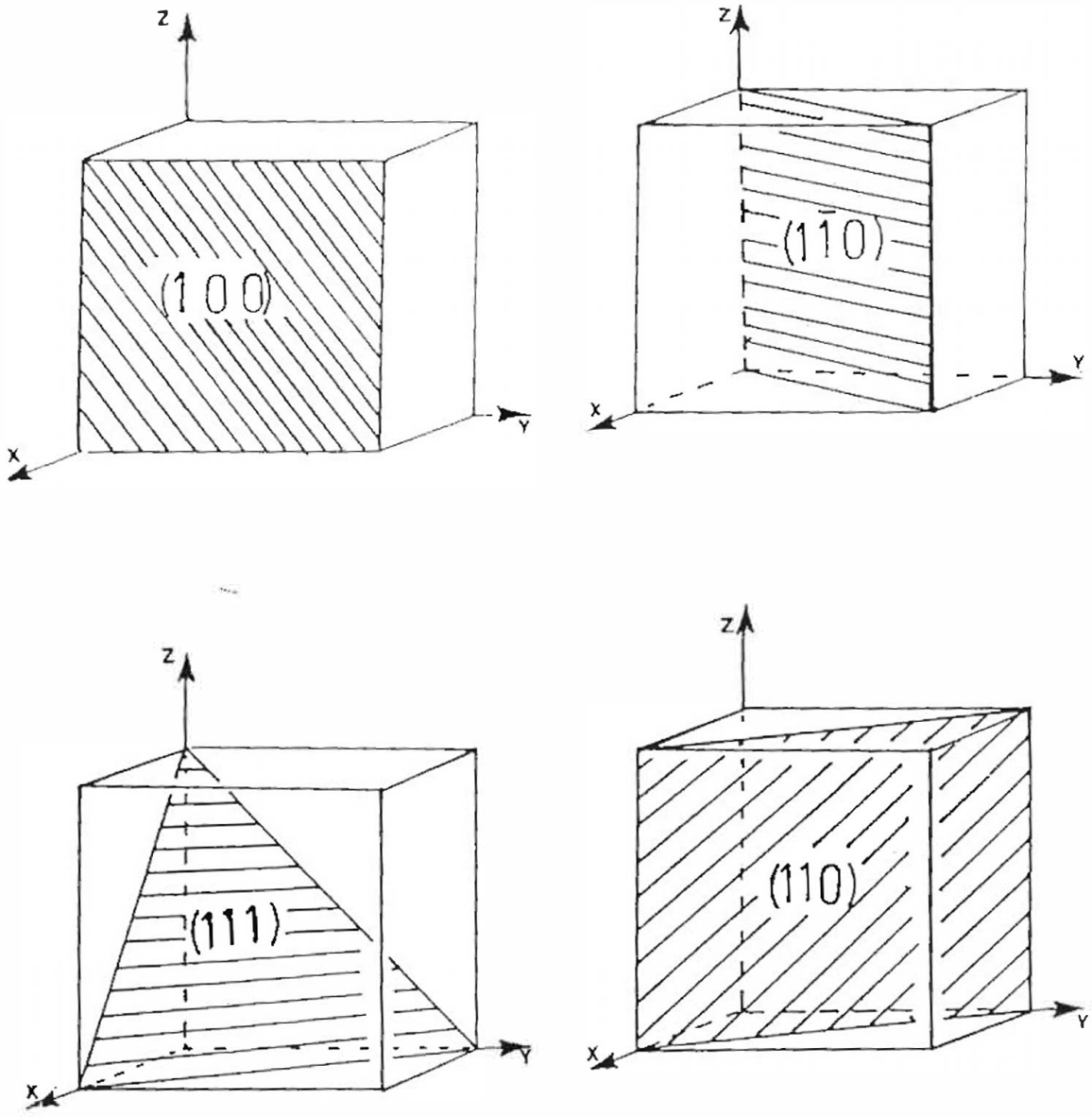

Fig 2.2: Examples of crystal plane nomenclature in a cubic crystal.

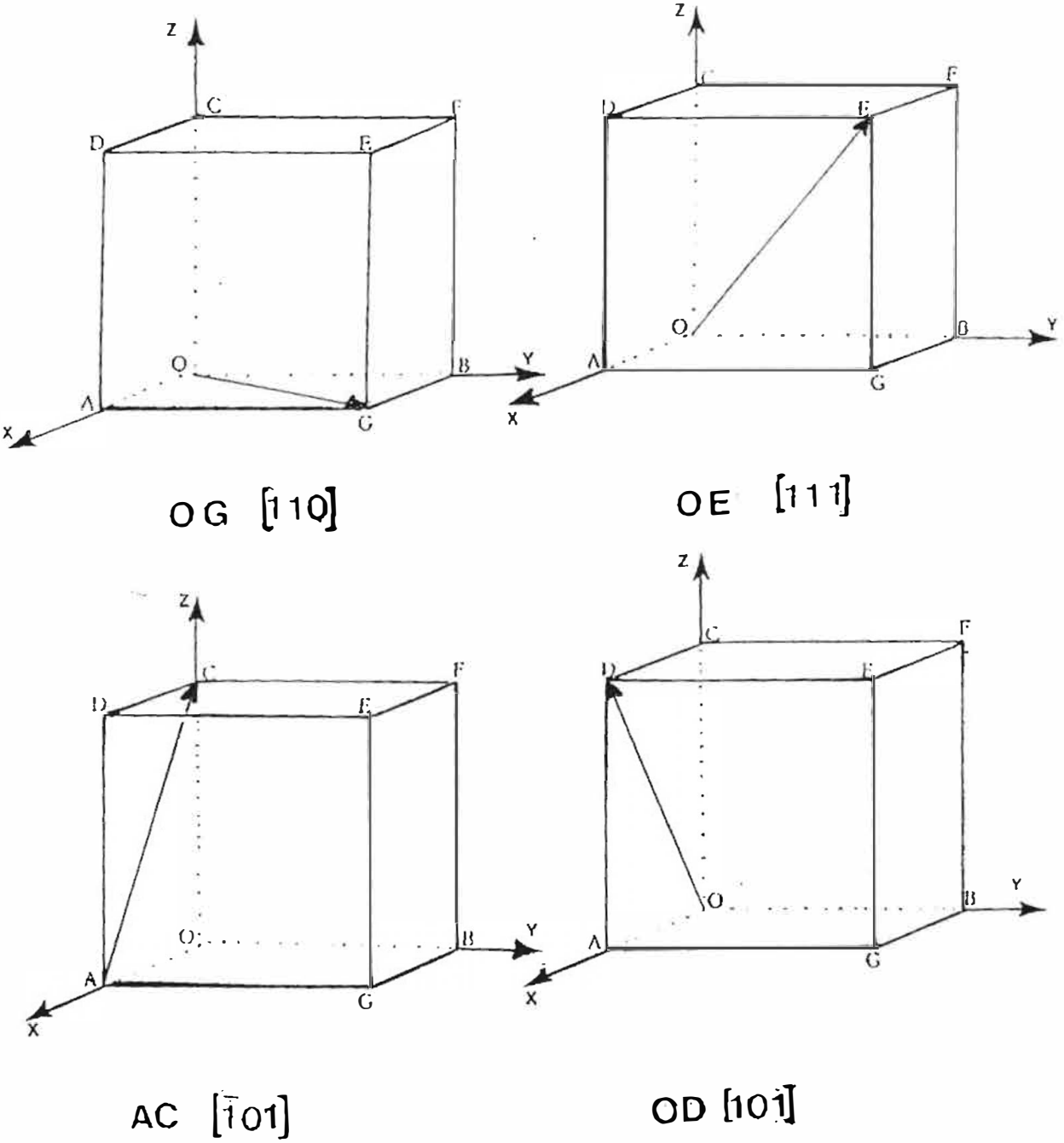

Fig 2.3: Crystal direction nomenclature in a cubic crystal.

stresses where the force is parallel to the surface across which it acts. The first subscript labels the direction of the force acting across the plane whose normal is parallel to the direction given by the second subscript. These components are called shear stresses. The stress tensor is written as a 3 X 3 matrix:

$$\begin{vmatrix} \sigma_x & \tau_{xy} & \tau_{xz} \\ \tau_{yx} & \sigma_y & \tau_{yz} \\ \tau_{zx} & \tau_{zy} & \sigma_z \end{vmatrix}$$

These stress components are shown in Fig 2.4.

The application of stress produces a deformation of shape in solids, and deformed solids are said to be strained. Strains are measured by specifying the components of the second rank symmetric tensor ε_{ij}. A strain is a dimensionless ratio of some measure of distortion of the body being stressed, to the original form of the undistorted body. Tensile strain, for example (see Fig 2.5(a)), is the ratio of the linear elongation of a solid to the original length of the same solid. Shear strain (θ), which can be expressed as $\theta = \tan^{-1}(\frac{a}{d})$, is shown in Fig 2.5(b) (13, 14, 16, 17).

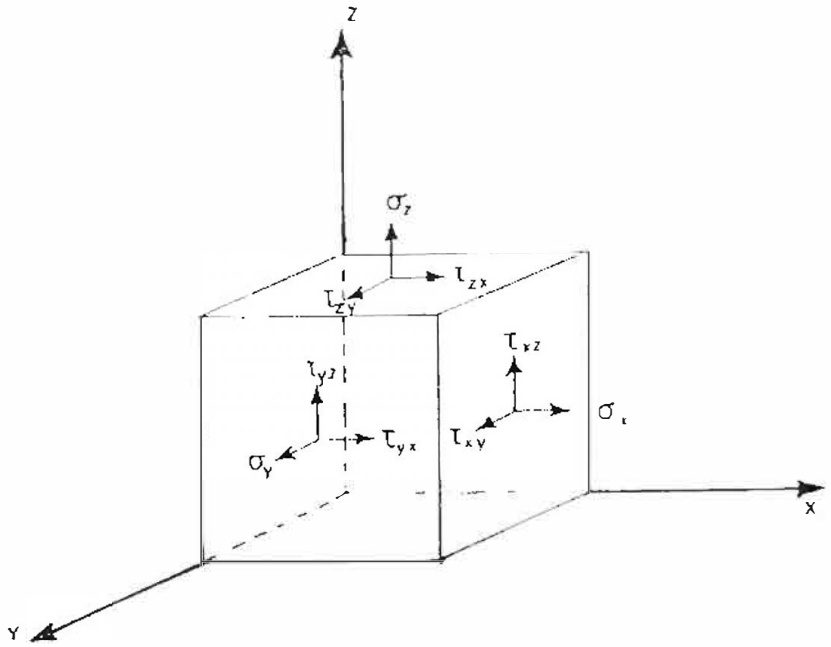

Fig 2.4: Stress components acting on a cubic volume element of a solid.

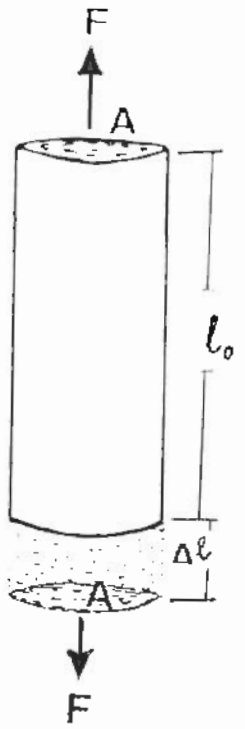

(a) A crystal rod of original length l_o and a cross-sectional area A being elongated by the force F by an amount Δl

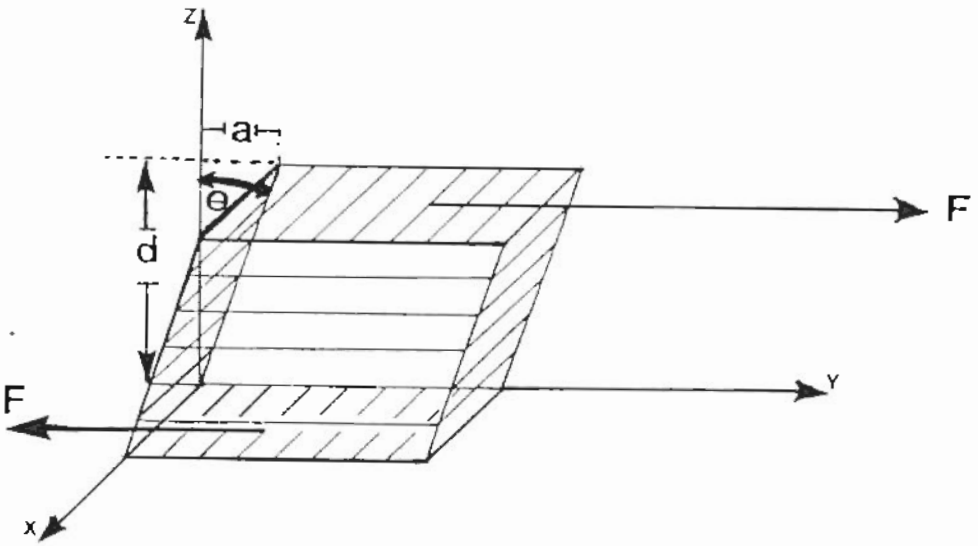

(b) A cube of side length d is sheared over displacement a by force F .

Fig 2.5: Deformed solids, subjected to (a) a tensile stress (b) a shear stress.

2.3 METAL DUCTILITY

A conventional way of representing the response of bodies to stress is to plot a graph of stress vs strain. The ratio of stress to strain below the elastic limit is a constant specific to the material being tested and is called the elastic modulus of the material. Beyond the elastic limit, stress-strain curves show remarkable differences for different solids. Figs 2.6 and 2.7 show the stress-strain curves for crystalline solids and amorphous solids (e.g. glass) where (for a crystal) stress τ is plotted against strain ε. At low stresses (below about a thousandth of elastic modulus of the material), stress is proportional to strain, obeying Hooke's law, and the curve is a straight line up to a yield point τ_y. In this linear region of the curve, solids deform elastically and will return to their original sizes and shapes if the deforming stresses are removed (8, 15, 18).

At the end of the linear region, plastic deformation sets in, and the test object no longer recovers its original shape when stress is removed. The curves for the crystalline and amorphous solids diverge in the plastic region. For example, consider an fcc crystalline solid, which deforms according to the curve in Fig 2.6. This solid deforms plastically over a wide range which can briefly be divided into three regions, also undergoing work hardening as it deforms. The first region marked Stage 1, where the slope of the curve is small, is a region of easy glide, where little work hardening occurs. The second region marked Stage 2 is where the metal work hardens rapidly with the increasing slope of the stress-strain curve. Eventually the curve bends over in a parabolic fashion at Stage 3 where work hardening decreases until the rupture point (10).

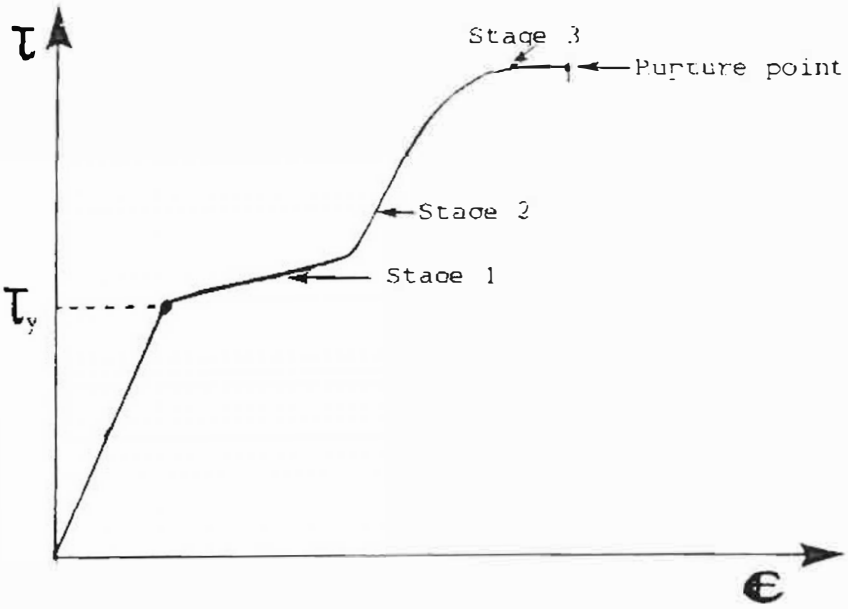

Fig 2.6: Shear stress-strain curve for a crystalline (fcc) solid.

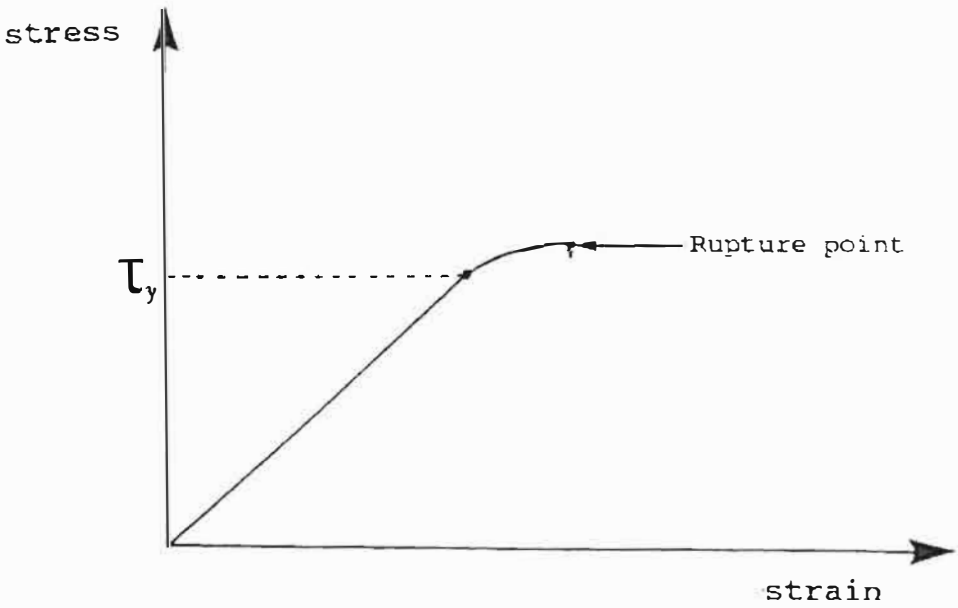

Fig 2.7: Shear stress-strain curve for an amorphous solid.

It is work hardening that makes metals, which are crystalline in structure, suitable for manufacturing and construction because they can flow plastically and strengthen beyond their elastic limits when they are stressed. Metals become stronger as they deform plastically and work harden so that the work hardening phenomenon provides a safety factor in construction (4,5,23). An example of work hardening can be made of a beam in the structure of a steel bridge that could accidentally be stressed beyond its design limit, it may flow plastically and strengthen rather than fail in a brittle fashion.

Because metals are so widely used, the fundamental physical mechanisms involved in the plasticity of metals are of interest. When plastic deformation in metals is closely studied, results reveal that shear occurs parallel to specific crystal planes called slip or glide planes. Glide planes contain the highest density of atoms. Shear occurs also in specific directions, called glide directions. These are directions in the glide plane in which the atoms are most closely spaced. Thus in an fcc metal like copper, glide occurs parallel to {111} planes in the close packed direction <110> (13,19,22).

In studying metal plasticity much attention has been focused on single crystals. Specimens for testing and examination are grown into a rod shaped single crystal form. Testing then consists of subjecting this rod-shaped single metal crystal to a tensile stress and measuring the resulting tensile strain. Plastic shear during the tensile testing is hardly ever homogeneous. It is to a lesser or greater extent concentrated into groups of neighbouring glide planes. The unit event in plasticity is then the

spread of shear across a packet of parallel glide planes (as in Fig 2.8). When such a glide packet intersects a surface that does not contain the slip direction, steps are formed on the surface. These steps may at times be coarse enough to be visible to the naked eye if formed on a polished surface (20,21).

2.4 DISLOCATIONS IN CRYSTALS.

Microscopic observation of sheared metals shows that shear on the atomic scale is not continuous, but that displacements between glide planes occur in quanta of a single interatomic spacing (19,21). When one atomic plane shears over its neighbouring plane by one atomic spacing, it could in principle happen in two ways:

1. Shear could occur as a plane of close-packed atoms moved simultaneously over the entire area of the plane, or

2. Shear could spread from one region of the plane to the other.

In practice the second mechanism always operates. Appreciable plastic glide starts when the shear stress on the glide plane, resolved in the glide direction, reaches a specific value called the critical resolved shear stress (CRSS) (19,24).

Shear then spreads gradually across the glide plane. There exits a boundary line between regions over which the shear has spread (sheared region), and those over which shear has not spread (unsheared). Near this boundary line

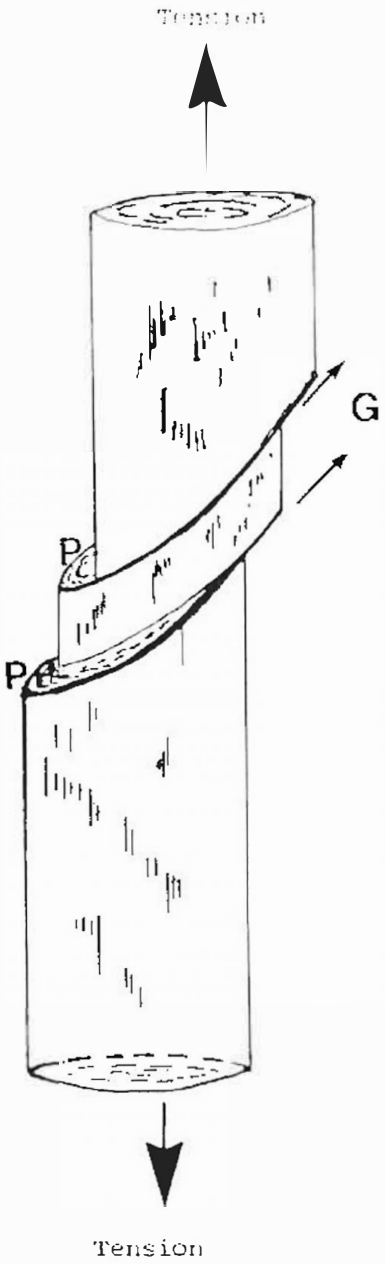

Fig 2.8: Crystal rod under tensile stress, with lamellae slipping along glide planes P in glide directions G .

the crystal lattice is elastically distorted. The boundary is called a crystal dislocation. As shear spreads, the dislocation traverses the glide plane, and atoms above the glide plane undergo a displacement **b**, relative to those below the glide plane. The vector **b** is in the direction of the slip and defines the magnitude and the direction of the spreading shear. **b** is called the Burgers vector of the dislocation (19,21).

Because dislocations distort the crystal lattice, dislocations can be seen in thin metal foils, when examined by electron microscopy. The electron microscope has therefore become an essential tool for studying how crystal plasticity results from generation and movement of dislocations. For review of this subject see Basinski and Basinski (25).

In practice, the spreading of shear across a neighbouring group of glide planes occurs by the cooperative movement of many dislocations, gliding together as a group. The considerable experimental evidence for such group behaviour is described by Neuhauser (26).

Because dislocations glide in a group, their discrete nature (each dislocation consisting of a line with which is associated a Burgers vector of atomic magnitude) is less evident in plasticity than is often thought to be the case (21).

2.5 CONSERVATIVE AND NON-CONSERVATIVE GLIDE

Dislocation lines are not confined to a single glide plane. They usually extend through three dimensions and have shapes that are sometimes of biological complexities. The direction of a dislocation at any point is defined by a unit vector $\hat{\mathbf{l}}$, which lies along the line. The sense of $\hat{\mathbf{l}}$ is arbitrary, but the sense must be chosen so that $\hat{\mathbf{l}}$ does not reverse direction as one proceeds along the line.

A surface that contains both $\hat{\mathbf{l}}$ and $\underline{\mathbf{b}}$ for the same dislocation is a possible glide surface. Shear may spread on the surface without matter being added or removed in the vicinity of the dislocation line. Such glide, that does not require the addition or subtraction of matter is called conservative glide (2,3,4). If a dislocation moves on a surface that does not contain $\hat{\mathbf{l}}$ and $\underline{\mathbf{b}}$, its motion requires addition or removal of matter and is called non-conservative glide. For an arbitrary dislocation, the angle between $\hat{\mathbf{l}}$ and $\underline{\mathbf{b}}$ lies between 0° and 180°. There are two special cases, the edge dislocation, for which $\hat{\mathbf{l}} \cdot \underline{\mathbf{b}} = 0$ and the screw dislocation for which $\hat{\mathbf{l}} \cdot \underline{\mathbf{b}} = 1$ or -1.

A dislocation line that extends into three dimensions will in general have at various positions along its length segments that are parallel or perpendicular to $\underline{\mathbf{b}}$. Segments for which $\underline{\mathbf{b}} \cdot \hat{\mathbf{l}} = \mathbf{b}$ are called screw dislocations. Segments for which $\underline{\mathbf{b}} \cdot \hat{\mathbf{l}} = 0$ are called edge dislocations. Segments where $\underline{\mathbf{b}}$ and $\hat{\mathbf{l}}$ are neither parallel nor perpendicular are said to have mixed character.

It is important to remember that a glide surface is not a predefined surface that existed in a crystal before it was sheared. The glide surface only becomes defined as glide spreads. Consider a simple situation, in which glide spreads on a surface that is initially plane. Since a dislocation line cannot end in a crystal, it must either form a closed loop, or end at a surface. Suppose a dislocation line forms a loop as in Fig 2.9 (a) on the plane surface A (1,8). At the points E the dislocation is in edge orientation, at S is in screw orientation. Along the arcs SES the surface on which the conservative glide can occur is well defined: it is the plane A shown in the figure. But at S, $\hat{l}$ is parallel to $\underline{b}$, and the dislocation is free to glide on any surface that contains $\underline{b}$, for example, the surface C. Glide may therefore be diverted on to plane C (Fig 2.9(b)). This process of transferring glide from a plane such as A to a plane such as C is called the cross-slip of a screw dislocation segment, as shown in Fig 2.9 (10,19,21).

Cross-slip may cause a glide surface to become more complex than a single plane, as shear spreads. In crystals, because of the crystallographic nature of glide, a glide surface must consist of segments of crystallographic planes, joined along lines parallel to the slip direction $\underline{b}$. Two factors may inhibit the transfer of slip and consequent complication of the shape of the glide surfaces. Firstly, because of the crystallographic nature of the glide, dislocations may be inhibited from cross-slip if there are no planes onto which glide can be easily transferred. In a close packed structure glide planes are inclined at large angles (70° in fcc). If the stress on one plane is large enough to promote glide, it may not be large enough on the cross-slip plane. Secondly, in crystals, dislocations

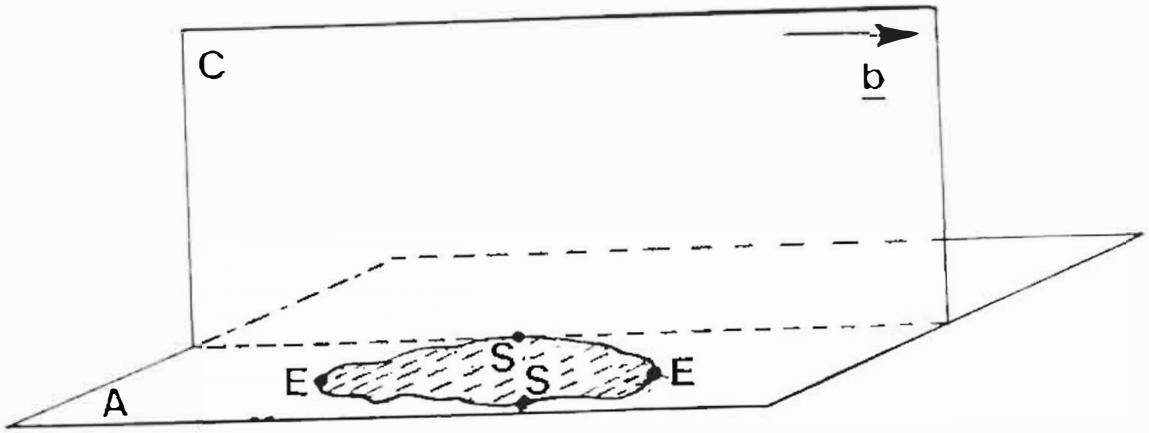

(a) Slipped area (shaded) on plane A. Slip is about to spread onto plane C when the screw segment S moves onto plane C.

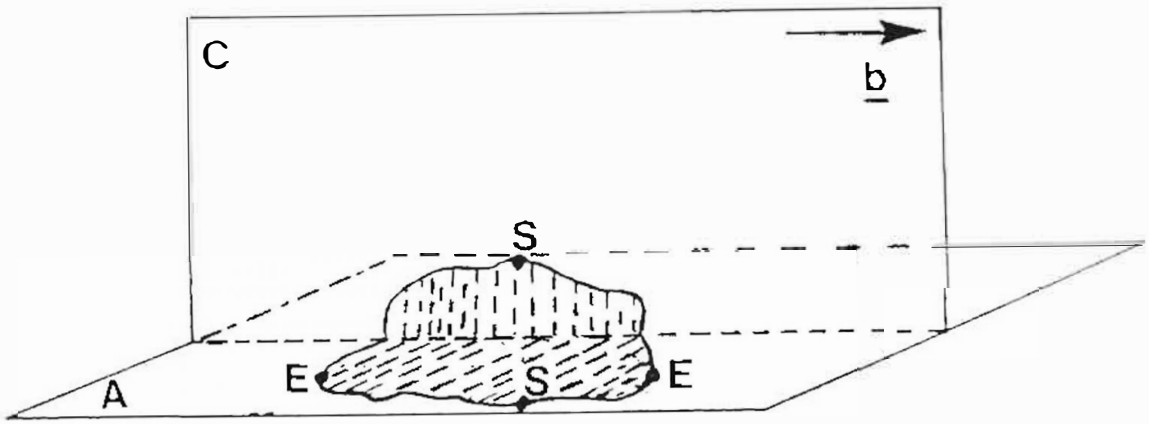

(b) The slipped area as in (a) above, but after cross-slip. Slip on C has spread over the vertically hatched area.

Fig 2.9: The screw segment S undergoing cross-slip.

may not be simple lines, but often have slightly spread out cores that have a two- or three-dimensional shape, e.g. in fcc metals, dislocations are ribbon shaped, with the ribbon plane parallel to the glide plane of edge dislocations, while in bcc crystals such as iron, a dislocation may be spread on to three separate planes (2,3).

Such details of the shape of dislocation core make it difficult for cross-slip to occur, or in some cases, prevents it entirely. Under these circumstances, the glide surfaces that develop have a strong planar character. Such planar surfaces may nevertheless be stepped and corrugated along the glide direction by occasional cross-slip, as shown in Fig 2.10. Since the glide surface develops as shear spreads, there is also the possibility that the surface can become split and bifurcated as explained below.

When the screw segment of a spreading dislocation loop undergoes cross-slip, the edge segment of the dislocation will continue to glide on the original plane. The screw segment that undergoes cross-slip may do so by following a path of least resistance in order to avoid an obstacle on its original plane. This is how bifurcation occurs. In the process a cusp may develop in the slip front e.g. A in Fig 2.11. For further discussion on the details of corrugation and bifurcation see Jackson (28).

A screw segment of a spreading dislocation loop which undergoes cross-slip is illustrated in as in Fig 2.11. Here slip continues to spread while bifurcation develops in the glide surface. Repeated bifurcation of glide surface can eventually result in the glide surface acquiring analmost biological complexity (2).

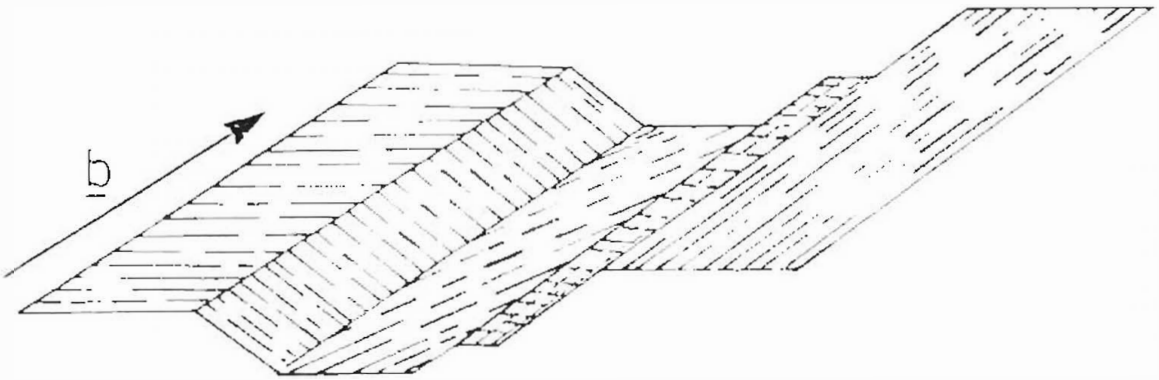

Fig 2.10: A corrugated and stepped glide surface. The Burgers vector is as indicated by an arrow.

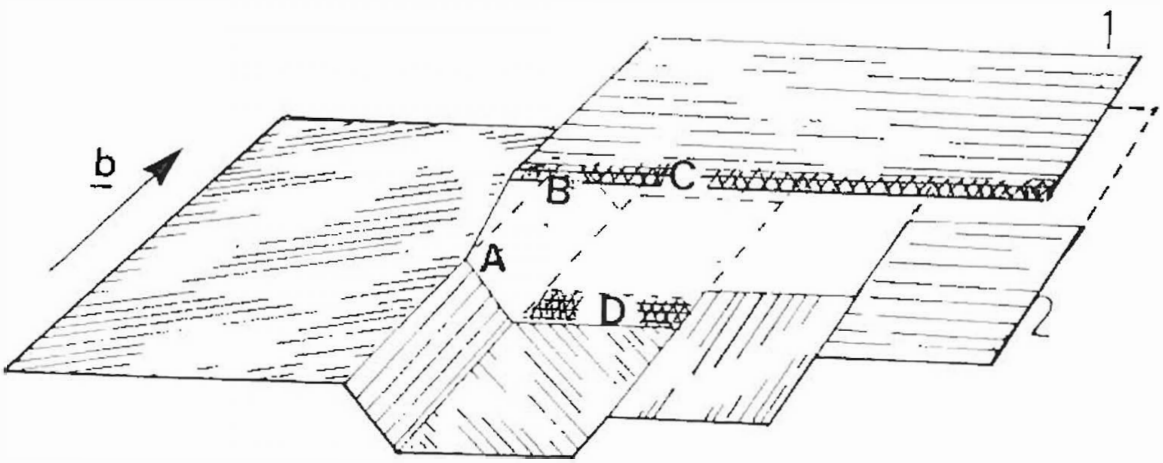

Fig 2.11: A glide surface on which cross-slip has occured along AB splitting the surface into two segments 1 and 2.

2.6 DEVELOPMENT OF INTERNAL STRESS IN CRYSTALS

Glide that is predominantly planar in character has been called lamellar glide (4,21). Such glide is characteristic of hexagonal close packed metals, such as cadmium, and of some face centred cubic alloys such as copper-rich aluminium alloys. Lamellar glide is associated with a small degree of work hardening. Rapid work hardening occurs in pure fcc metals, and is associated with glide that is neither planar nor lamellar in character. Such glide is called turbulent glide, and is accompanied by the development of complex three-dimensional dislocation microstructures, and the presence of internal stresses. It has been suggested that internal stresses are primarily a consequence of non-planar glide (29). Consider a glide surface that has been bifurcated by cross-slip as shown in Fig 2.11: as glide continues to spread, the upper surface develops further in the direction $-\underline{b}$ in the hatched region C, while the lower surface develops further in the direction $+\underline{b}$ in the hatched region D.

It can be shown that internal stress then becomes concentrated in the volume between C and D (30). In metals, these stresses are relaxed plastically, and this impedes further spreading of shear. The net results of many such events is that the crystal as a whole becomes more resistant to plastic deformation, i.e. the crystal work hardens.

2.7 SHEAR IN AMORPHOUS MATERIALS

Certain elements of the process of shear described in previous sections, apply also in the spreading of shear in amorphous materials. An example was observed in the deformation and faulting of Wombeyan marble by Patterson (18). Firstly, when shear spreads on a well defined surface, rather than in the bulk of the solid in a viscous fashion, a description in terms of dislocations may be useful. A case in point is the formation of geological faults.

Although rock is a coarse and complex polycrystalline material, the displacement involved in faulting on a crustal scale is so much larger (measured in metres) than that in crystals (measured in nanometres) that for many purposes the progression of shear can be regarded as if it has taken place in an amorphous material. The boundary of the region that has undergone faulting is called a tip line by geologists: it is this "tip" of the fault that marks the edge of the fault. A tip line is a geological analogue of a large group of dislocations in crystal plasticity (28,31,32,35).

The second relevant feature of dislocation glide is the distinction between conservative and non-conservative glide. This distinction is valid when the fault plane is vertical or nearly vertical, and the glide direction is horizontal. Such a fault is called a strike-slip fault (see Fig 2.12). The restrictions placed on the spreading of shear by the requirement that glide be conservative, means, for example, that a vertical tip line of the strike-slip fault may propagate only in the plane of the fault. Shear may

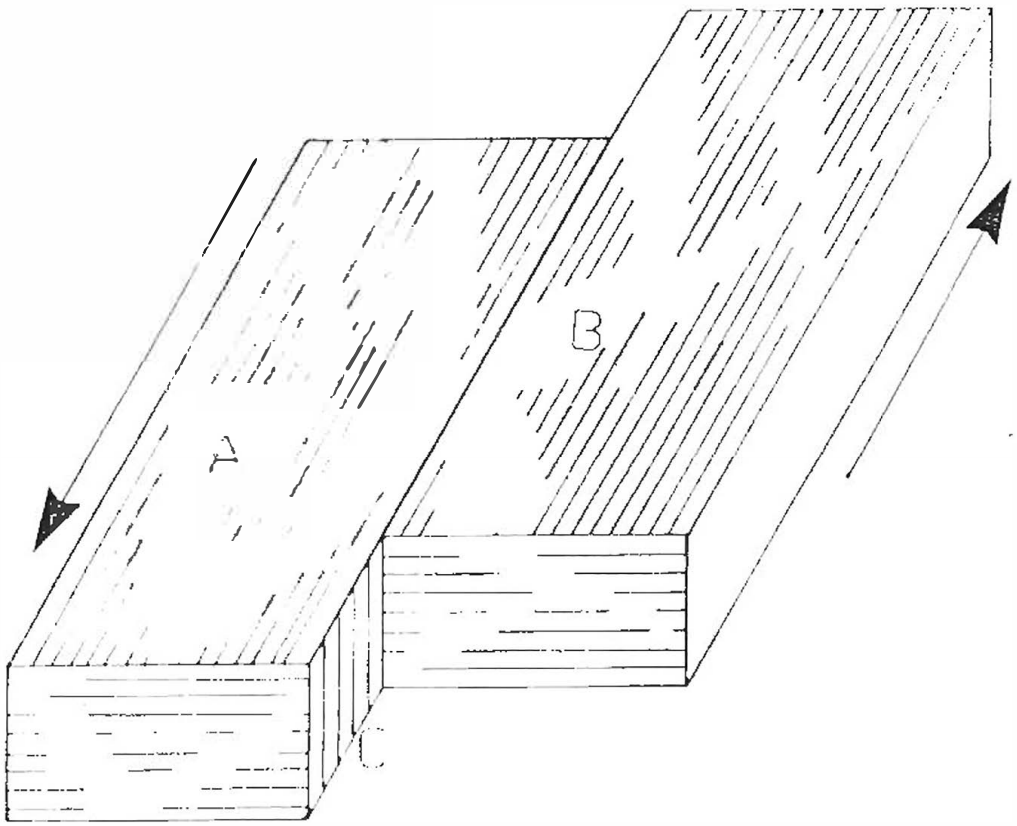

Fig 2.12: A strike-slip fault. Surfaces A and B are parallel to earth's surface and are displaced parallel to this surface. Such displacement parallel to the surface is called "strike". Hence the name: "strike-slip".

deviate from the plane only where the spreading fault is bounded by a horizontal tip line, which is the analogue of a screw dislocation (35,36).

As in the case of crystals, such deviations are likely to result in a fault surface becoming more complex than a single plane. It should be noted that restrictions imposed on the formation of the fault surface by the need for a shear to be conservative are less severe in the case of thrust faults where the fault is horizontal in crustal deformation than in the case of crystal dislocations (37).

The outer shell of the earth's crust is about 250km thick, and consist of two layers: the outermost layer being the lithosphere, about 50km thick and the inner being the asthenosphere, about 200km thick. The study of plate tectonics suggests that these layers, though rigid, are divided into a series of crustal plates bounded by oceanic ridges and strike-slip faults, sometimes called transform faults. The tectonic plates are buoyed up and float on a denser plastic mantle beneath, the plates rise and sink occasionally to establish equilibrium (33,34,38,39). In a thrust fault, the fault surface is horizontal or inclined shallowly to the horizontal. Because of the proximity of a free surface (earth surface), the tip-line may deviate from planar motion and move upwards, for example so relaxing the constraint on non-conservative glide. This results in a plate block of the earth's crust being displaced above the earth's surface as illustrated in Fig 2.13 (31).

The third useful feature that may be adopted from dislocation modelling to the larger scale of geological faulting is the distinction between edge and screw dislocations, and the concept of dislocation cross-slip.

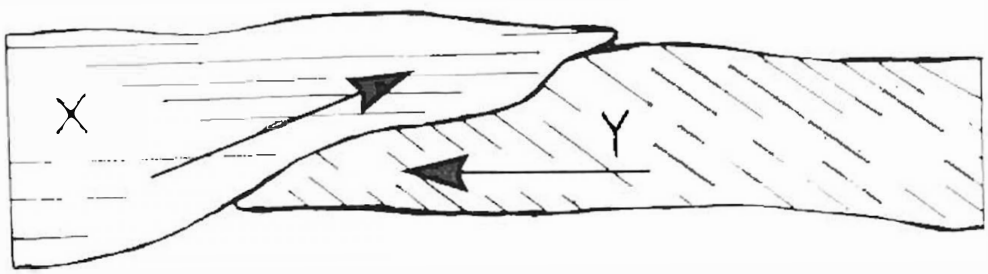

Fig 2.13: Block X of the earth's crust displaced over the earth's surface Y in a thrust fault. Arrows show movement direction of each block. The fault surface is roughly horizontal.

Tip lines that are perpendicular to the direction of faulting are analogues of edge dislocations, while those parallel to the faulting direction are the geological analogues of screw dislocations. In crystals, restrictions on cross-slip such as the shape of the dislocation core may constrain glide to be planar (section 2.5), but in an amorphous solid, there are no such restrictions, and glide surfaces are free to develop corrugations by cross-slip, provided the corrugations lie parallel to the direction of glide (31). As in crystals, glide surfaces may become split and bifurcated when cross-slip occurs. Indeed, because there are no restrictions on cross-slip in an amorphous material, it is difficult to see why glide surfaces should remain planar. In general, then, the morphology of the glide planes in amorphous material should be dictated only by the following two factors.

1. The pattern of the external stress that is applied to the crust, and the pattern of the internal stress that develop as a result of glide, say, in earth crustal deformation, or any material under examination, and

2. The restriction imposed by the need for the glide to remain conservative, which are severe for strike-slip faults, but somewhat relaxed for thrust faults.

In crystals, turbulent glide may be enhanced by the presence of inhomogeneities. For example, turbulent glide occurs from the onset of plasticity in crystals that contain a dispersion of small particles, as in the dispersion hardened copper alloys. For a review, see Humphries (40).

When shear spreading on a surface encounters an inhomogeneity, the inhomogeneity may be by-passed aided by cross-slip which enables shear to transfer to surfaces that do not intersect the inhomogeneity (28,31).

Suppose now that this description of cross-slip is extrapolated to a situation where a real material can be expected to behave like an amorphous solid, such as the large-scale deformation in the earth's crust that accompanies strike-slip faulting at the edge of tectonic plates. One may then expect that the fault surface (the analogue of glide surface in crystals) will frequently be non-planar and corrugated along the glide direction. Corrugations parallel to directions inclined to the surface terminate on the surface. Such corrugations should appear as stepped arrays called in geological terminology en-echelon faults. Such an array is illustrated at the bottom in Fig 2.14(b).

Corrugations and en-echelon faults may develop as follows: as a fault spreads along its incipient glide surface, it is likely to encounter hard regions that resist the shear. At such encounters, the cross-slip of screw dislocation components that develop as shear encircles this hard region can enable shear to by-pass the hard region. When such cross-slip occurs, the surface becomes bifurcated. The bifurcation of geological fault surfaces can cause the intersection of the fault surface with the earth surface to become stepped as shown in Fig 2.14.

When strike-slip geological faults are mapped on the surface of the earth, stepped en-echelon segments are often observed. The origin of these en-echelon faulting is not well understood, It is suggested here that the

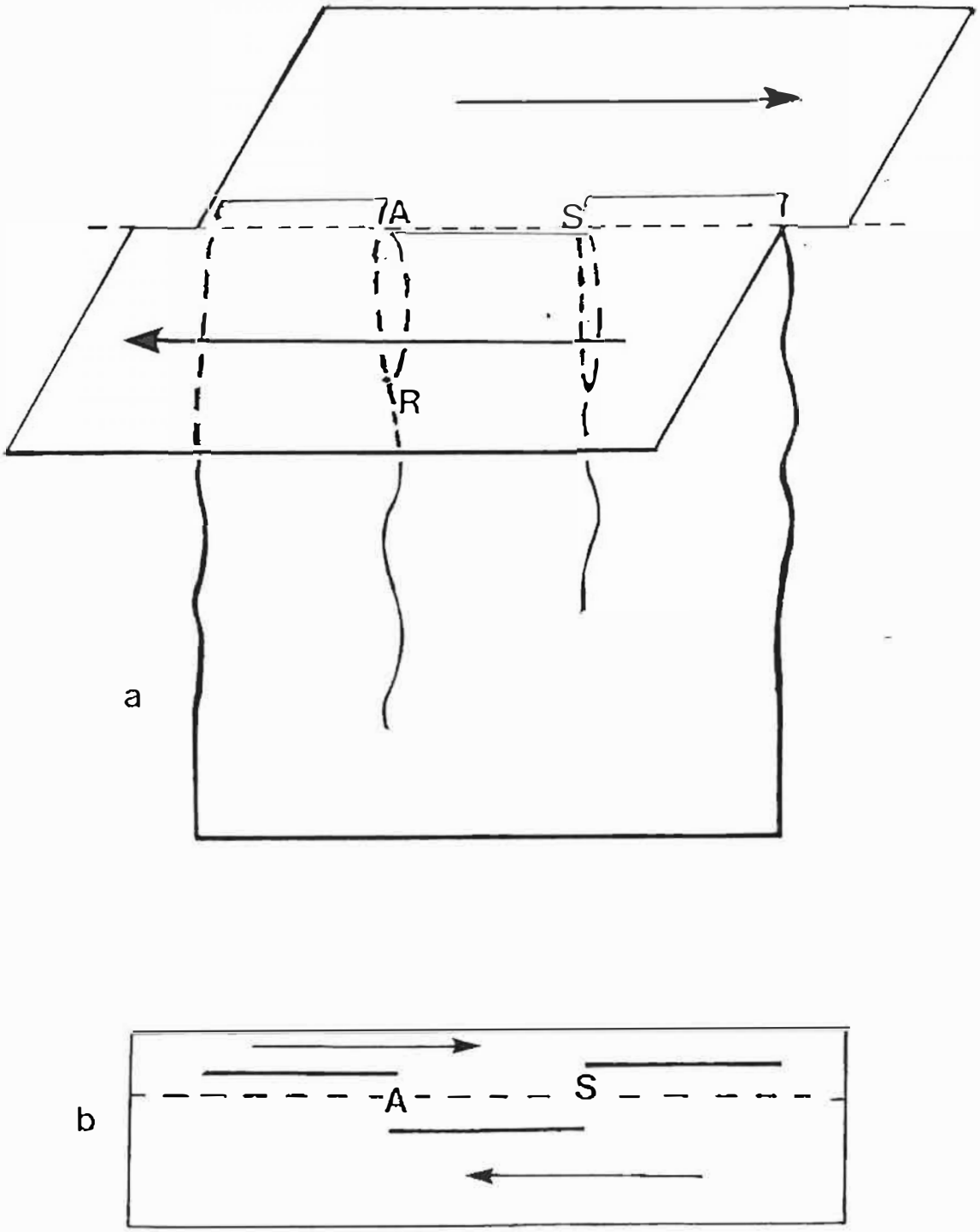

Fig 2.14: (a) Bifurcated fault surface in a strike-slip fault.
(b) Plan view of the faulted surface showing en-echelon faults.

cross-slip of the tip lines below the earth's surface could provide a simple explanation for this commonly observed feature of strike slip faulting (41,42,43).

The phenomenon of en-echelon faulting may be connected to the origin of earthquakes. Earthquakes are vibrations of the earth caused by the rupture and sudden movement of the earth's crust when it is strained beyond its elastic limit. At a rupture point, crustal material under strain fractures and the shock generates vibrations named seismic waves (33,38,39).

In geological terminology, a step in the mapped trace of a fault, such as in Fig 2.14(b) is called a jog (as distinct from so-called dislocation jogs in crystals). A is a dilational jog, while S is an antidilational jog. This feature may have originated deep in the crust of the earth at a point such as R, in Fig 2.14(a). Antidilational jogs are so called because further progress of faulting is restrained at S; such jogs offer frictional resistance to slip in a strike-slip and may thus inhibit further slip by forming a potential locking point. The opposite end of the same fault surface segment, marked A, is called a dilational releasing jog. Here no major impediment to slip exists. Sibson (42) has suggested that the antidilational jogs are favoured sites for earthquake origins; it is therefore important to understand how and why such defects on otherwise planar fault surfaces develop; further discussion on the dilational and antidilational jogs appears in chapter 5 with reference to Fig 5.1.

A difficulty in tracing the origins of such features is that the morphology of the fault surface cannot be easily deduced. Experiments of shear on a small scale in model amorphous solids could help to establish the morphology of the shear surface, and in particular, whether there is a tendency for glide surfaces to be split and bifurcated, and to be corrugated parallel to the direction of shear. A device often used to demonstrate and model shear on geological scale is the shear of wet or slightly damp granular solid such as sand, in an experimental shear box (44,45,46).

2.8 PREVIOUS WORK ON MODEL STRIKE SLIP FAULTING

Several research workers have investigated the rupture patterns that result from strike-slip faulting in model amorphous solids; most of these patterns have been studied from sand models. The results obtained from these models may help geophysicists to understand earthquake mechanisms. Sand, as amorphous solid, is a suitable material for the purpose of model construction since it faults and ruptures on deformation, while clay, an alternative material is more suited for investigating the phenomenon of folding. Although such laboratory experiments are on a very small scale, the results concerning horizontal translation of amorphous solids have been extrapolated (36, 44, 45) to the tectonic scale both in surface mapping and geophysical interpretation of the fault patterns below the surface of the earth.

Two groups of research workers have been active in this field. The first group, laboratory workers, worked with models. The second group, field workers, discuss data from real earthquakes.

2.8.1 LABORATORY WORKERS

Emmons (45) investigated the subsurface patterns of deformation generated by two types of strike-slip displacement: (1) a strike-slip displacement on which the surface followed a straight course and (2) a strike-slip displacement that followed a curved course. For (1), the sheared sand was contained in a box that was 22 inches long, 8 inches wide and 14 inches deep. This box was divided in two halves in such a way that the two halves could slip relative to each other in opposite directions without separating, (see the similar box used in the present work, Figs 3.1 and 3.2. A similar box was used also by Mandl (36), whose experimental work will be discussed below). Emmons' box was filled with sand that was vibrated to close packing. The sand consisted of alternating horizontal layers of contrasting colours. One half of the box was the translated by 2 inches, to induce a strike-slip fault in the material. Without giving further details as to how he conducted the observation, Emmons reported as follows:

1. Deformation of the sand was confined to a narrow zone above the joint between the two half-boxes. This joint was called the basement, and the narrow zone to which the deformation was confined was called the rupture or fault zone.
2. Near the base of the box the rupture zone was confined closely to the division of the container.
3. The rupture zones widened (with a tulip-shaped cross section) towards the surface by spreading groups of branching faults (see Fig 2.15).

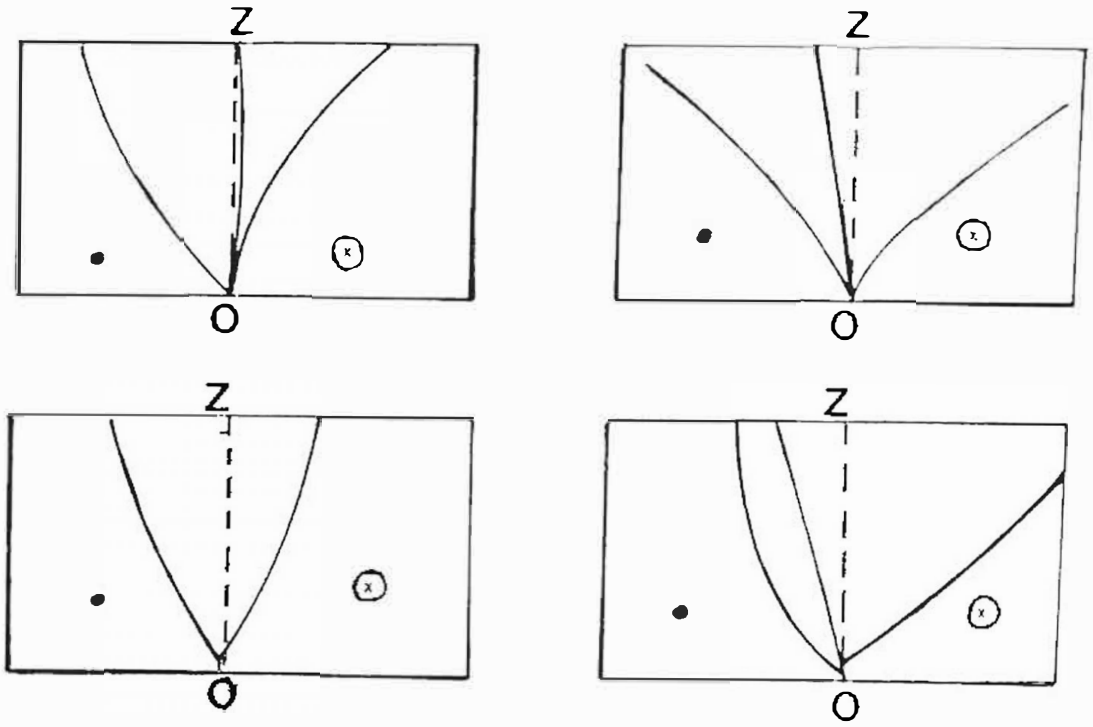

Fig 2.15: Series of cross-sectional views of the fault surface according to Mandl (36) and Emmons (45) after the shearing of the experimental box along the center line. ● indicates the box half that was sheared in the direction outward from the page with respect to ⊗ which was inward.

4. The fault surfaces were not planar, nor did they form simultaneously.

5. These fault surfaces were twisted and wavy, that is, they were warped in cross sections both vertically and horizontally.

Richard *et al* (47), investigated how faults initiate and develop above a basement (see Emmons above) in strike-slip faults. They used a similar experimental configuration to Emmons. Their experimental box was divided into two halves so as to allow each half to move horizontally relative to the other. The box was 800 mm long, 450mm wide and 25mm high. It was filled with sand and crushed glass in alternating horizontal layers 5mm thick to the height of 25mm. The container was then sheared at a velocity of 30mm per hour. The total shear displacement was 30mm. An imaging technique, namely, computerized X-ray tomography,was used to scan the cross-sectional images. (This technique, the principle of which was first derived by Cormack in Cape Town, may be used to measure the density and atomic arrangement inside opaque bodies). They were able to monitor the fault development inside the model, without destroying it. For further details of this technique see Richard *et al* (47).

It was found that faults start at the base of the model immediately above the junction (that is, at the basement) and diverged into two or three branches as they approached the free surface. In cross section sketches these branching faults were seen to deviate from the vertical at angles between 70^{o} and 90^{o} over a fault or rupture zone 30mm on both sides of the basal junction (basement) of the experimental box, as in Fig 2.15. The fault was divided into complicated smaller faults oriented at almost right

angles with the direction of the shear. These faults are called transverse faults.

Mandl (36) in an experiment similar to that of Emmons, investigated the subsurface geometry of strike-slip faults. His experimental box, which was cut into two to allow horizontal glide as in Emmons experiment, was 1000mm long, 500mm wide and 100mm deep. The box was filled with white sand alternating with blue sand in horizontal layers. Again, the shearing was in the horizontal direction so as to impose a simple shear, where the undeformed parts of sand in the box were carried along passively by the moving base of the box, resulting in a vertical shear surface.

Mandl mapped a series of vertical cross-sections of the sheared overburden at intervals of 10cm along the strike, or shear direction (as in Fig 2.15). He also mapped cross-sections perpendicular to the shear direction (strike) to determine how the fault branched into sub-branches. This branching occurs as the deformation spreads out into a wider fault zone as it approaches the surface of the packed sand. The different vertical mappings are shown in Fig 2.15. The three experiments described above give an indication of how the subsurface geometry in large scale crustal deformation might develop when large scale strike-slip faulting occurs.

2.8.2 FIELD WORKERS

Field workers have attempted to deduce fault morphologies by mapping faults on the earth's surface at their natural sites. The workers considered below discussed their results in the frame work of the theory of plate tectonics. This plate tectonic theory states that the earth's crust is divided into plates that support the continental land masses. The plates themselves float on the mantle of the earth.

Press (48), noticed that the earthquakes occur along boundaries of tectonic plates, and hence concluded that crustal instabilities due to earth's movements cause shearing stress on plates lying next to each other. When this stress is large enough to overcome frictional resistance between the plates, fracture occurs, a strike-slip fault develops between the two plates and the earthquake occurs.

Fröhlich (49), contributed to the theory of earthquake eruption during his research report about deep earthquakes. Deep earthquakes were defined as those whose origin is below150km. These deep earthquakes occur in the following manner: when two crustal plates collide, the edge of one plate glides onto the top of the second plate while the second plate edge gets subducted into the earth's mantle underneath the first plate. When the brittle edge of the subducted plate comes into contact with the hot mantle, it melts under increased pressure and increased temperature. Because it fails in this melted state to sustain the gliding plate, the crustal material ruptures at the plate junction resulting in an earthquake at this depth. Fröhlich's work shows that it is not only in strike-slip faults that earthquakes result.

Sibson (42), like Press and Fröhlich referred to the plate tectonic theory where the earth's crust floats on a viscous hot magma of the mantle below. He suggested that this floating crust has two strata. The upper stratum of the crust, 10 to 15km in thickness, consisting of brittle material whose behavior during plastic deformation is dominated by friction between fractured pieces, he called the seismogenic régime; while the lower stratum between the mantle and the seismogenic régime, was assumed to be aseismic quasi-plastic régime. When a shearing stress is applied to continental crust, frictional resistance occurs in the seismogenic régime; this friction constitutes an obstruction analogous to an obstacle in crystal deformation that results in cross-slip. (see section 2.5, Fig 2.11). If this shearing stress applied becomes more than the resistance due to friction within the seismogenic régime, strike slip faulting occurs, triggering earthquakes at the sites of friction; the earthquake shocks from these triggered earthquakes fracture the seismogenic crust like porcelain, segmenting the slip surface into en-chelon faults. This is why the en-echelon structures would be seen on the free surface of the earth.

Jackson (31) also suggested that the fault surfaces in crustal deformation will not be planar but will corrugate along the direction of the strike-slip, basing his suggestion on an analogy with the glide surface in crystals.

Segall and Pollard (41) speculated about how the en-echelon faults occur on the surface of the earth. They suggested that since the adjacent ends of the en-echelon segments of a fault dip toward one another, they coalesce to form a single fault at depth as illustrated in Fig 2.16.

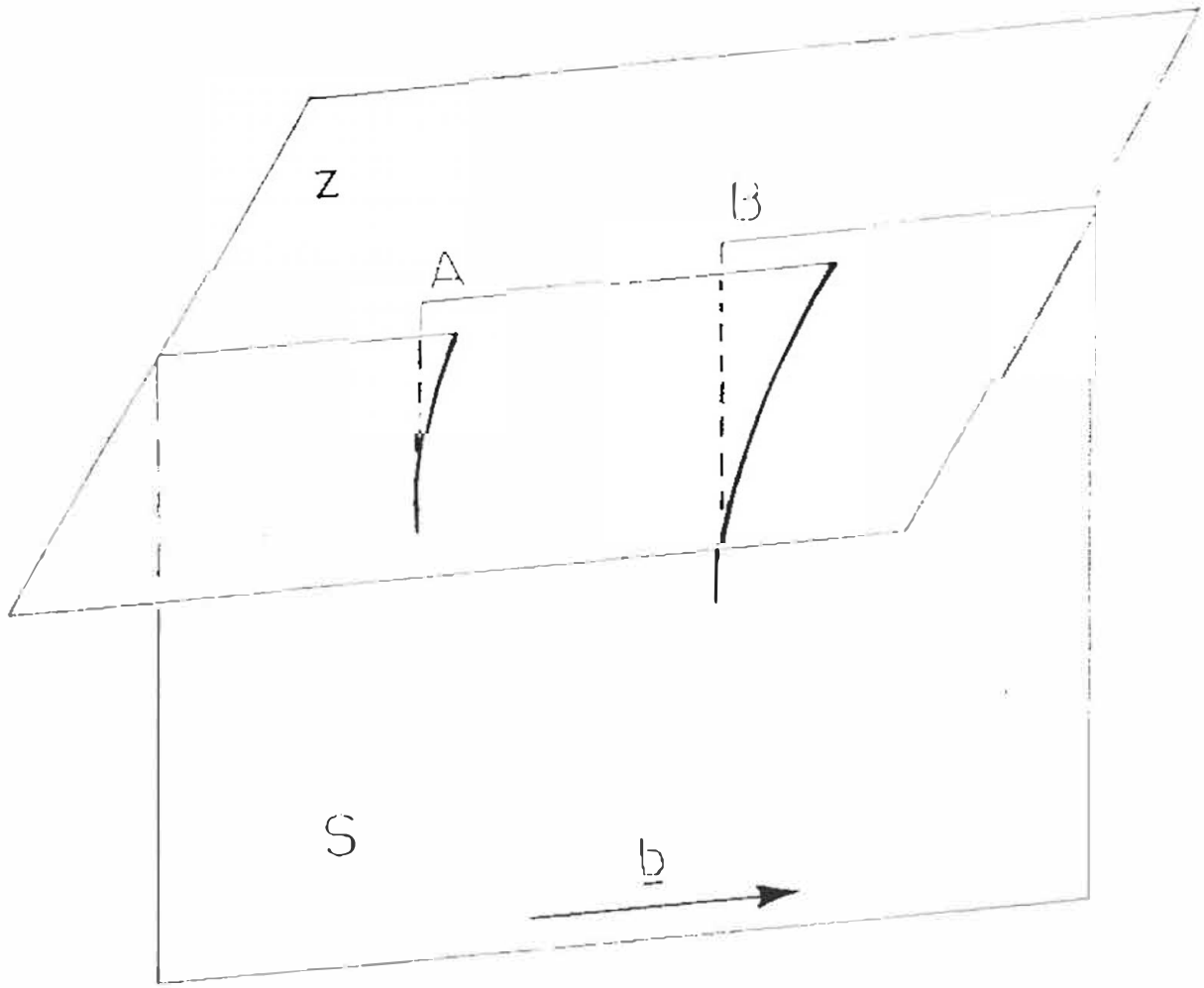

Fig 2.16: En-echelon segment A and B of a strike-slip fault coalescing to a single fault surface S below the surface Z (earth's surface).

2.9 CONCLUSION

Field workers have speculated about the morphology of fault surfaces involved in crustal deformations, in attempting to account for the earthquakes and en-echelon faults that occur in fault zones. The main difficulty with field observation is that below the surface the crust is impossible to examine on a geological scale. The laboratory workers however, devised various experimental procedures to assist in clarifying some of the hidden aspects of crustal faulting in an analogous but smaller scale. These experimental procedures may be used to develop an understanding of how slip surfaces develop in amorphous solid. If there could be a way of extrapolating the findings from the fault surface in amorphous solids to crustal faulting with success, such extrapolation could greatly elucidate some aspects of geological shear.

CHAPTER 3

EXPERIMENTAL METHODS AND APPARATUS

3.1. INTRODUCTION

Pure homogeneous river sand (average grain diameter 1mm) was placed in a wooden experimental box that could be sheared along a vertical plane that bisects the box. As a result of this shear, one half of the box was displaced relative to the other half, as in a strike-slip geological fault.

Displacement markers, consisting of a mixture of sand and distemper similar in particle size and moisture content to the sand in the experimental box, but of a contrasting colour to the sand, were introduced into the sand in the form of transecting lamellae (called vertical colour markers) before the box was sheared, to indicate the movement of the sand resulting from shear.

Observations of these markers were made at different levels. To do this, thin layers of sand were scraped away to expose a series of fresh surfaces, starting from the top of the sand, and continuing until the bottom of the experimental box was exposed. These observations provided information on the shape and morphology of the fault surface.

Several sets of experiments were carried out (two or three experiments being done in a set to ensure the reproducibility of the results obtained). The sets labelled 1 to 6 were used for preliminary investigations. Observations made on sets 7 and 8 showed both sets to be similar, hence only set 7 is presented in more detail.

The appearance of the markers on the sand surface after shear was noted. The positions of the markers were copied onto transparencies and photographed as follows: over every freshly exposed sand surface, an A4 size transparency was placed, and the shapes of the markers were traced onto the transparency. A camera was also used to photograph each newly exposed sand surface. The information gathered both from transparencies and photographs was used to build up a three dimensional model of the glide surface.

Transparencies clearly showed the offsets due to shear on each lamella at every sand height. Individual displacements of each offset from the center line at successive levels were determined and mapped on paper sheets 70mm wide and 100mm long for each vertical colour marker. These offset maps which traced out the path the fault surface followed through the colour marker, were enlarged to A4 size and their shapes were transferred onto perspex sheets 3mm thick.

The perspex sheets, arranged in the same order as the vertical colour markers were placed vertically, at 200mm intervals. The perspex sheets were then kept fixed by a frame of steel wire 6mm in diameter. Holes were drilled at offset positions of the fault surface on each sheet. Strings threading through these holes then lay in the fault surface, and provided a three dimensional model of this surface. (The method of model construction will be described in Section 3.4.1).

The advantage of such a model is that it can be examined from all angles. The intersection of the fault surface at every vertical colour marker is particularly clear. The data compiled from the marker positions was used to create and to clarify the morphology of the fault surface between two sheets.

3.2 APPARATUS USED

3.2.1 THE EXPERIMENTAL BOX

To shear the sand, a wooden box was used (Figs 3.1, 3.2). The box was 400mm long, 300mm wide and 100mm deep. It was cut into two halves which were attached to each other by a soft cloth (along strip CC' in Fig 3.4), so that the two halves could be displaced relative to each other by 40mm, so as to model a strike-slip fault in the sand. The purpose of the connecting soft cloth was to ensure that the two halves could maintain contact while sliding past each other as in a strike slip fault (see Fig 3.3) without falling apart.

The box was filled with river sand sifted through a wire gauze so that the maximum grain size was 1mm. The optimum moisture content of the sand was found to be 16% by weight. Lesser moistures caused sand particles to have insufficient cohesion. For greater moistures the body of the sand was too wet to maintain its form. The sand was then compacted by being pressed down with a piece of wood to achieve maximum density. It was important to use compacted sand with an optimum moisture in order to produce a well defined shear surface.

3.2.2 THE VERTICAL COLOUR MARKERS

To prepare the vertical colour markers, pieces of masonite hardboard of 4mm thickness were made with lengths just less than 300mm, so as to fit the inside of the experimental box. These boards were placed vertically in the

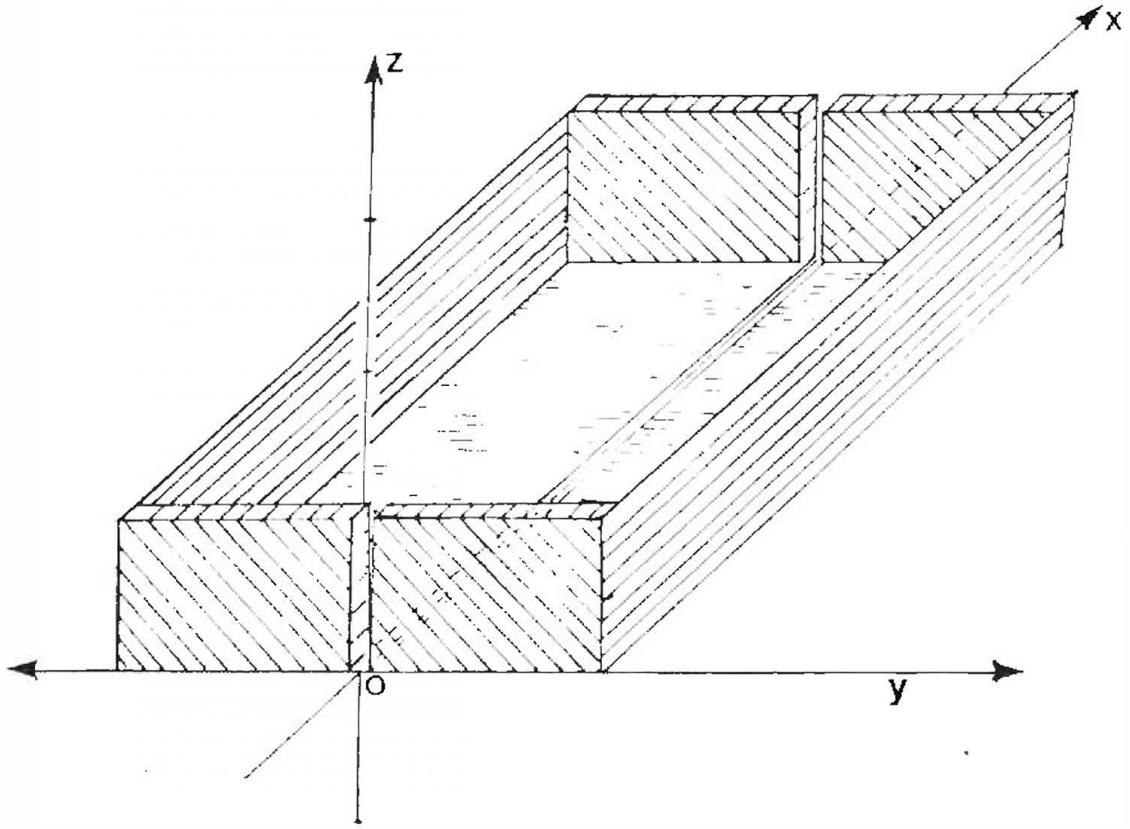

Fig 3.1: The experimental box and the coordinate system used to describe the experiment.

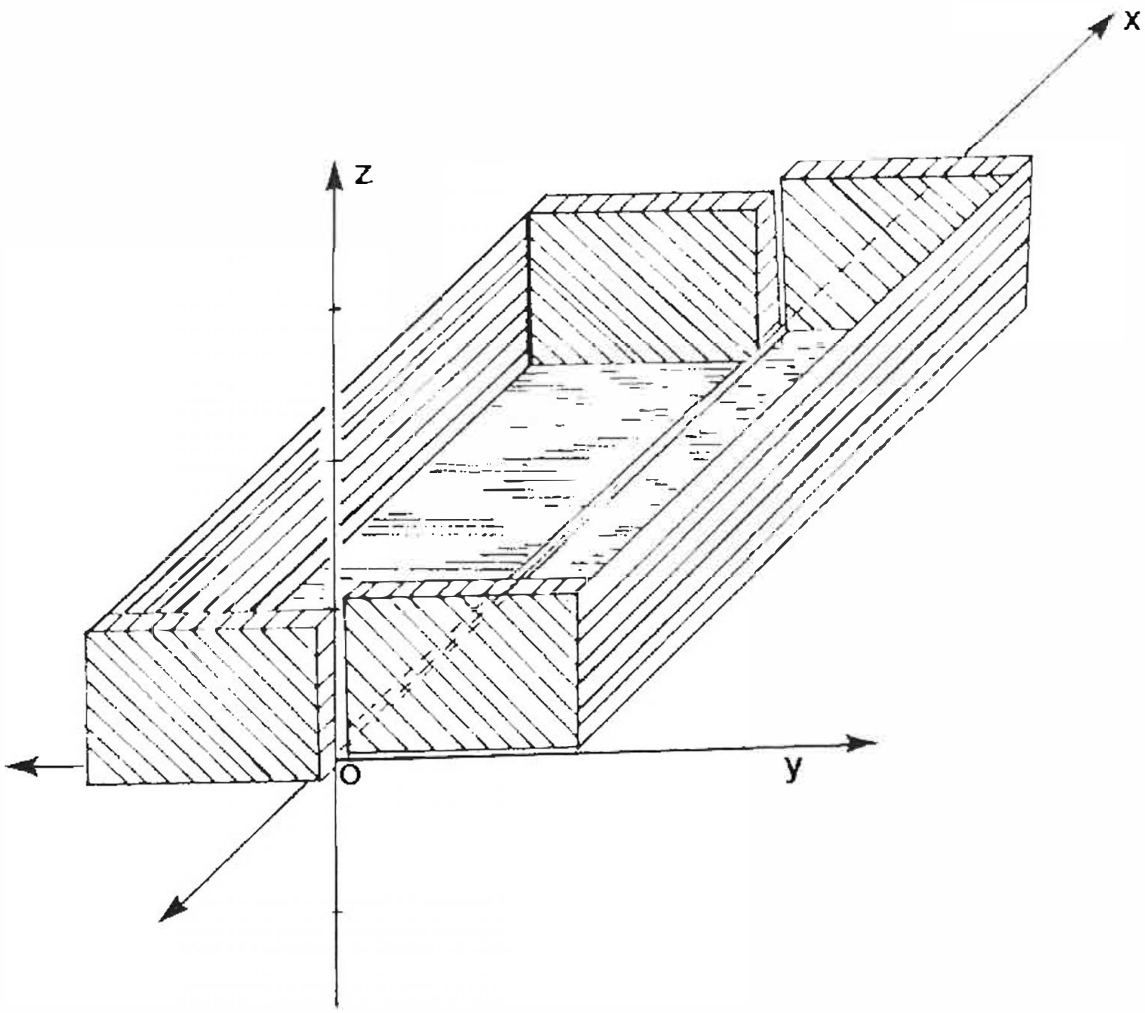

Fig 3.2: Experimental box after shear along the x-axis across the X-Z plane.

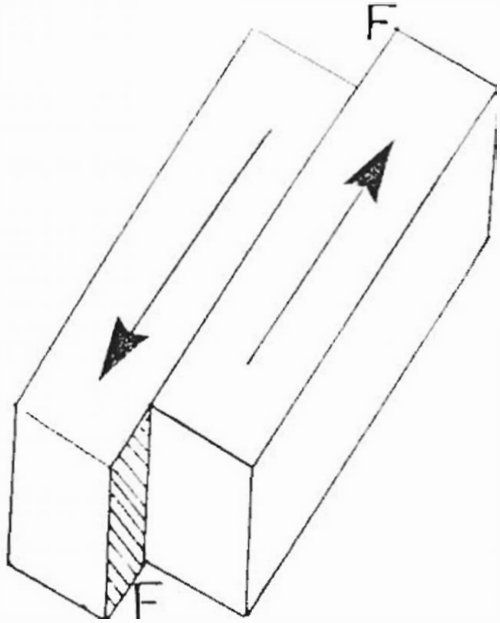

Displacement associated with a sinistral strike-slip.

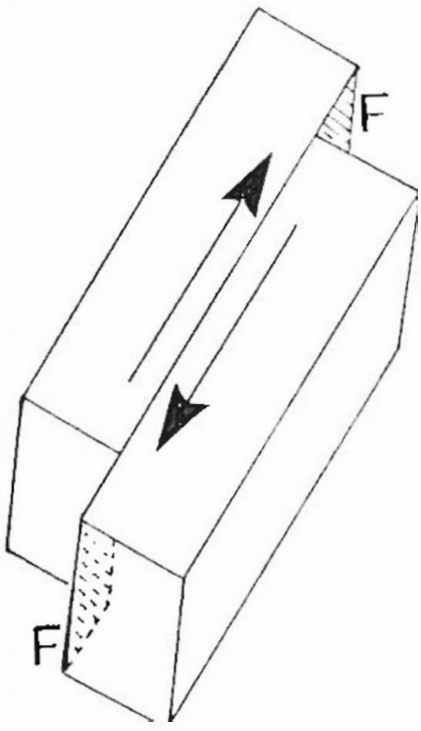

Displacement associated with a dextral strike-slip.

Fig 3.3: Strike-slip faults. The arrows indicate the direction of slip. FF denotes the glide, slip or fault surface.

box at equal intervals of 40mm. A total of 6 markers was used. For 30mm intervals, a total of 8 markers was used (Fig 3.4).

Distemper powder (obtained from a hardware store) contrasting in colour with the sand specimen, was used as a marker in the sand. Pink distemper proved convenient. Since this distemper powder consisted of smaller particles than sand, the distemper was mixed in equal proportions with sand. The presence of the markers then affected the propagation of shear in the sand minimally.

3.2.3 THE SCRAPER BOARD

A scraper board (Fig 3.5) was used to remove layers of sand of even depth. It was 100mm wide. It had the same depth as the experimental box. Lines were drawn on the scraper board which were 5mm apart. These lines were horizontal when the scraper board was placed vertically inside the experimental box. Adjustable pegs PP were provided. These pegs controlled the depth of the board in the box, and hence the depth of the sand layer removed by scraping.

3.2.4. TRANSPARENCIES, RULER, CAMERA, etc.

A transparency of A4 size was placed on every freshly exposed surface. The positions of the distemper markers were recorded on these transparencies by means of a marking pen. A plastic ruler (300mm) was used to draw a straight line that marked the plane along which the two half-boxes slip, i.e. along CC' in Fig 3.4. CC' was named the center line. A 35mm camera was used to photograph each freshly exposed surface during the progress of the test sets, which are set 7 and set 8.

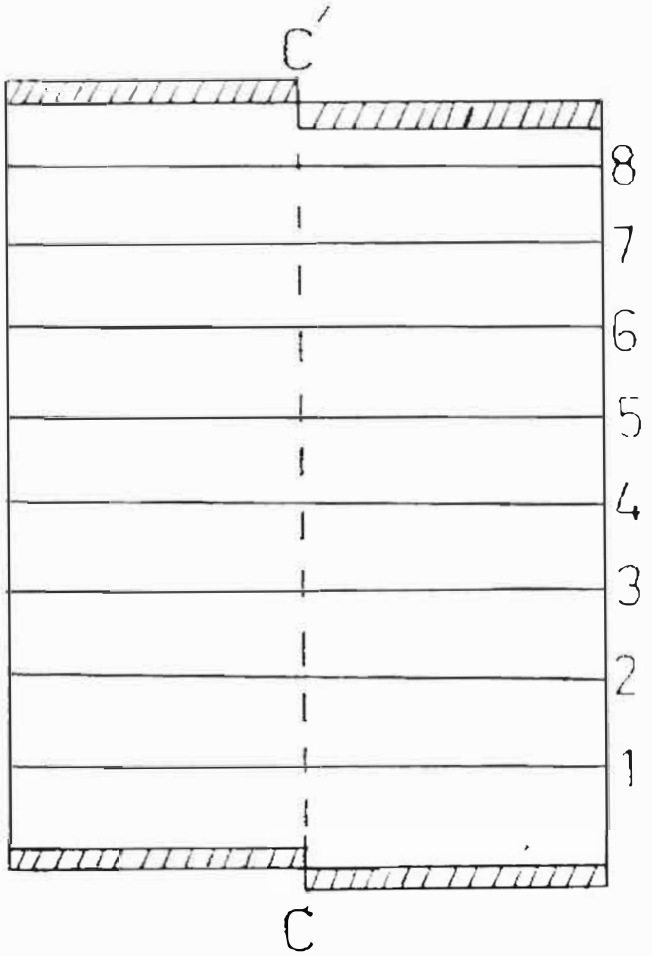

Fig 3.4: Experimental box, right laterally slipped, with eight hardboards in their positions, before shearing.

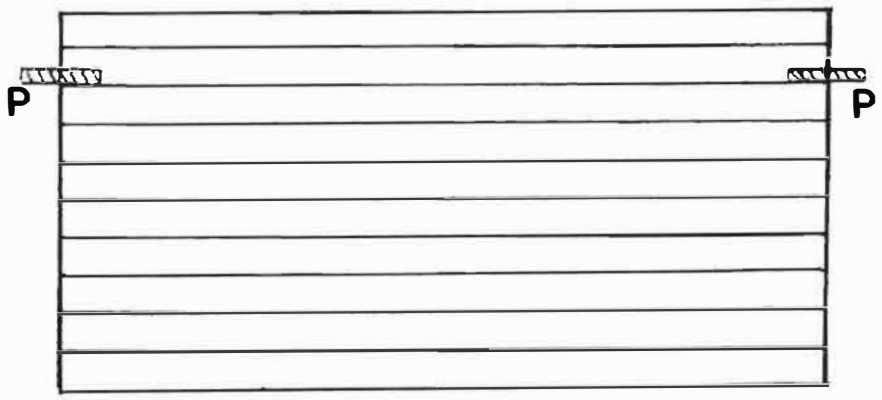

Fig 3.5: The scraper board, adjusted with two pegs PP at the 80mm mark to allow the scraper board to be used to remove a uniformly 80mm thick sand, leaving 20mm thick sand in the experimental box.

3.3 THE EXPERIMENTAL PROCEDURE

3.3.1. SAMPLE PREPARATION

In geophysics, a strike-slip fault where material on the left is displaced towards the observer relative to the material on the right is called a sinistral or a left lateral strike-slip fault, while a fault in which material on the right is displaced towards the observer is said to be right lateral or a dextral strike slip. Such faults are shown in Fig 3.3.

The procedure began with the experimental box in a right-laterally slipped position as in Fig 3.4 with the masonite hardboards numbered 1 to 8 placed vertically as indicated (Fig 3.4). Washed, damp river sand was taken as prepared above (see section 3.2.1), and poured carefully into the experimental box so as not to disturb the positions of the hardboards.

After filling the box the scraper board was used to level the sand to the height of the walls of the box. The hardboards were thus just exposed and were carefully removed from the sand, one after another without disturbing the rest of the sand. Each removed hardboard left an empty lamella (or cleft) in the sand. Care was taken to ensure that the walls of the lamella did not collapse while the boards were being removed. A pair of pliers was used to remove the boards. A 50:50 mixture of pink distemper and sand was prepared. For every experiment, a litre of this 50:50 mixture was sufficient to provide all markers. The mixture was then poured into the lamellae left by the removed boards until the lamellae were full. In this way each vertical colour marker was placed in position until all markers were completed.

3.3.2. SHEARING THE SAMPLE

The experimental box was then sheared horizontally so that the two halves of the box, each filled with compacted sand, were displaced relative to each other defining a shear surface as the slip occurred, in the manner of a left-laterally slipped strike slip in geophysical terms.

CHAPTER 4

DATA ACQUISITION, ANALYSIS AND RESULTS

4.1 INTRODUCTION

Observations were made on eight sets of experiments with the purpose of studying the details of the shape of the fault surface in the sand that is sheared. When the sand in the box is sheared, steps develop along the vertical colour marker lamellae which are called offsets. The offsets denote the positions where the fault surface intersects each lamella. Plotting these intersection points on the same level on a transparency and connecting them traces out the path or trail of the fault surface at that level. We shall call this the horizontal trail of the fault surface at that level. When all the sand has been scraped away until the last (bottom) level is exposed, the intersection points can be mapped vertically along the vertical colour markers. These maps will be called the vertical trail maps of the fault surface at each lamella position. Such vertical trail maps give vertical sections of the fault surface at the position of each lamella similar to those shown by Mandl in Fig 2.16.

The first six sets of observations were preliminary sets to develop the experimental technique; while set 7 (which was similar to set 8), was taken as the test set from which the data was subsequently accumulated. The experimental procedure and its development from set 1 to set 7 is described below.

4.2 REPORTS AND COMMENTS ON INDIVIDUAL SETS.

SET 1

The first set was a rough preliminary investigation of the method. It was carried out with sand that was not of homogeneous particle size. Three marker boards were inserted in the experimental box, randomly spaced; hence no proper measurements could be taken. The experimental box was filled with sand, the marker boards carefully removed, and the voids filled with distemper-sand mixture to act as a colour marker. The system was then sheared. From the results it became clear that more markers were needed to provide a more detailed map of the fault surface. It also became evident that a more systematic and accurate procedure had to be devised for removing sand to expose the colour marker offsets at different levels.

SET 2.

The second set incorporated improvements devised during the preliminary set. In set 2, six vertical colour markers were introduced into the experimental box, spaced 40mm apart. The specimen was sheared by approximately 30mm. A trowel was then used to scrape away 10mm thick layers of sand between observations of vertical colour marker positions. The observations on set 2 were as follows:

1. Each exposed surface of the sand that was to be examined was not uniformly levelled because a trowel was used to scrape away sand.

2. The vertical trail maps of the fault surface produced in this experiment were considered too complicated for effective analysis, and

it was decided to reduce the shear displacement from 30mm to 25mm in an effort to produce a simpler fault geometry.

3. Intervals of 10mm between exposed surfaces were rather large to map the fault surface due the shear.

Fig 4.1 shows the maps of the vertical colour marker lamellae offset trails after the shearing in set 2, with each lamella marked numerically from the origin.

SET 3

In set 3, sand layers were removed by an improved method. Scraping was done with one of the masonite hardboards, and the depths between the levels were measured with a ruler. Again there were six vertical colour markers. The specimen was slowly sheared by 25mm. Transparencies were used as follows: after exposing every fresh surface, a transparency was placed over the sand to trace the positions of the offsets in the vertical colour markers. Eleven transparencies had been used when all sand was scraped away to the bottom of the experimental box. Each transparency showed how the positions of the colour markers had shifted at each offset at every level below the original surface. The following observations and conclusions were made:

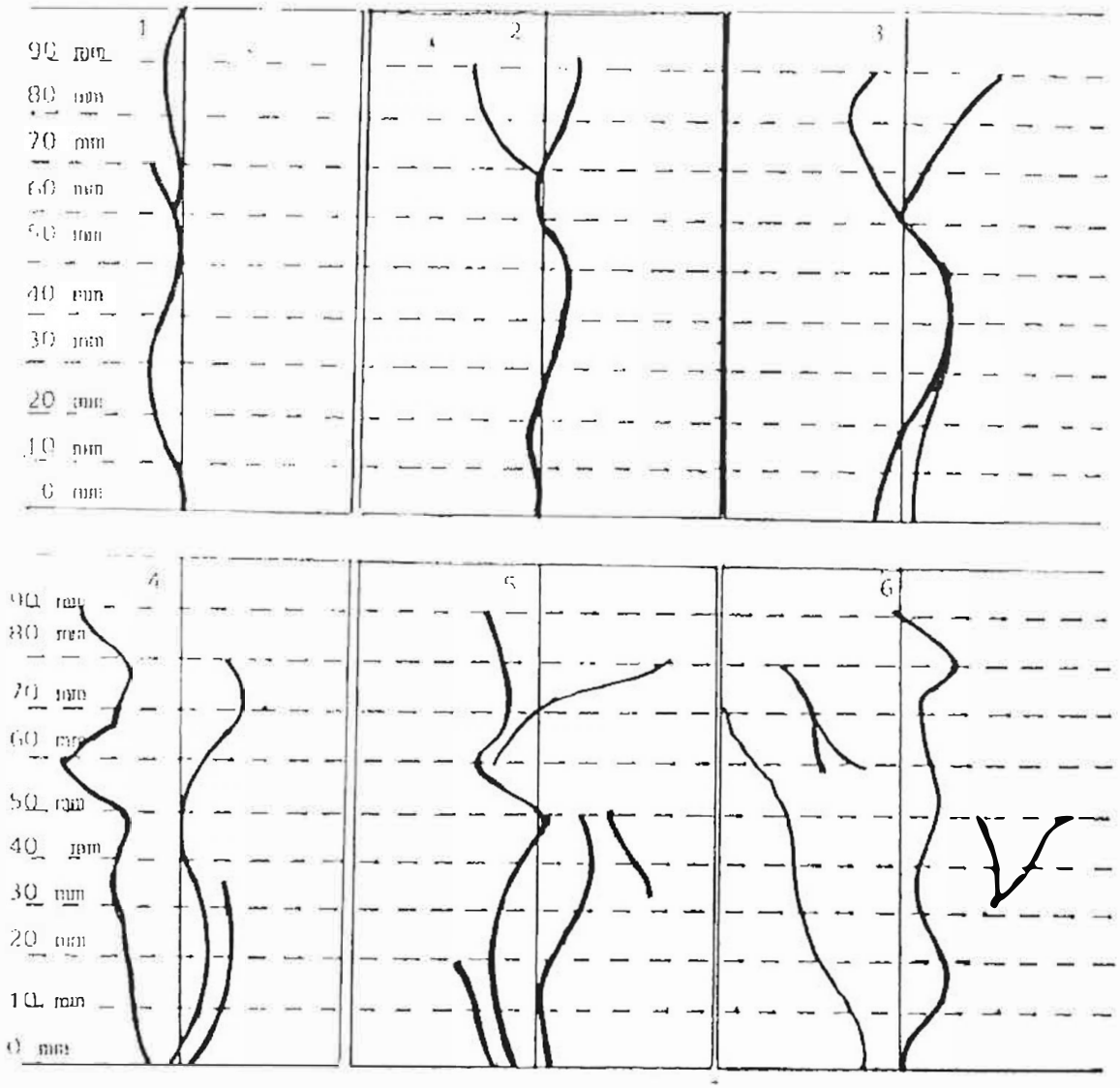

Fig 4.1: The vertical colour map trace for the fault surface in set 2.

1. The use of a ruler for depth measurements did not ensure that each exposed surface was uniformly levelled.

2. The 10mm intervals between newly exposed layers were still too large.

3. The maps of the fault surface trail through vertical colour markers were less complicated than in set 2 (see Fig 4.2).

Fig 4.2 shows the maps of the vertical colour marker offsets after the shearing of the experimental box and its contents.

SET 4

Set 4 was obtained in the same manner of processing and examining as set 3. Two of the 10mm intervals were each halved to increase the resolution of the fault morphology. Intermediate intervals were established with difficulty since the 5mm intervals were estimated using a ruler. Surfaces 5mm and 25mm above the bottom or the zero surface were created and observed as extra surfaces. The inclusion of these surfaces in observations showed that the fault surface trail through the colour markers had corrugations that might be missed if only the 10mm intervals were observed between freshly exposed layers. Whereas previous sets of experiments were achieved by a rapid shear (the time taken in shearing process was not at this stage considered to be of any significance), shearing in set 4 was carried out slowly; a shear displacement of 25mm was completed in 30 seconds. This gentle, slow shear process resulted in a simpler fault surface in set 4. Fig 4.3 shows the maps of the colour marker trail traces of the set 4.

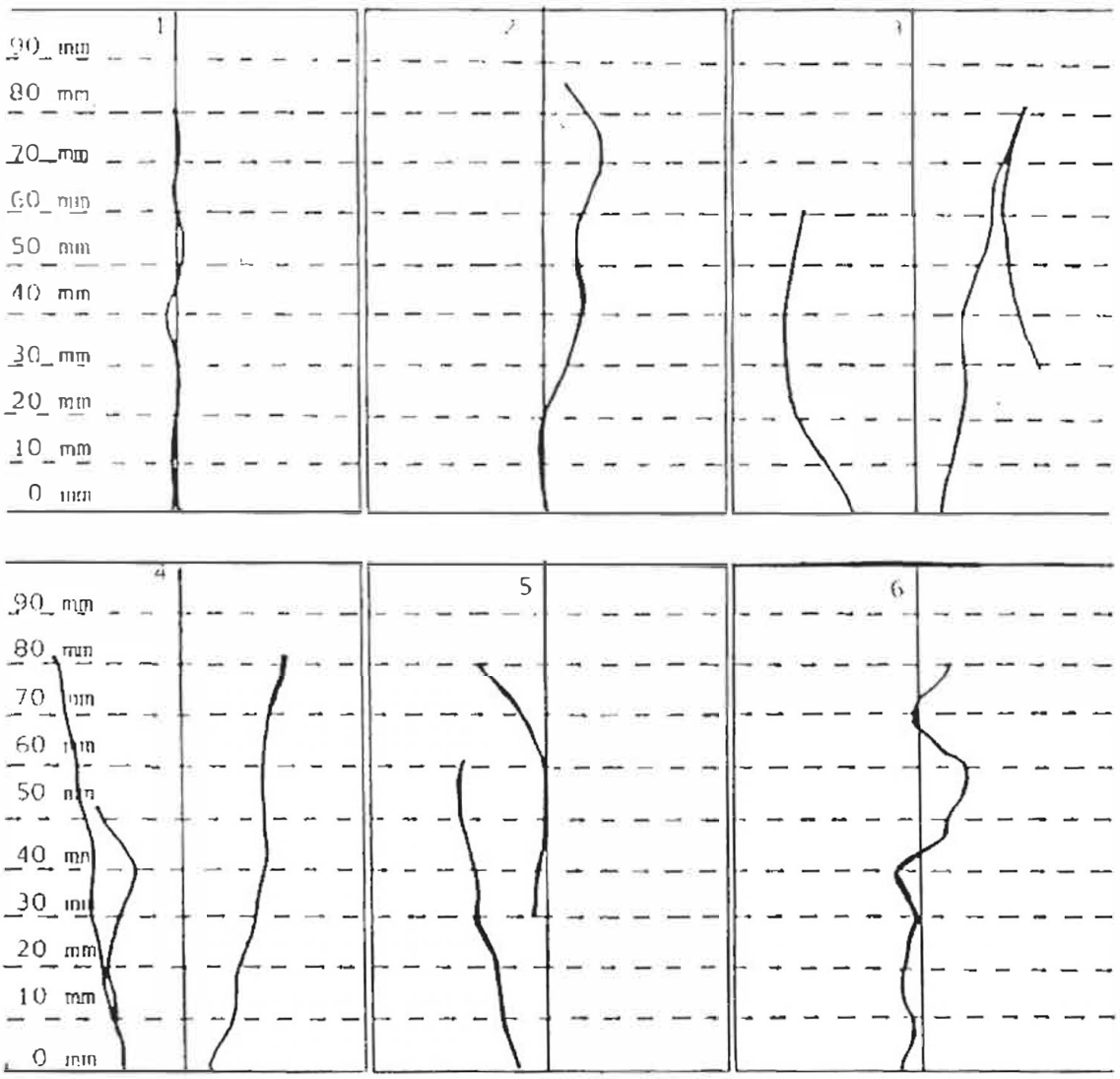

Fig 4.2: The vertical colour map trace for the fault surface in set 3.

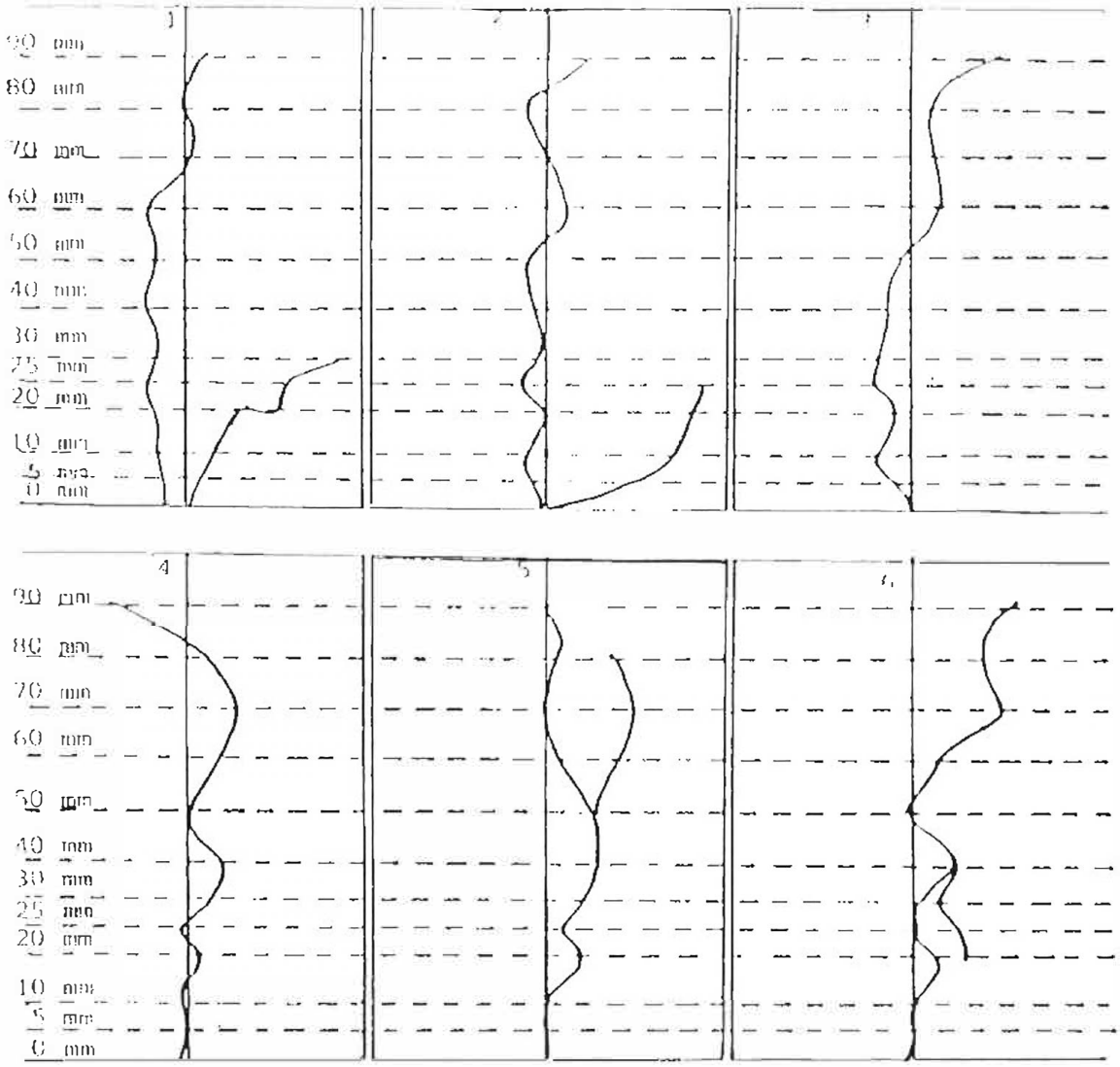

Fig 4.3: The vertical colour map trace for the fault surface in set 4.

Considering the bottom of the experimental box to be the zero height as indicated in Fig 3.1 and Fig 3.2 (where the experimental box was placed on the coordinate system, as mentioned under section 3.2.1) along the Z-axis of the coordinate system, the zero height of the XY-plane was examined as well as the 5mm height, and 25mm height as the extra surfaces in the examination processes. The following observations and conclusions were arrived at from set 3 and set 4:

1. Although a plain masonite hardboard was useful in scraping away the sand levels, a uniform, level, horizontal surface was difficult to achieve evenly everywhere in the experimental box; a more accurate scraping device was clearly needed. The scraper board described in Section 3.2.3 was then made and used in scraping sand layers away for set 6 and the subsequent sets.

2. The rate of the displacement during the shear was reduced to ensure that the fault surface was not too complicated.

SET 5.

Set 5 was carried out under similar conditions as set 3 and set 4, except that it was sheared more rapidly to confirm that the complication noted in set 2 was due to the rapidity of the shearing process. Similar freshly exposed XY-plane surfaces (as shown in Figs 4.7 to 4.10), at different depths were examined. Fig 4.4 shows the maps of colour marker offset positions in set 5. However the maps were too complicated to be analysed. Indeed the complication led to the conclusion that the complexity of the fault surface maps through colour markers depends on the velocity with which the shearing process is carried out.

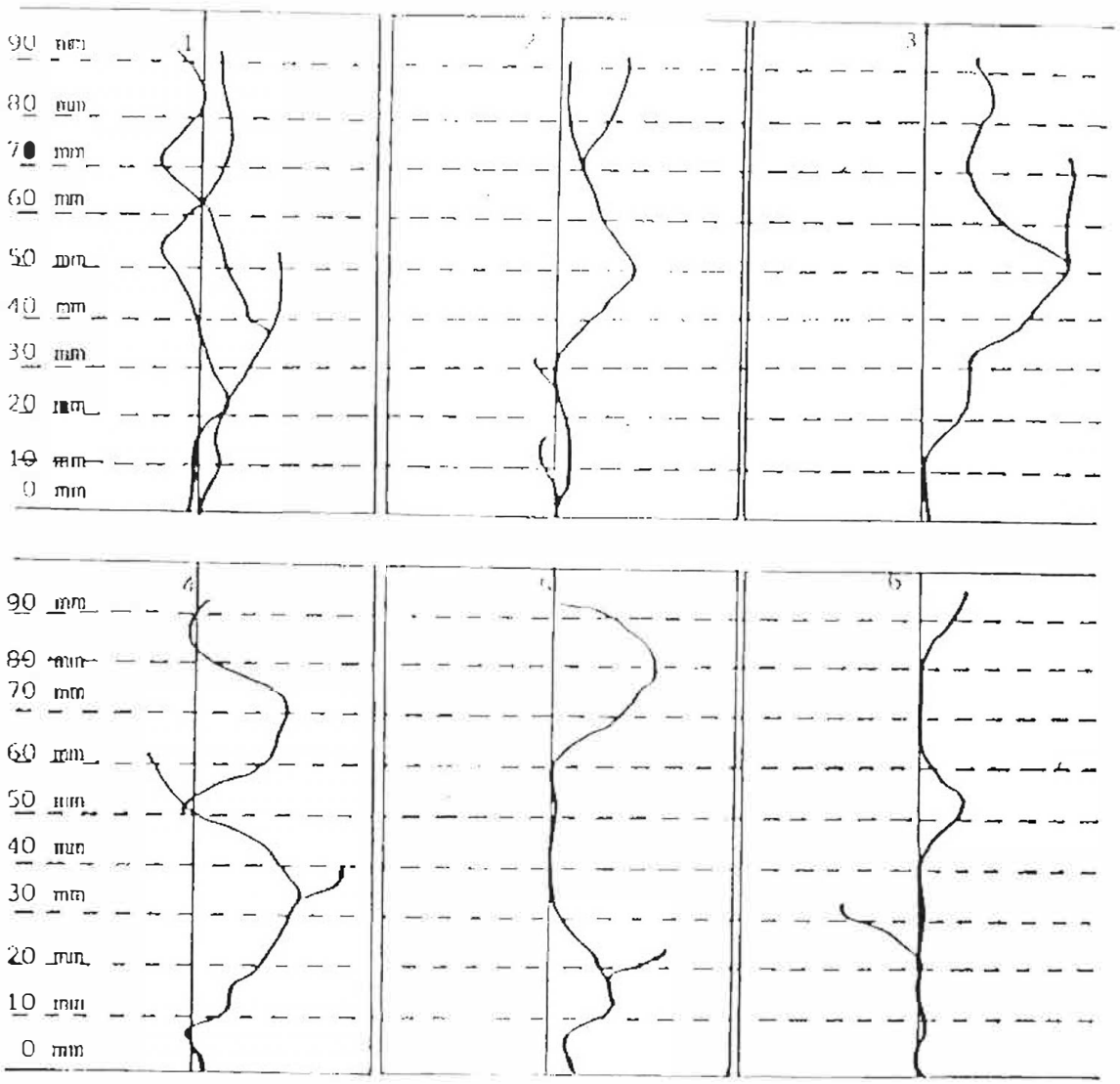

Fig 4.4: The vertical colour map trace for the fault surface in set 5.

SET 6.

Scraping away of the sand layers in set 6 was carried out with the scraper board as described in section 3.2.3; and at depth intervals of 10mm.

The experimental box was filled with the sand which was then compacted by being pressed down with a heavy piece of wood. The compacting was done in each compartment, provided by the divisions of the colour marker boards, individually, to the maximum density of the sand in each case, taking care not to disturb the final positions of the marker hardboards. The scraper board was calibrated in intervals of 10mm. In this experiment the right half of the experimental box was inadvertently moved 8mm in the Y-direction while shear was occurring in the X-direction. The results of this deviation was that the positions of the vertical colour marker offsets shifted to the left of the center line. The six maps of set 6 are shown in Fig 4.5. These maps show that the deviation led to a great complexity in the maps. It was then concluded that:

1. Compacted sand was more representative than the uncompacted sand as a model non-crystalline solid.

2. A scraper board was suitable if marked at 5mm intervals. The scraper board used in set 7, was therefore provided with 5mm divisions.

3. It was decided to use eight (rather than six) colour marker lamellae, spaced at intervals of 30mm, so that the fault surface could be examined in greater detail.

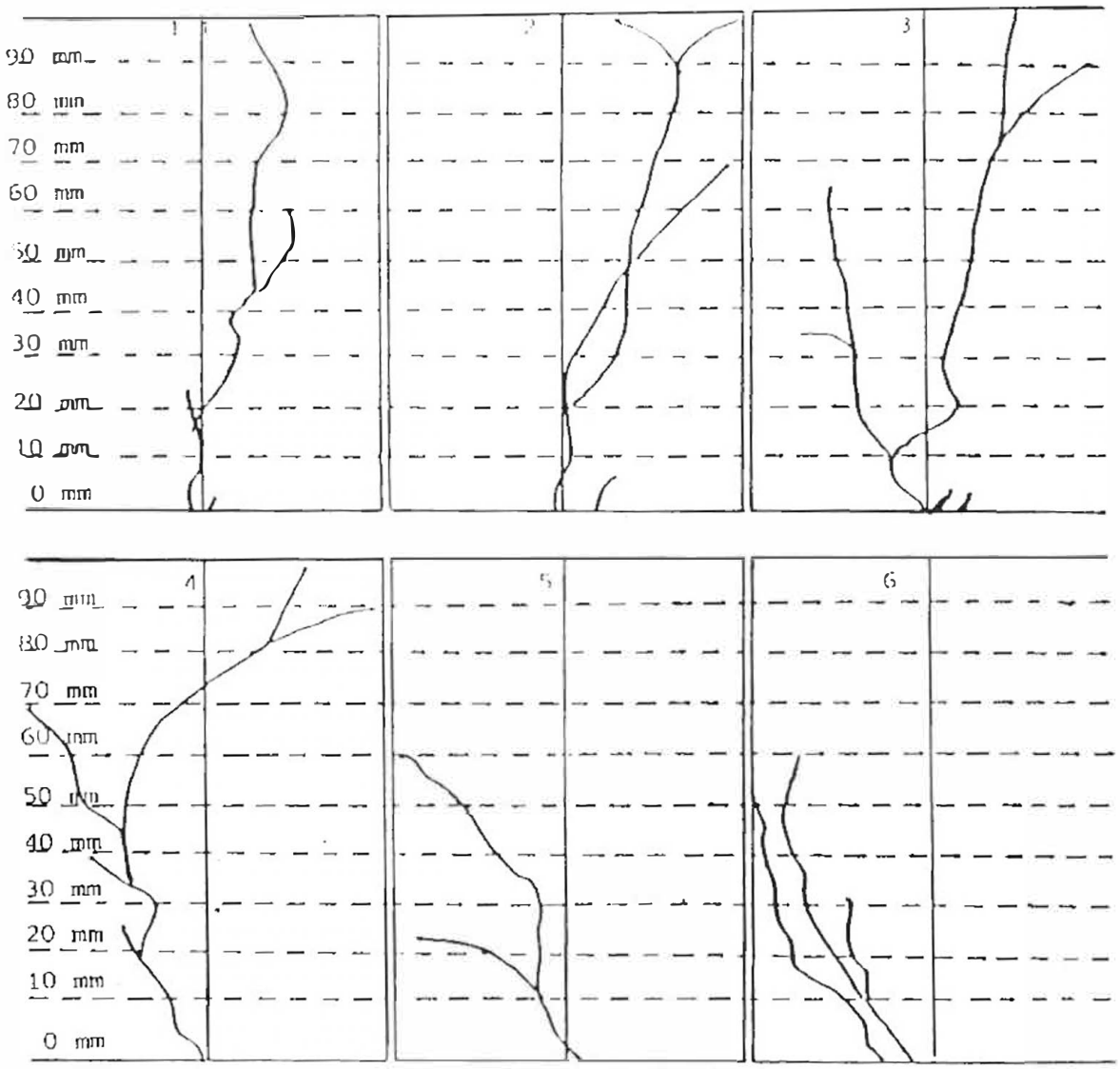

Fig 4.5: The vertical colour map trace for the fault surface in set 6.

SET 7.

The experimental box was prepared with eight hard boards in place, spaced 30mm apart. The sand was poured into the box and was compacted as previously. Distemper colour mixture was prepared to fill the clefts left after the hard boards had been removed. Since it was now known that slow shearing process would yield a less complicated set of fault surface maps, shear was then carried out very slowly: a shear displacement of 25mm was carried out in 4 seconds. The camera was also used to record every freshly exposed surface, after which a transparency was placed over the sand body, and the positions of the offsets on each colour marker were traced onto the transparency.

After the shearing, a thin layer of loose sand was blown away carefully. The positions of the offsets on the colour markers along the XY-plane of the experimental box at the height of 100mm from the bottom of the experimental box were measured relative to the center line that coincided with the plane bisecting the experimental box along the interface of the two box halves. Fig 4.6 shows the transparency traces of the colour marker offset positions at Z = 100mm, that is, the XY-plane of the sand at the height of 100mm from the bottom of the box. With the aid of the scraper board, adjusted by pegs on both sides, as the adjusting device, as mentioned in section 3.2.3, 5mm thick sand layers were scraped away to expose fresh surfaces, which were then photographed. The offset positions of the colour markers were traced onto the transparencies. This process was repeated at 5mm depth intervals from the 100mm height of the experimental box, down to the zero height at the bottom of the experimental box. Fig 3.2 shows how the experimental box was introduced onto the coordinate system.

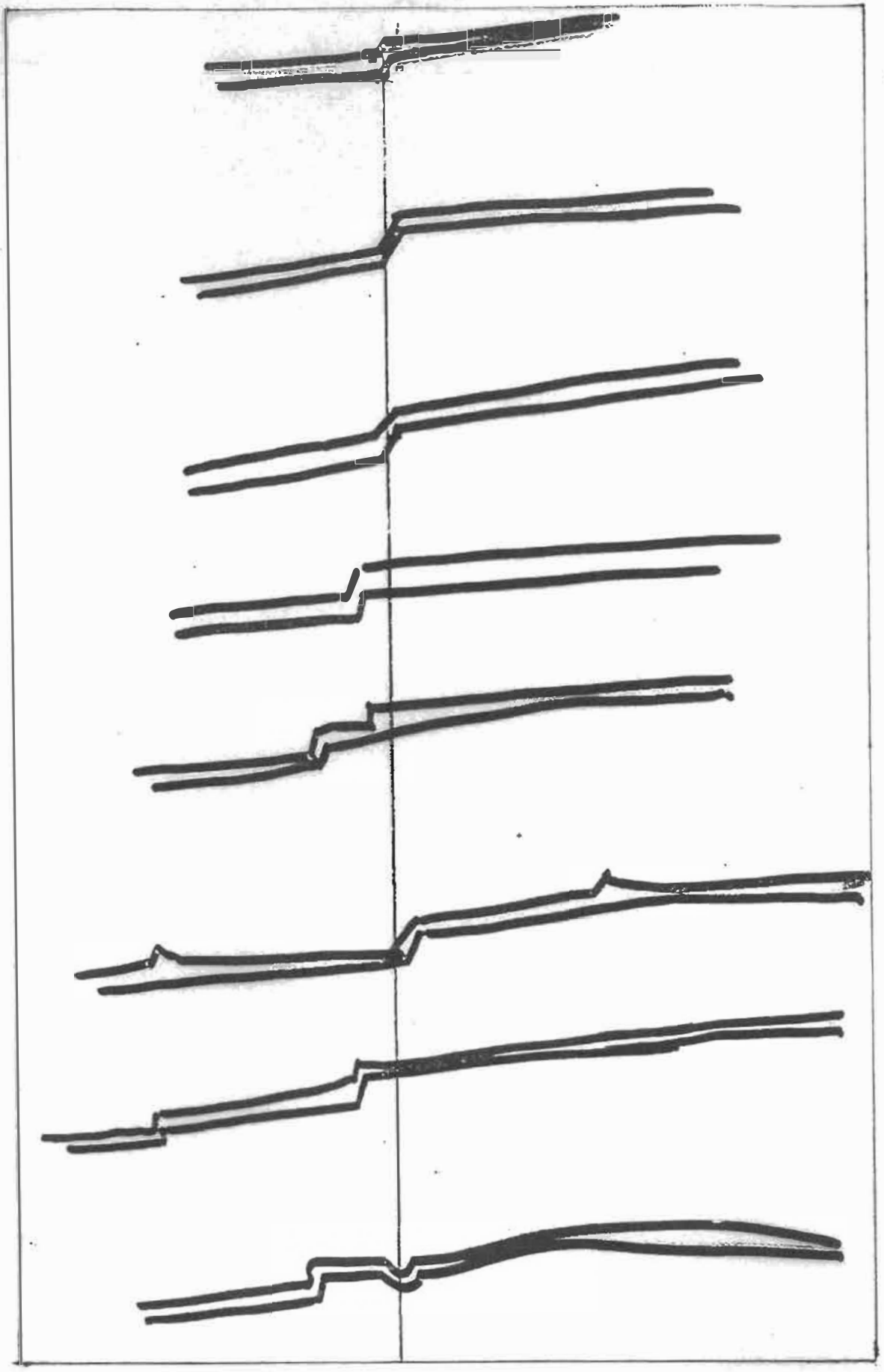

Fig 4.6: Transparency trace of the colour marker offsets at the height of 100mm (top surface).

The photographs were always taken at every freshly exposed surface. Figs 4.7 and 4.8 show photographs of the sand surface and the positions of colour markers and their offsets at the height of 40mm and 45mm for the experimental set 7.

SET 8.

SET 8 was carried in the same way as set 7 in order to verify if the results of set 7 were qualitatively reproducible. The results on transparencies and photographs prove indeed to be similar (although not precisely the same). For the sake of comparison, Figs 4.7 and 4.8 of the set 7, and Figs 4.9 and 4.10 of set 8 are shown. These results are so similar that either set could be used for measurement. It was decided to use set 7. The coordinate system applied in set 7 was used to describe the shear process. Fig 4.11 shows the experimental box with the positions of the hardboards before the shear; while Fig 4.12 shows the experimental box having been sheared, or left laterally slipped according to geological naming, showing the colour marker positions as having been shifted, while Fig 4.13 is the sheared experimental box on a coordinate system.

4.3 DATA ACCUMULATION (FROM SET 7)

The first transparency was placed on the XY-plane at the height of 100mm along the Z-axis, that is, on the top surface of the sand body. The straight line along which the central xz shear plane of the box (Fig 4.13) intersects the sand surface was recorded on the transparency, as were the positions of the colour marker planes and their offsets. Such a record is shown in Fig 4.6 where the clear positions of the offsets along the distemper

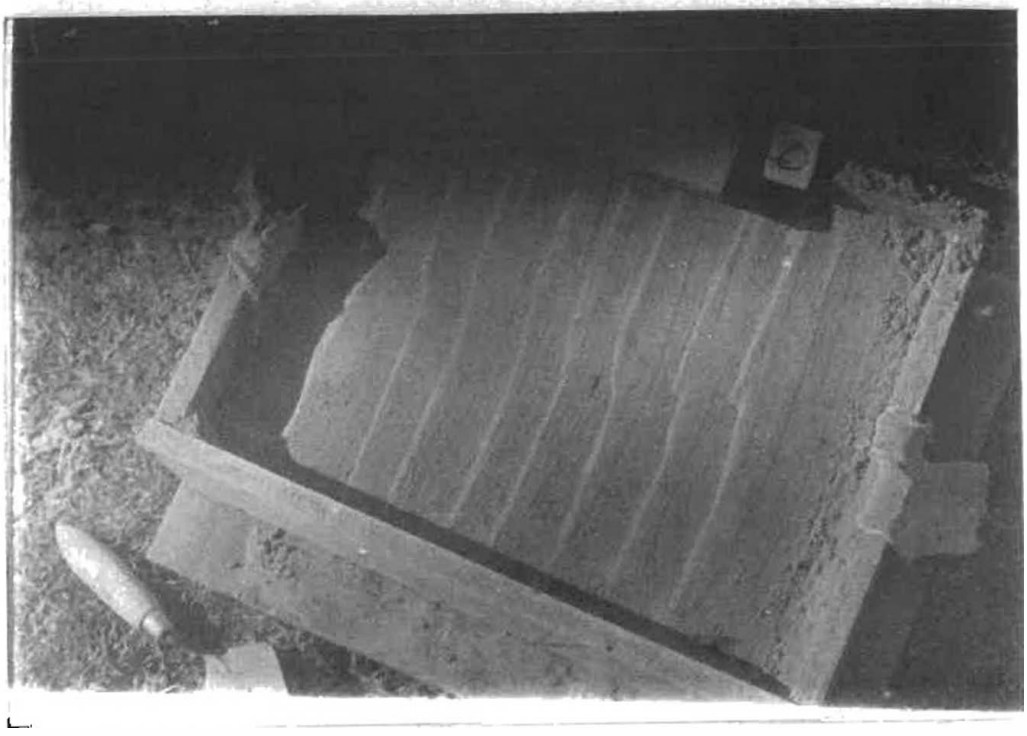

Fig. 4.7 Freshly exposed XY-surface at 40 mm along Z-axis in Set 7.

Fig. 4.8 The Surface at 45 mm along Z-axis in Set 7.

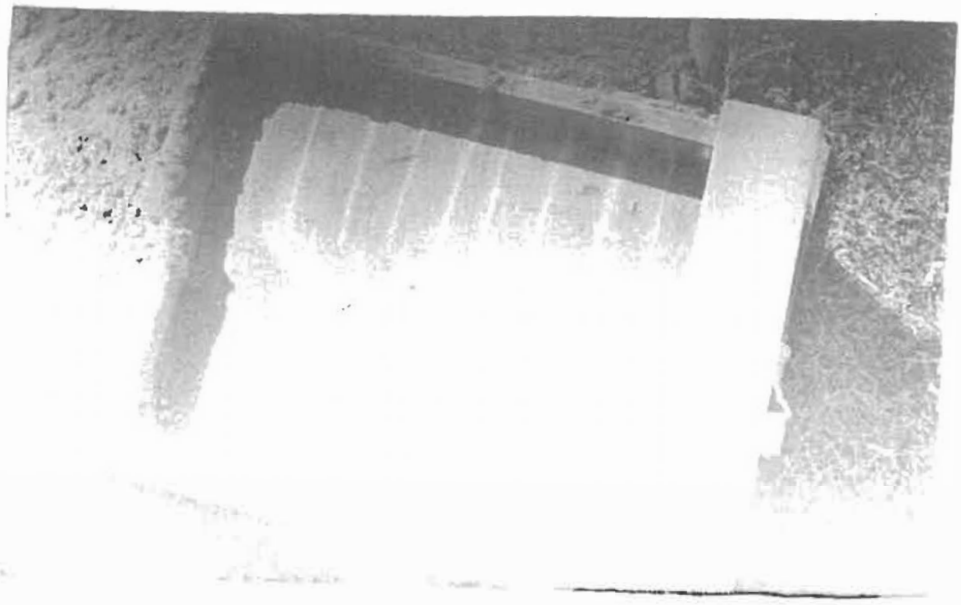

Fig. 49 Freshly exposed XY-surface at 55 mm along Z-axis in Set 8.

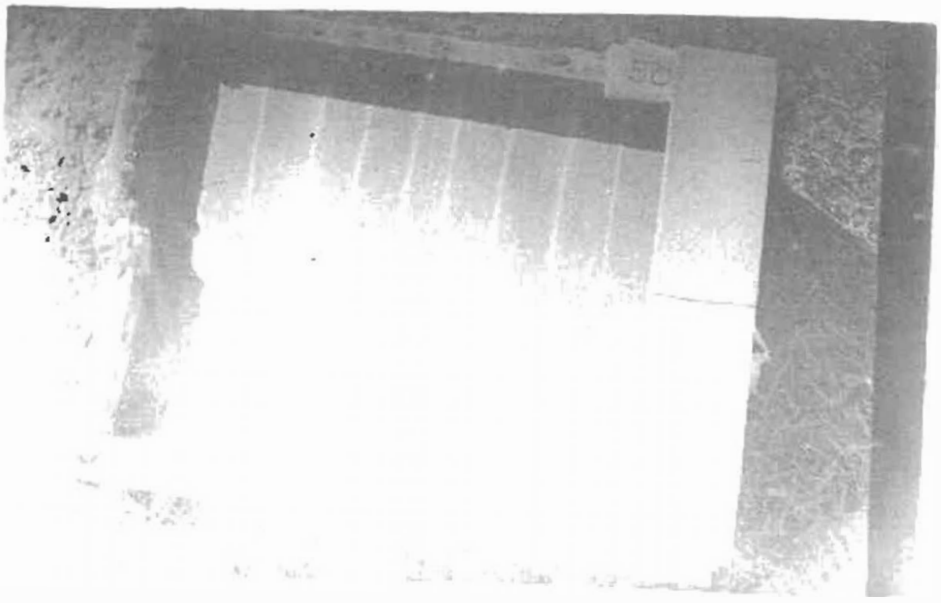

Fig. 4 .10 The Surface at 50 mm along Z-axis in Set 8 .

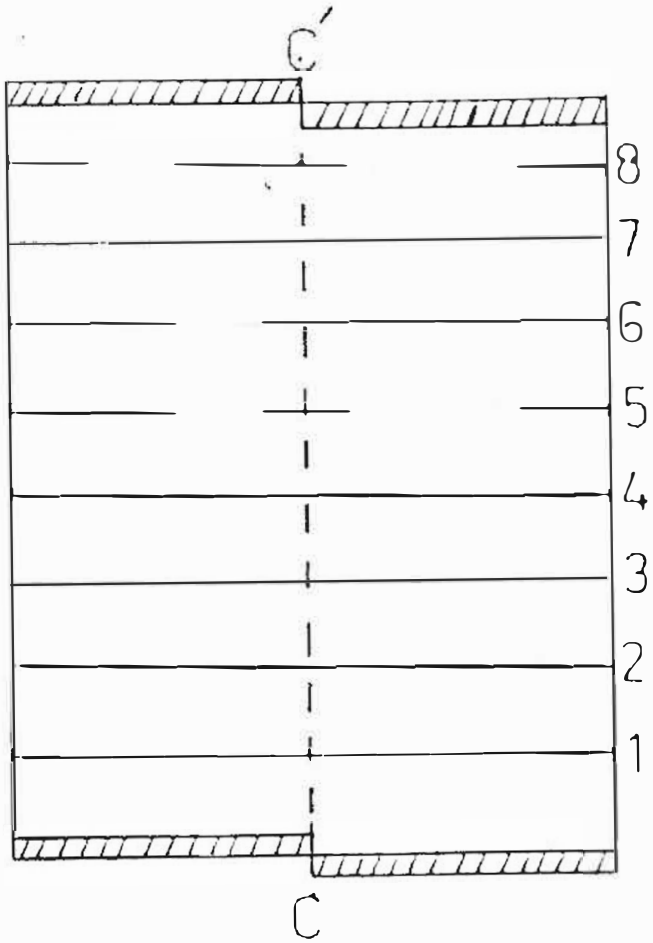

Fig. 4.11 The Experimental Box before Shear. The Numbers denote the Hardboards at the positions of the Colour Markers.

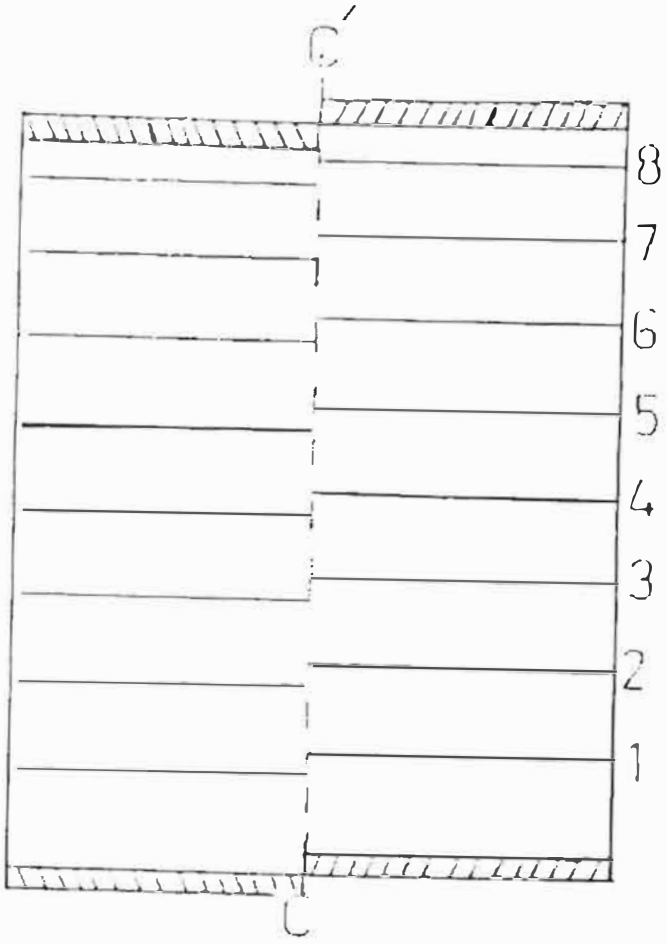

Fig 4.12: The experimental box after shear. Colour markers were expected to shift as shown due to the shear.

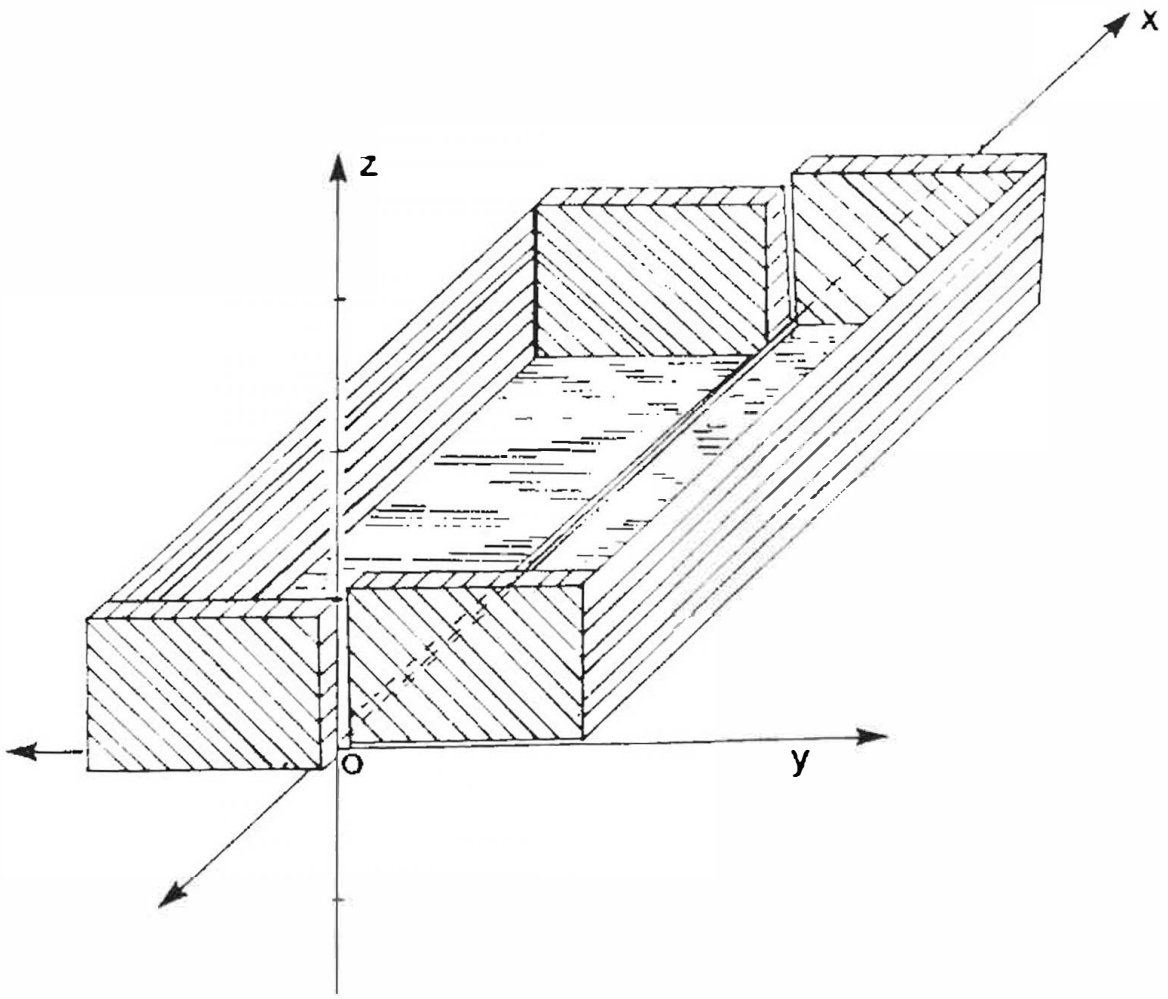

Fig. 4.13 Sheared Experimental Box showing the Coordinate System used to describe the location of Points where displacements occurred.

colour markers across the XY- plane at 110mm along the Z-axis can be seen.

The colour markers were numbered from 1 to 8 as shown in Fig 4.11. The positions of the markers were: 1: x = 35mm; 2: x = 85mm; 3: x = 110mm; 4: x = 160mm; 5: x = 190mm; 6: x = 220mm; 7: x = 260mm; 8: x = 300mm. Each colour marker lay in the YZ-plane across the experimental box, extending from y = -150mm to y = 150mm, while extending over the range 0mm to 100mm along the Z-axis. With the offsets traced onto the transparencies, the XY-plane surface of the sheared sand was also photographed.

With the aid of the scraper board (Fig 3.5), controlled by the pegs both sides to set the desired depth, a 5mm thick layer of the sand was scraped away to expose a fresh surface of the XY-plane at the height of 95mm. Again a transparency was placed on this surface, center line drawn, and markers drawn onto the transparency, as well as the photo taken.

Further 5mm sand layers were scraped away, exposing more fresh surfaces from which the transparency records were taken, and the surfaces were photographed. The scraping away and the recording were repeated to obtain a series of observations, continuing to the bottom of the experimental box.

The transparencies showed that the markers had offsets at different positions and different heights of the sand body; measurements were taken from each offset along a marker, to the center line from all transparencies at all levels of height for the range -35mm to 35mm along the Y-axis. These measurements of offset displacements, supplied the data which was collected in Table 4.1.

Z-coordinate	Y-coordinates, sometimes more than one value for their corresponding X and Z values as indicated.							
	(x = 35mm)	(x = 85mm)	(x = 110mm)	(x = 160mm)	(x = 190mm)	(x = 220mm)	(x = 260mm)	(x = 300mm)
(mm)	(mm)	(mm)	(mm)	(mm)	(mm)	(mm)	(mm)	(mm)
0	0	0;8	0;2	-3	0	0	1	0
5	1	0;14	-4;5	-1	0	0	5	0
10	0	1	0;5	-4	-3	1	2	0
15	3;9;15;23	4	2;6	0	5	4;10	6;13	0;10
20	2;12	8	8;18	0	3	0;12	2	-2
25	2;13	7	7;15	1	4	1	3	1
30	3;16	7	8;18	2	6	4	7	3;7
35	4;16	7	6;21	0;18	4	0	2	0
40	2;15	5	2;19	0;16	5	0;10	3	0
45	0;13	5	3;11	5	10	2	6	6
50	0	9	6;20	10	14	4	1;10	10
55	0	6	3;16	8	18	1	1	10
60	0	10	0;17	5	0;25	-2	0	-3;0;3
65	0	4	-2;23	21	34	-1	-1	5
70	-2	7	-1;18	28	1	-5	-2	6
75	1	12	0;23	-3	2	-6	0	5
80	0	5;18	0;29	0	8	-5	0	7
85	2	6;25	-3;30	2	11	0	5	6;11
90	-1	8	-7;25	-3	14	-5	-2	4
95	-6	4	-4;95	-7	6	-3	-4	-3
100	-25	0	0	-10	-14	3	-8	-18

Table 4.1 The Offset Points positions accumulated after shearing the Set 7. This Data was used to plot the Fault Surface Path through the eight vertical maps in the set.

The column labelled Z-coordinate in Table 4.1, gives the Z-value (that is, the height from the bottom of the experimental box). Each value along the Z-axis denotes a level of a freshly exposed sand surface. Each column on the right, from the second to the ninth, denotes the X-coordinate of the colour marker. The numbers in the columns (2nd to 9th), are the points along the Y-axis, in the range -35mm to 35mm where the offsets occurred on a colour marker at the same level. For example, at a height of 15mm, the colour marker that was at x = 35mm along X-axis had offsets at 3mm, 9mm, 15mm and 23mm to the positive of Y-axis.

The data in Table 4.1 was plotted in YZ-planes to trace the shape of the fault surface in the sand from the top to the bottom, from the offsets on each marker. Fig 4.14 shows the plot of the offsets in the colour marker lamella that was situated at x = 35mm on the X-axis, according to the data in Table 4.1. Each colour marker lamella could then be mapped in the same way as that shown in Fig 4.14 and the plotted points could be joined as in Fig 4.15 to further trace the path (or trail) of the glide surface across the sand. Four other maps made from the plots of different colour marker lamellae positions appear in Fig 4.16 below.

While Fig 4.16 shows the individual maps of the offsets from the colour markers, Fig 4.17 is a 3-dimensional drawing of the maps in the order x = 35mm; x = 85mm; x = 110mm; x = 160mm; x = 190mm and x = 220mm. This figure shows how the fault surface is corrugated and bifurcated; indeed, this fault surface, unlike glide surfaces in crystals, is not planar at all. An enlarged version of Fig 4.17 could aid in clarifying the description of the fault surface in more detail. In Figure 4.18, three offset maps are shown

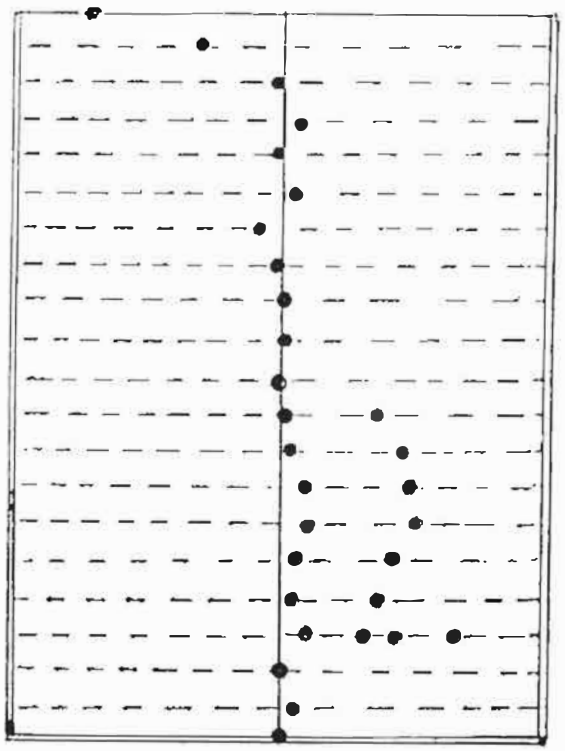

Fig 4.14: Plot of the offsets on the colour marker at x = 35mm.

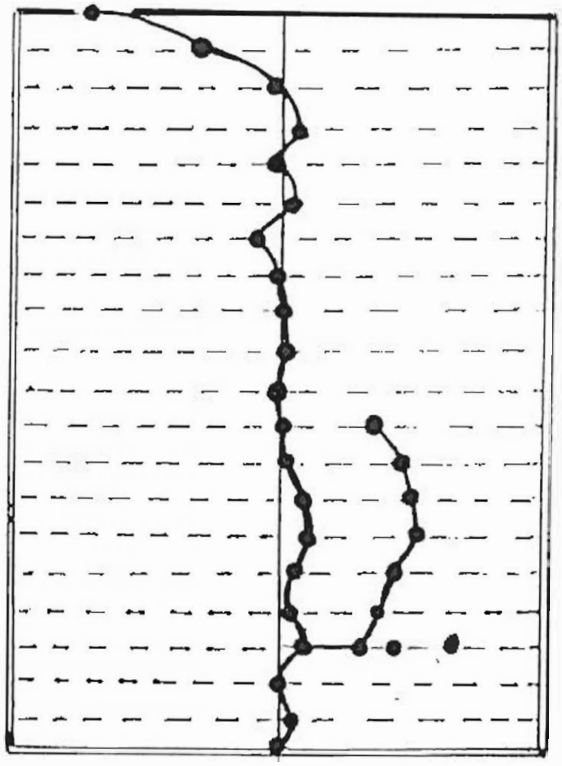

Fig 4.15: Mapping the offset points, indicating a possible path of the fault surface after shear.

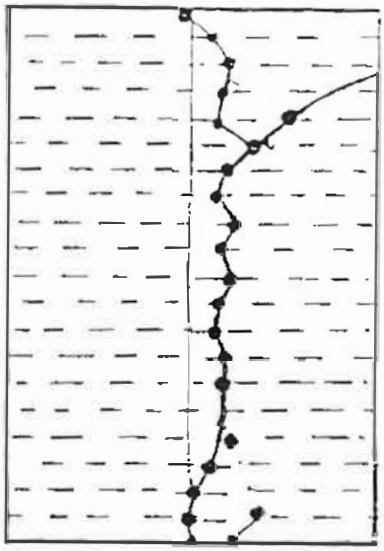

x = 85mm

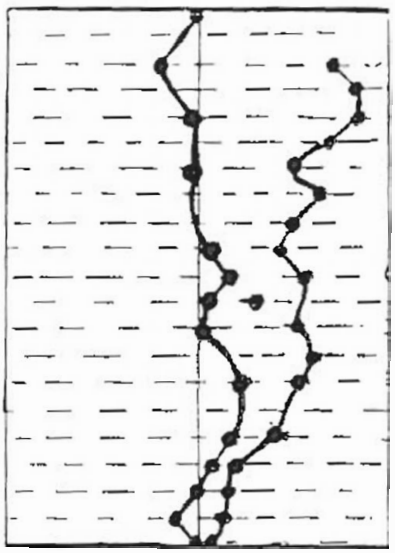

x = 110mm

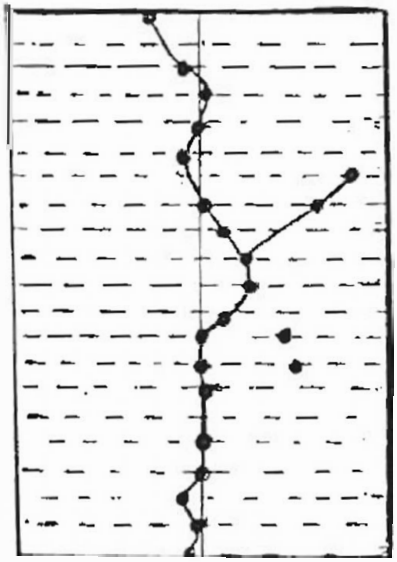

x = 160mm

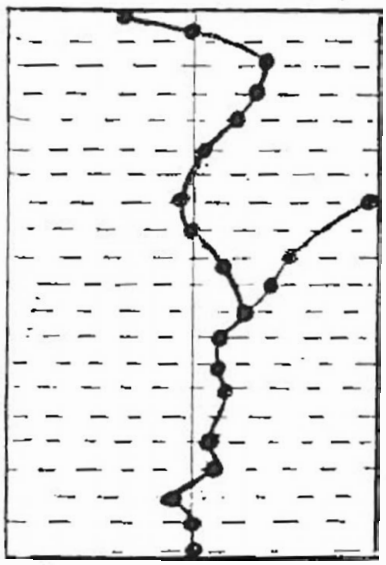

x = 190mm

Fig 4.16: Individual maps of the offsets points from the indicated colour markers.

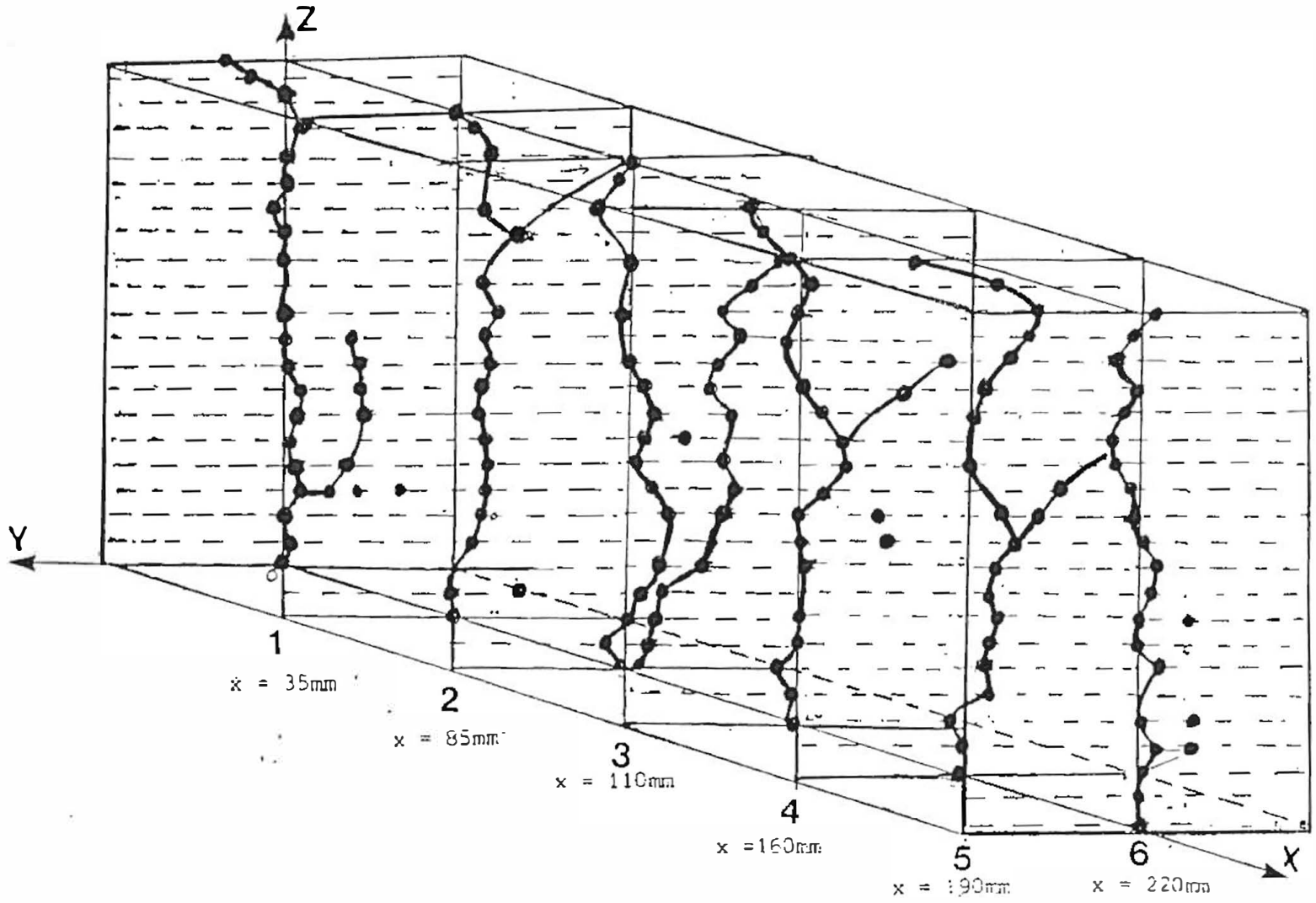

Fig 4.17: Six of the eight colour marker offset maps shown in perspective.

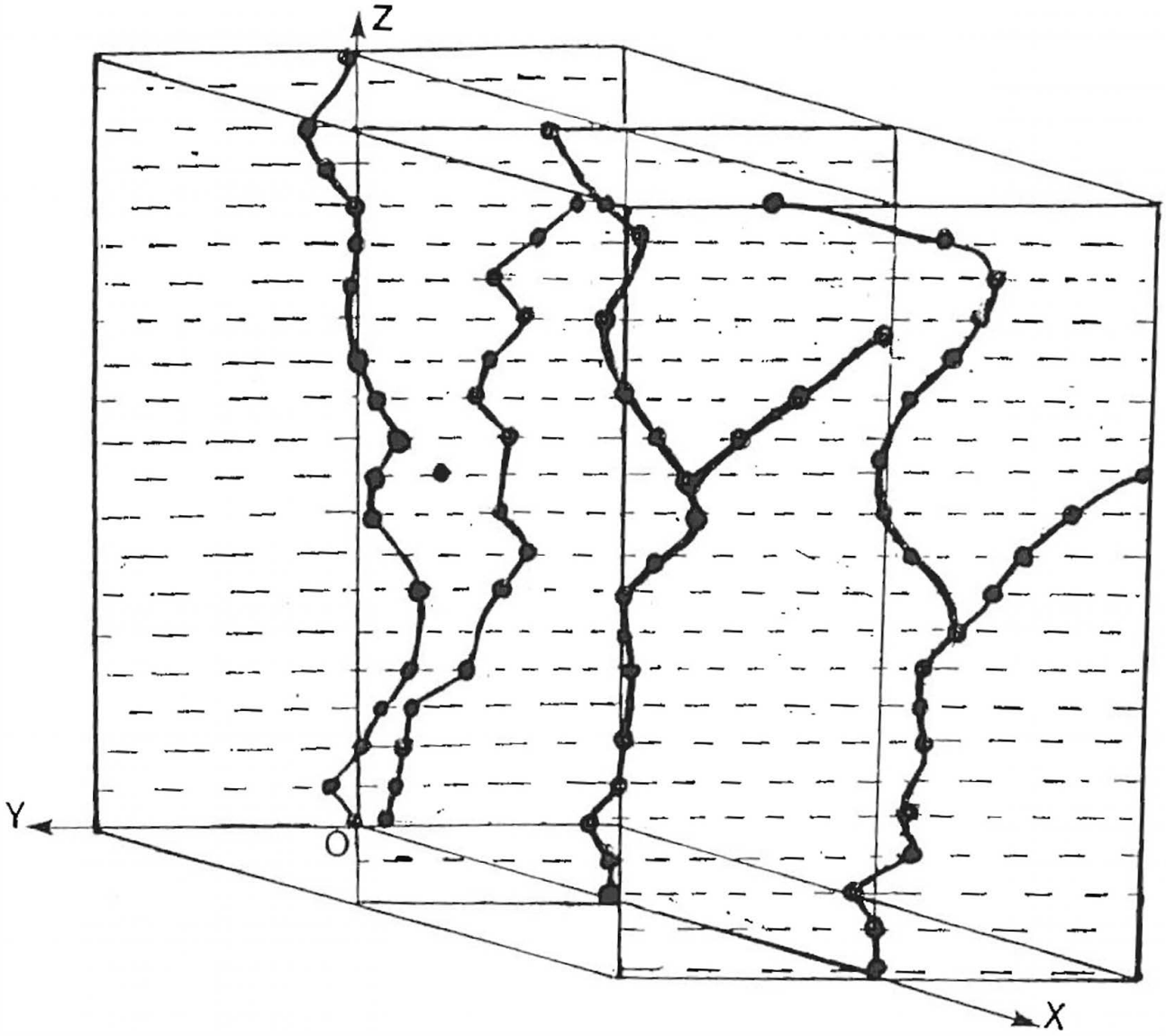

Fig 4.18: Three of the eight colour marker offset maps on a larger scale.

on a larger scale. The fault surface between colour marker lamellae maps at x = 160mm and x = 190mm was a single surface from the bottom of the sand at z = 0mm up to z = 45mm; then, the glide surface began to divide, branching to right and to the left. Both branches were located on one and the same side of the central plane, y = 0mm, which coincides with the center line.

Fig 4.19 shows how the figure further divided into two distinct surfaces at some height from the bottom of the sand; one surface is a small, branching surface. Such a surface, branching from the main surface is termed a splay in geological terminology.

When the individual maps, assembled from the offset points, were examined, it was observed that although the majority of the offset points fell on the predicted path of the fault surface, there were some extra points that did not lie on the lines tracing out this fault surface. This occurred when there was more than one offset point in one colour marker at a given level, as for example at the points (x,y,z) = (220,10,15) and (x,y,z) = (35,15,15). This either implied more than one path of the fault surface or shorter fault segments that resembled en-echelon faults. The presence of more than one offset along the same colour marker could also indicate that either there were more than one glide surface in the sheared sample, or that the offsets were associated with smaller fault surfaces (splays) branching from the main fault surface, being the en-echelon faults.

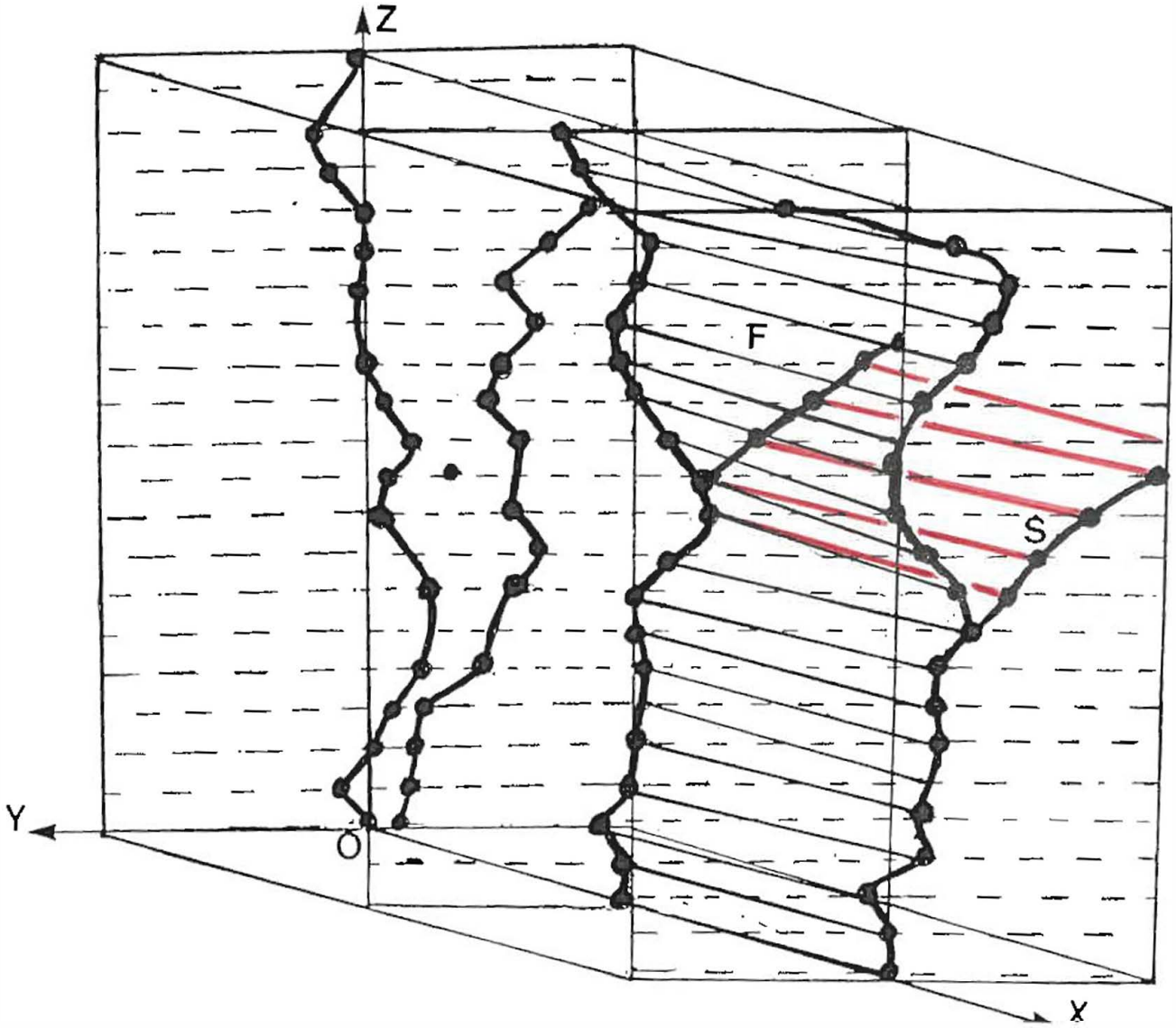

Fig 4.19: A splay S, (coloured red), branching from the main fault surface F, bifurcating it.

4.4 MODELS.

In order to be able to observe the glide or the fault surface from the sheared sand sample discussed above, it is helpful to build a three dimensional model of such a fault surface, using the data tabulated in Table 4.1. Such a model has the advantage that, unlike Figs 4.17 to 4.19, it can easily be examined from all angles. Models could be constructed from:

1. A transparent material, made of perspex, through which one can examine the inside of the structure, and

2. A computer model resident in the computer memory, which could be called up as required.

The models are described below:

4.4.1 The Perspex Model.

The vertical marker maps obtained from the plots in section 4.3, were enlarged on the photocopier to A4 size, so enlarging each map by a factor of 2.4. Such enlargements are shown on Fig 4.20 (for enlarged map of colour lamella x = 160mm) and on Fig 4.21 (for enlarged x = 190mm).

Perspex, being transparent and rigid, was found to be a suitable material to use for constructing a model for demonstrating the morphology of the glide surface generated by shear in the sand. A material like glass,

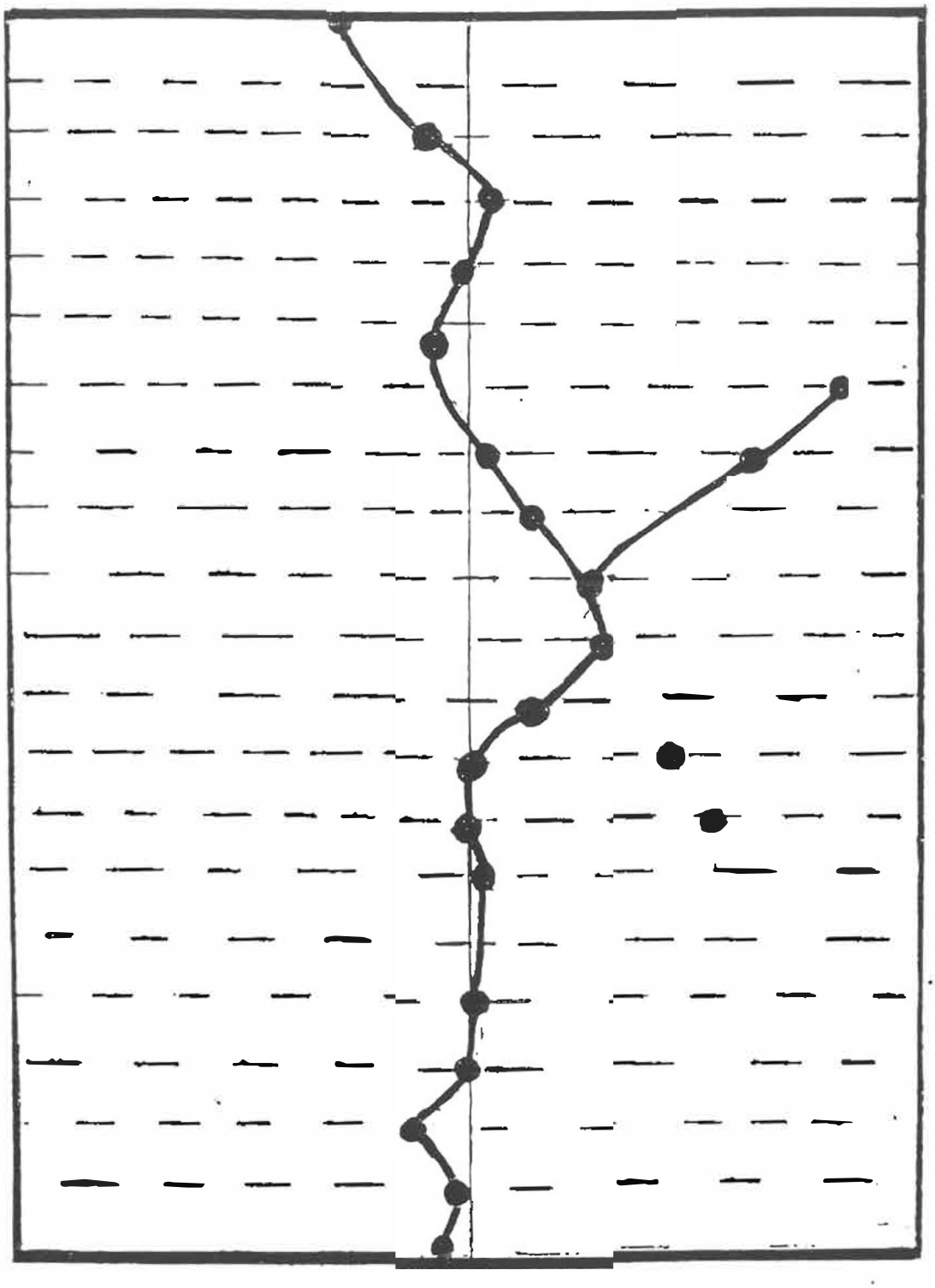

Fig 4.20: Colour marker offset map (x = 160mm), enlarged.

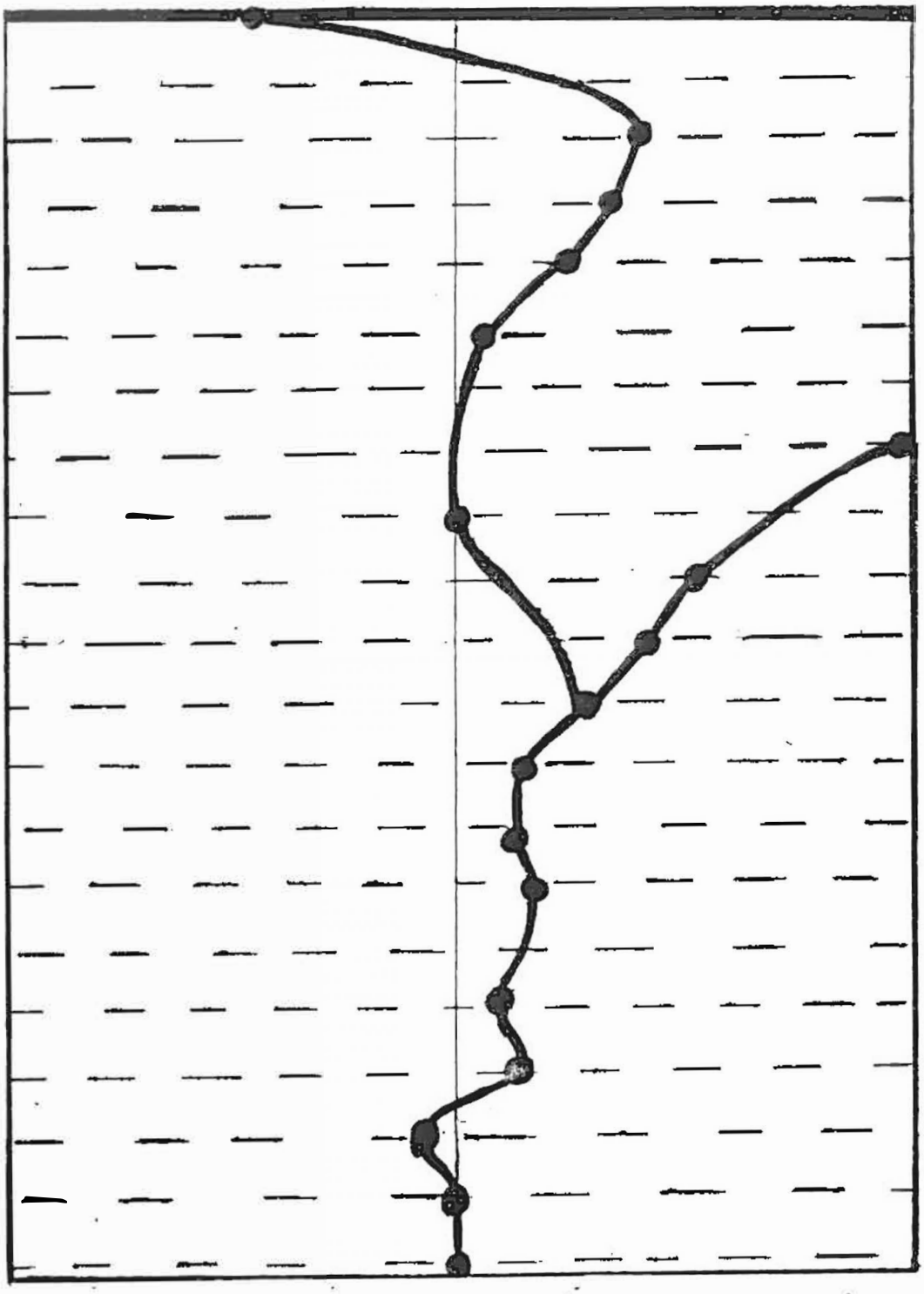

Fig 4.21: Colour marker offset map (x = 190), enlarged.

although transparent, would be too heavy and easily broken. Moreover, perspex is less expensive and has the essential advantage that holes are easily drilled through it. Eight 4mm perspex sheets were cut to A4 size, and each of the eight enlarged map sheets was used as a template to drill 4mm holes through a perspex sheet at the plotted positions of the offset points.The perforated perspex sheets were then placed at intervals of 200mm, along the the X-axis, in their original order, parallel to one another, in YZ-planes. A rigid structure was then made from these sheets by using 6mm diameter wire to support the structure.

Cotton threads were passed through the drilled holes on the corresponding horizontal level, from the first to the eighth perspex slab. On each level cotton was threaded through corresponding holes of each perspex sheet; where more than one hole on the same level of height, on the same perspex sheet existed, the cotton was made to branch into as many branches as the number of holes at that level. Threading the path of the fault surface on the top level, that is, the sand top surface, was carried out as follows: With the aid of transparency Fig 4.6, which traces the colour marker displacements at the surface of the sand, that is at Z = 100mm, the offset points, where there have been displacements due to the shear, were plotted (Fig 4.22). These offset points indicate all positions where the fault surface intersected the colour marker lamella, and these intersections appear on both sides of the bisecting center line CC'. The following facts were then immediately apparent from this plot of the offset points:

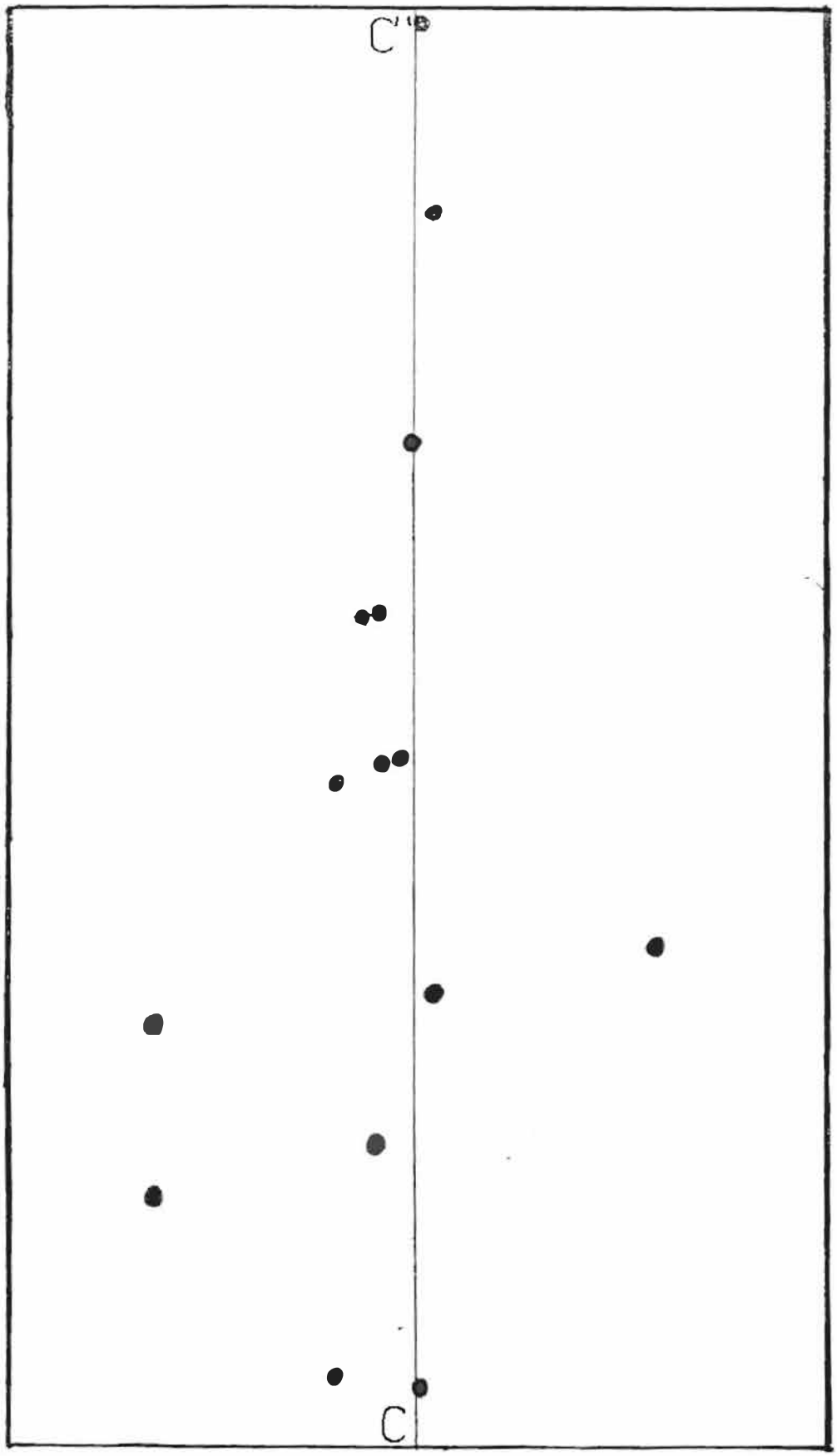

Fig 4.22: Offset points plotted from the transparency Fig 4.6 taken at z = 100mm after shear.

1. Although a single uninterrupted continuous shear was carried out, some disturbances and discontinuities of the fault were noted at several positions. These discontinuities will be referred to as "steps".

2. Although the sample was sheared along the center line CC' of the sand body, the offsets were widely displaced from the centre line, parallel to the distemper lamellae. These displacements from the centre line showed that a shear zone existed on both sides of the centre line. The shear zone was about 35mm wide.

3. Where two or more offsets occurred along the same colour marker lamella, it was possible that there were at least two fault surface segments.

4. Isolated offset points occurring on the colour marker lamellae could indicate short fault surface segments. It was not possible to determine where such segments started or ended, since they only intersected a single lamella.

Figs 4.23 and 4.24 show possible paths of the fault surface for which the threading was done here.

5. One difficulty that was presented by perspex slabs was that because the slabs were rigid, they could not be arranged to fit the shapes of the colour marker lamellae after the shear, and simultaneously support the structure without posing the positional inaccuracies for the offset points.

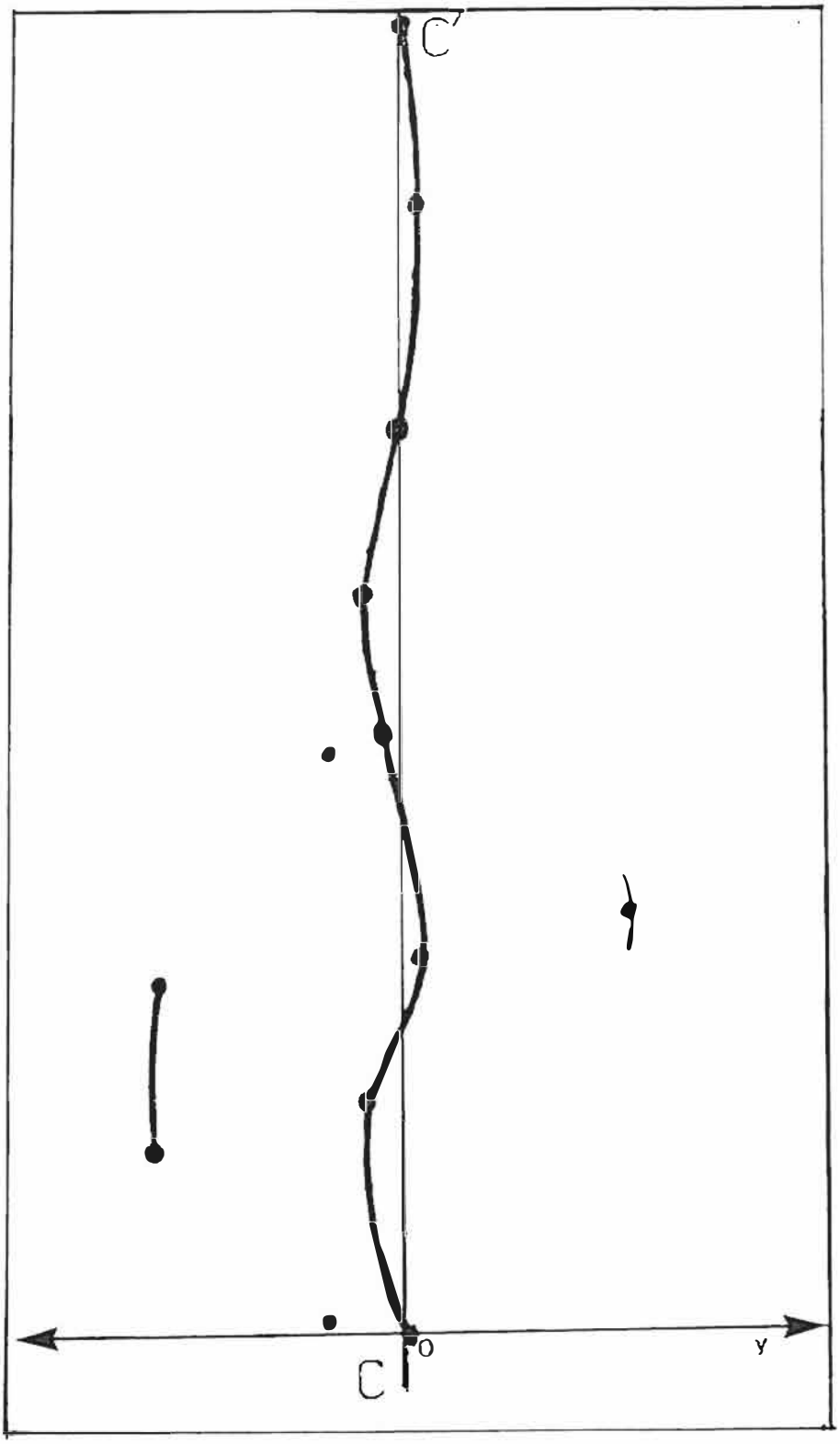

Fig 4.23: One way of linking up offset points plotted in Fig 4.22. The linking shows a possible path of the fault surface along the centre line.

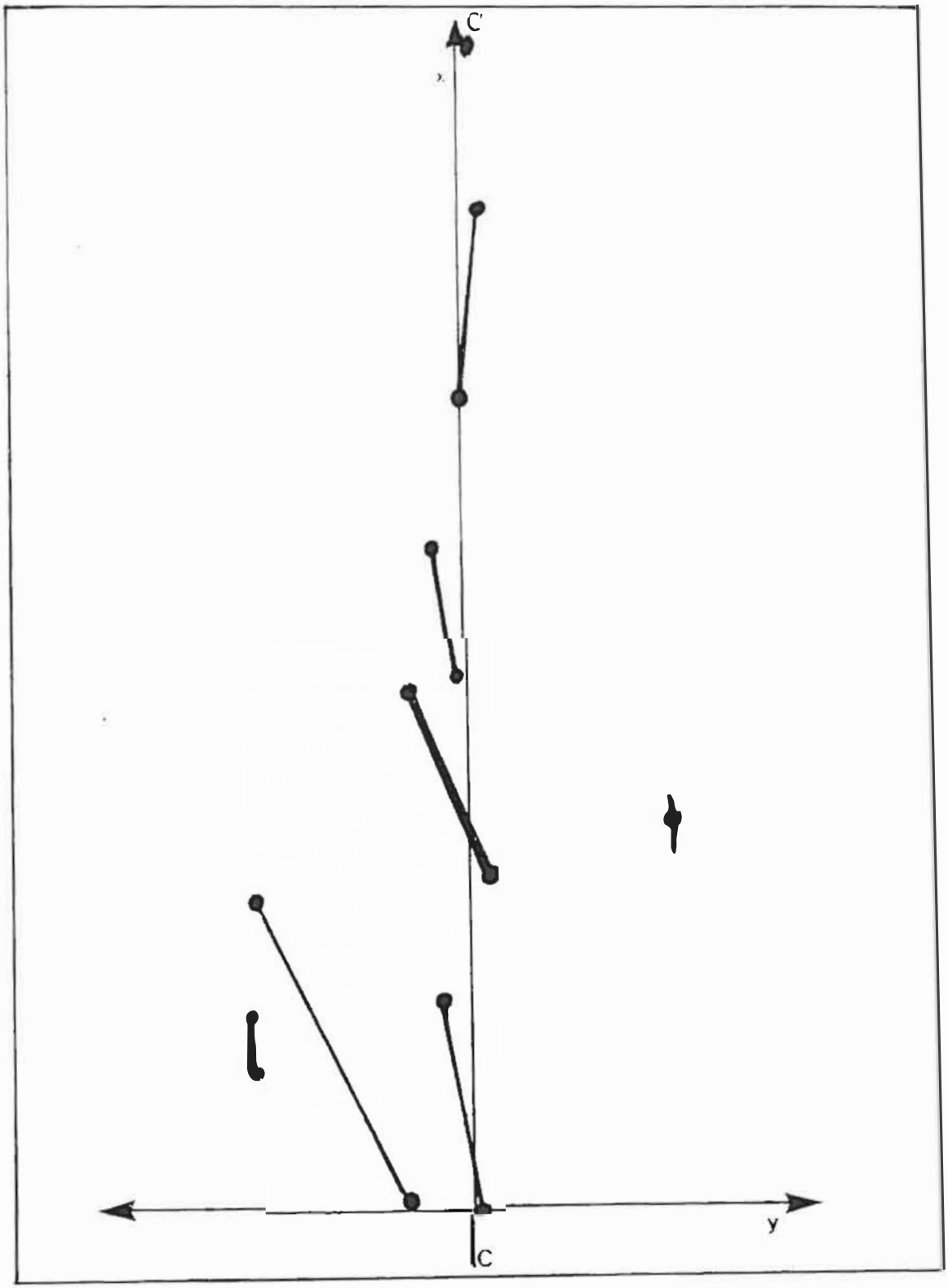

Fig 4.24: Another possible linking of the offset points.

6. Also, the fact that the structure was enlarged by a factor of 2.4 means that errors in mapping the offset points are likewise magnified by this factor.

4.4.2 The Computer Model

The data accumulated from set 7 and tabulated in Table 4.1 was used for the construction of a computer model. This data was programmed into a Personal Computer (P.C.) to plot the three dimensional picture of the fault surface structure, also showing how the fault surface corrugates and bifurcates as it branches away from the plane y = 0mm.

Programs in Basic were devised and several figures were plotted by these programs. Fig 4.25 is a general figure of the faulting in the sand, as derived from the data in set 7, but was, however, too complicated to analyse. This Fig 4.25 was plotted by Program A (attached). Program A was then edited to provide a simpler figure to analyse, Fig 4.26. The corrugation and the dividing of the fault surface on each map could then be seen. This figure was plotted by program B.

Program C was written so that the fault surface morphology between two fault surface trail maps, namely, map 4, (x = 160mm), and map 5, (x = 190mm) could be examined. This program was used to demonstrate the corrugation and the division in the fault surface. The program first enlarged the original map 4, which in the experimental box was situated across the x-axis at x = 160mm. Fig 4.27 shows this map, The map shows how the fault

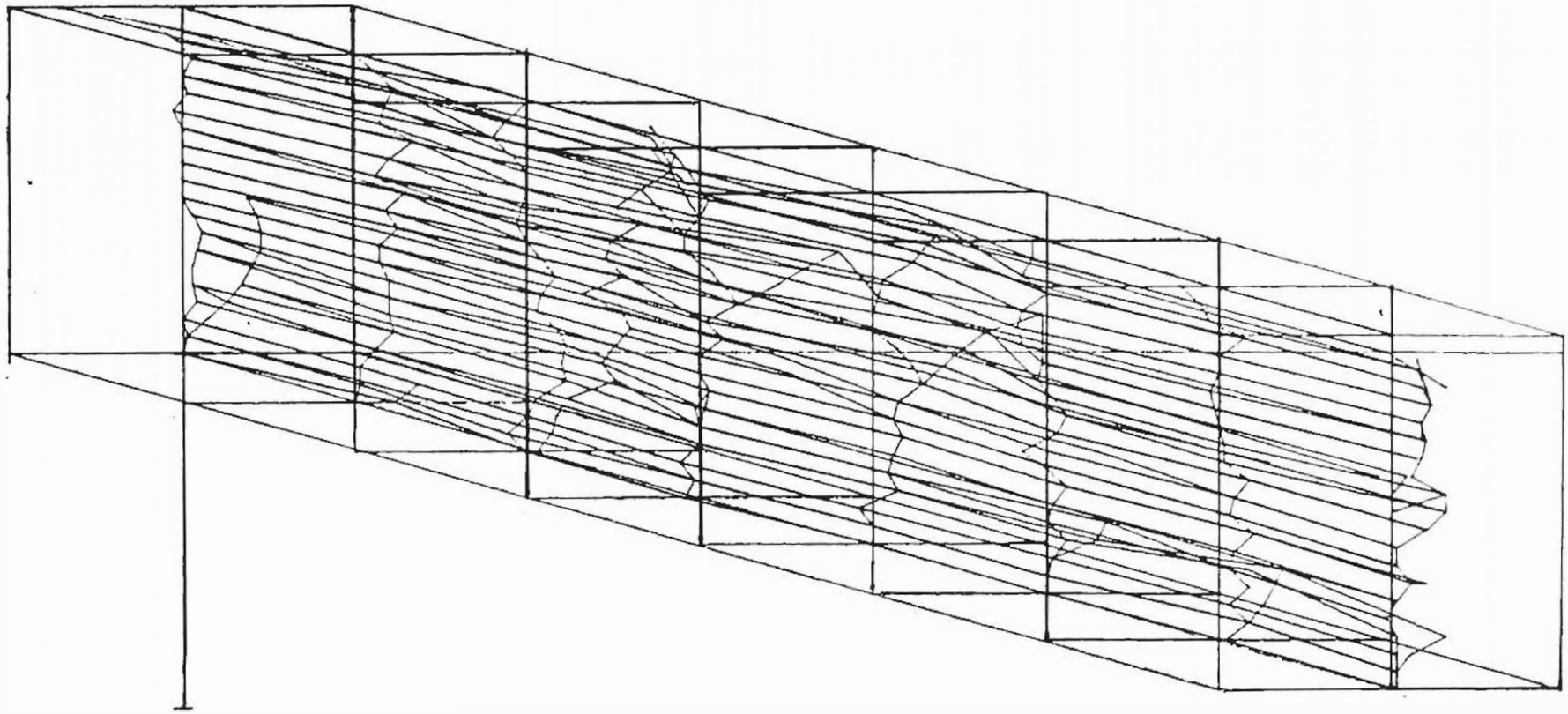

Fig 4.25: The computer model figure plotted from data. This figure is too complex to interpret.

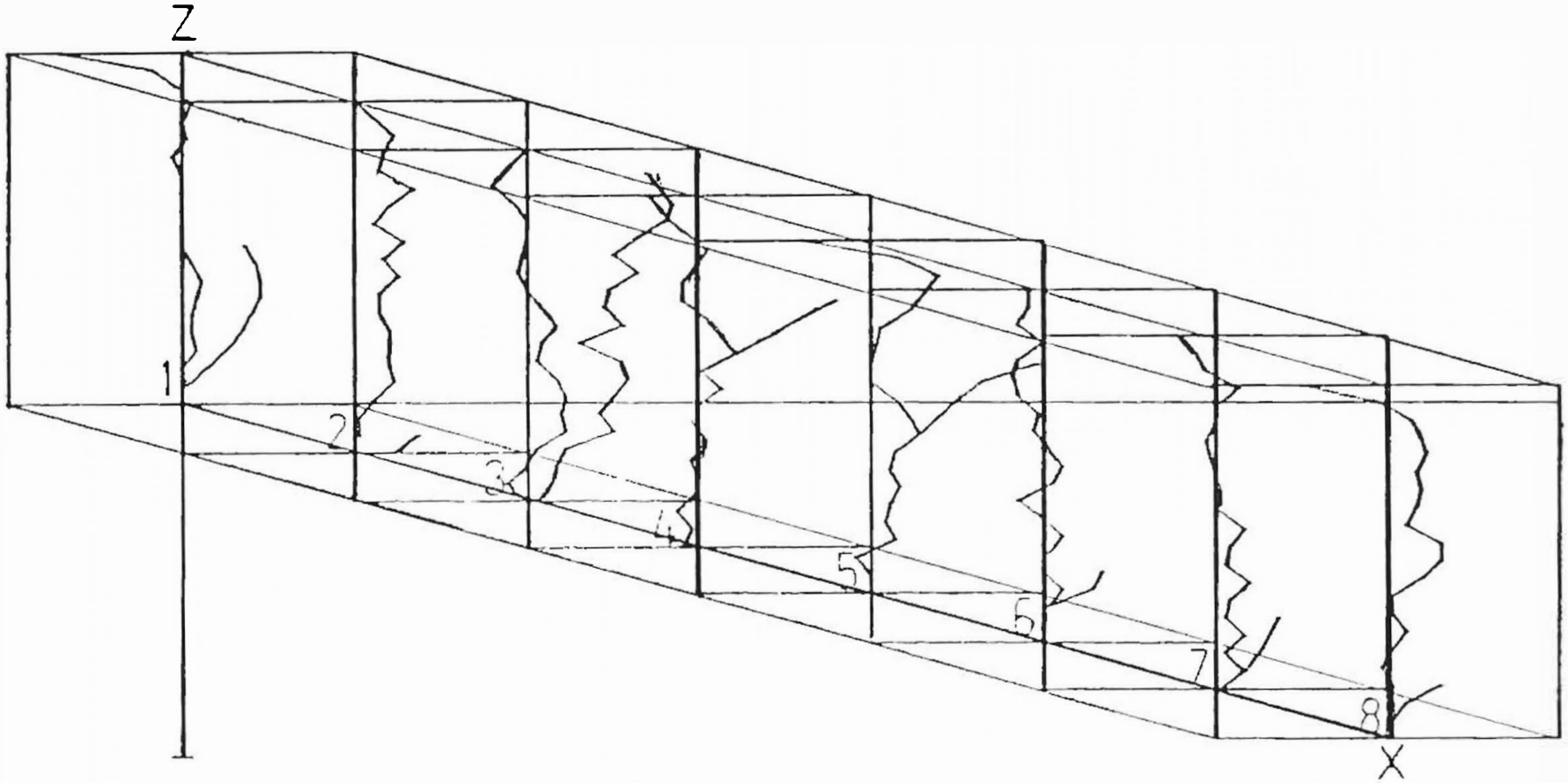

Fig 4.26: The computer drawn fault surface model with vertical colour marker map traces (YZ-plane sections) in their sequential order indicating how the fault surface was corrugated and branched.

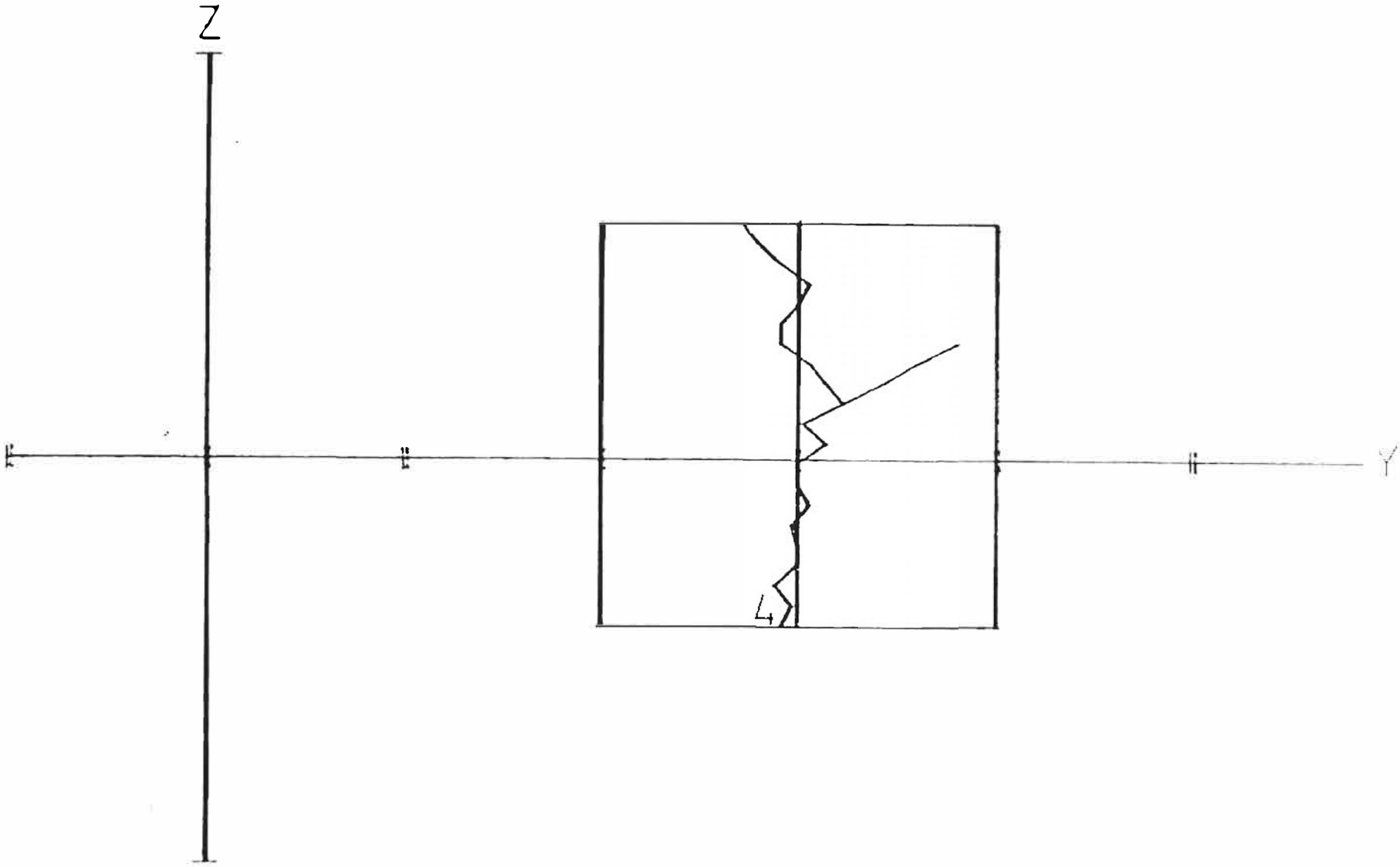

Fig 4.27: The vertical colour marker map No.4 (the YZ-plane section) enlarged and plotted by computer, showing the path of the fault surface at x = 160mm.

surface was corrugated and divided at x = 160mm and along the XY-plane. The program further singles out map 5 which lay at x = 190mm in the experimental box, and shows the corrugations enlarged in a similar way as was done to map 4. This map 5 is shown in Fig 4.28, while Fig 4.29 shows map 4 and map 5, arranged in their original order, that is, how they lay originally in the experimental box, also enlarged by a factor of 1.5. Further figures provided by the program C are Figs 4.30 and 4.31, which show the fault surface shaded between the maps 4 and 5, with a different pen where the surface was bifurcated into two, for the second surface, as shown in Fig 4.31.

4.5 CONCLUSION.

Although similar experiments were reported where fault surfaces were examined by other workers (See section 2.8.1), the method used here is simple, and has the advantage that only inexpensive materials are used.

Plotting the offset positions of the colour markers and joining them together (see Fig 4.14 and Fig 4.15 for the vertical shape of the fault surface on the YZ-plane) provided a picture of how a fault surface could be oriented at that position. Fig 4.6 (transparency) was used to plot the points in a similar way to provide a picture of how the fault might look on the top surface of the sand body after the shear. Fig.4.22 shows such offset points as were plotted from the transparency, while Fig. 4.23 shows the picture of the offsets linked together in what could be one of the many possibilities of what the fault surface looked like on the outside surface of the sand, i.e. on the XY-plane, at the height of z = 100mm. Once the colour marker offset positions for each lamella had been transferred to

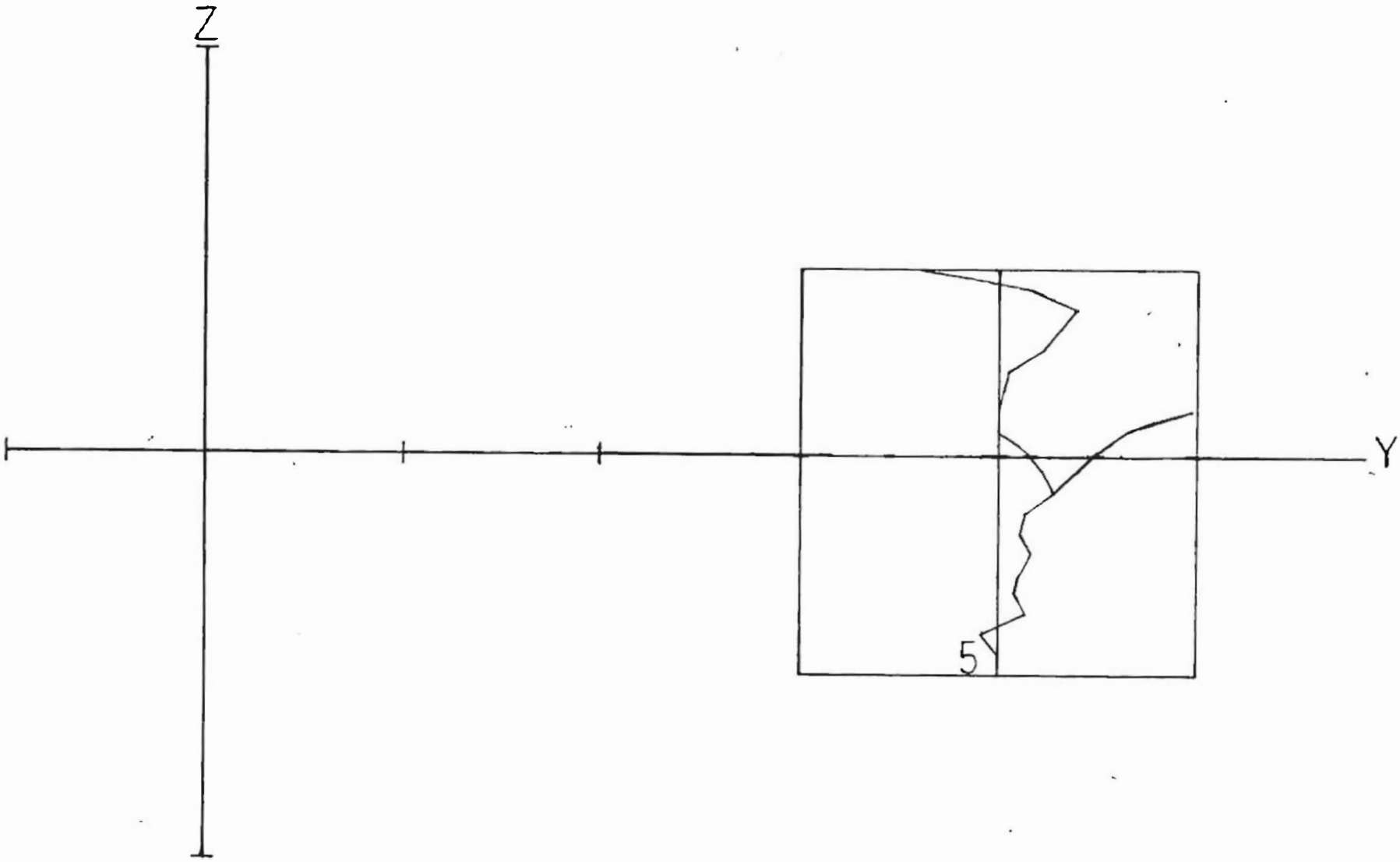

Fig 4.28: The vertical colour marker map No.5 (the YZ-plane section at x = 190mm) extracted by computer. Let the branching and the corrugation be noted here.

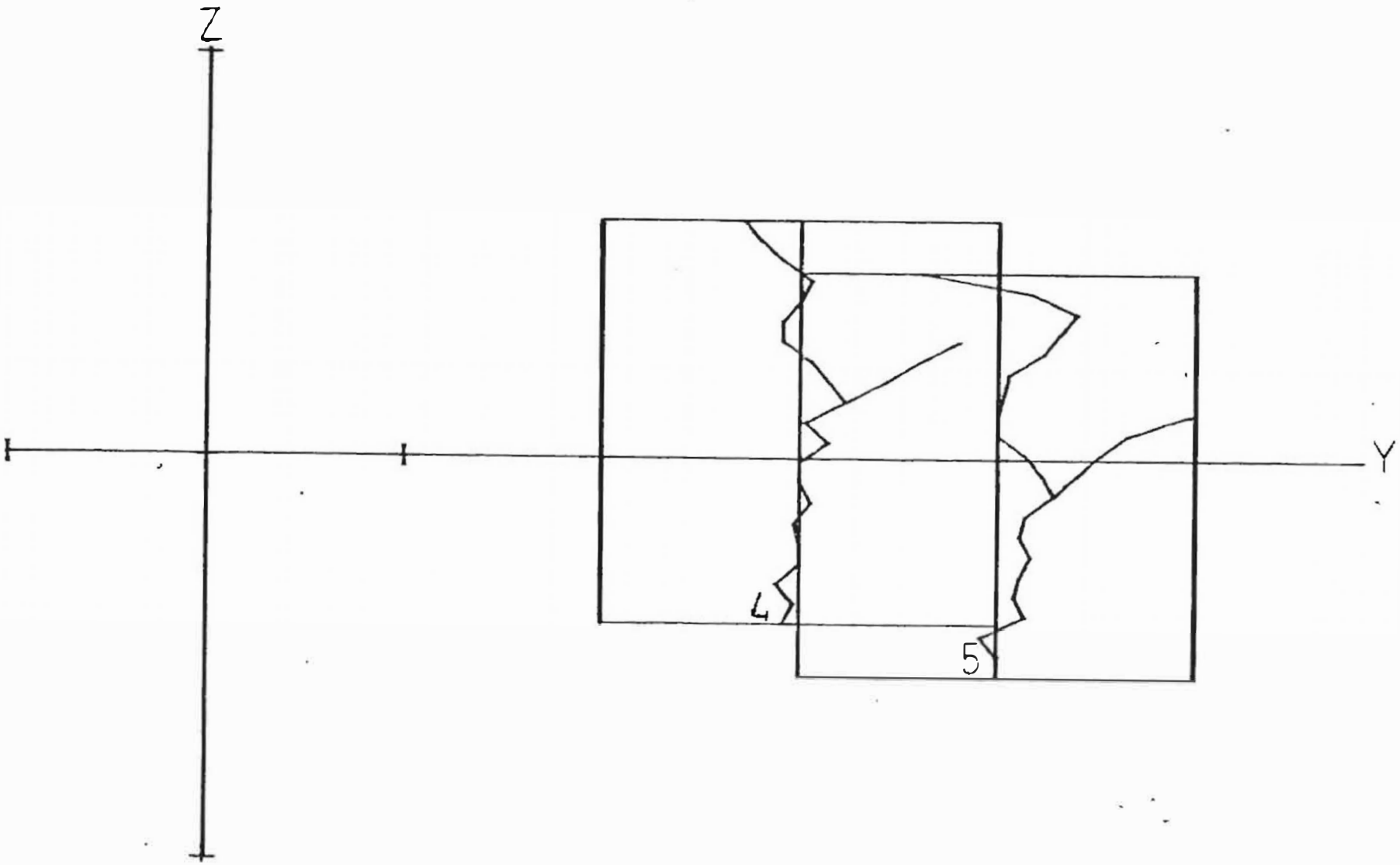

Fig 4.29: The map sheets No. 4 and No.5, arranged in sequential order for the mapping of the possible path of the fault surface between them.

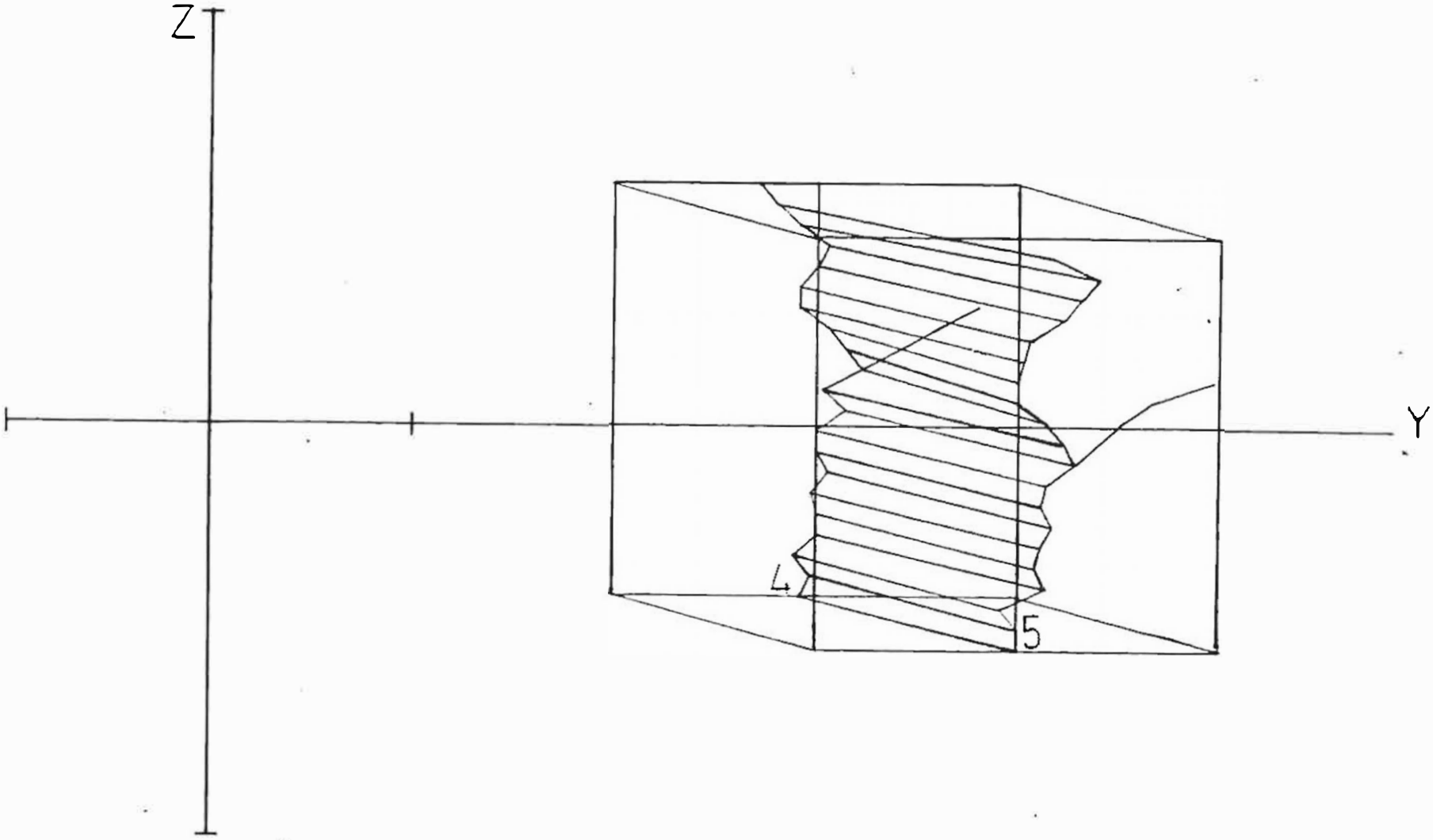

Fig 4.30: A corrugated fault surface traced between maps No.4 and No.5.

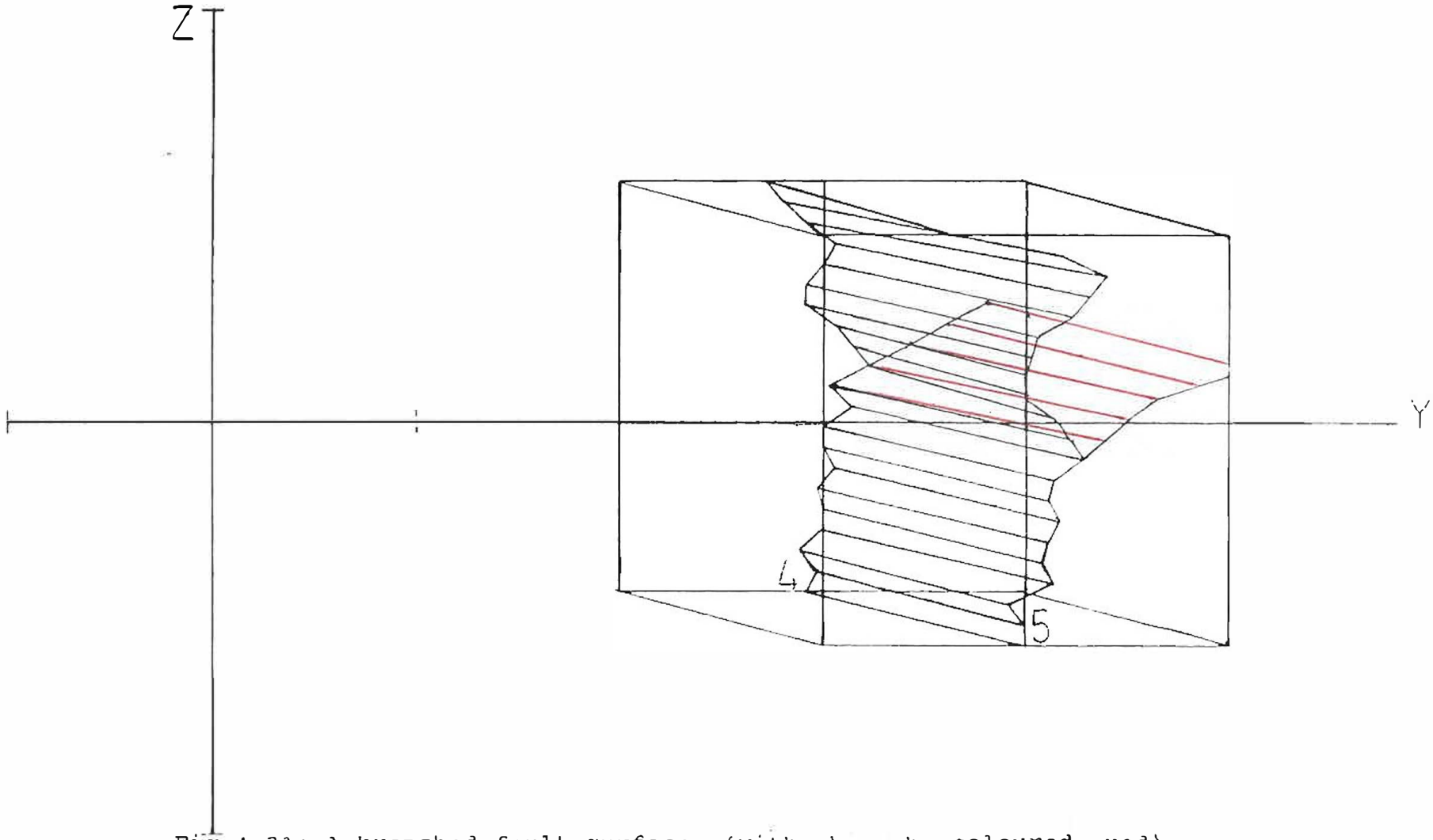

Fig 4.11: A branched fault surface (with branch coloured red) shows how the fault surface was bifurcated.

sheets of perspex, and holes drilled at these positions, the sheets were aligned in order, and suitable linking of the offset positions with thread provided a reconstruction of the fault surface inside the sand body which could be examined with ease.

The plotting of the offset positions further provided the data that helped to the construct a three dimensional computer model of the fault surface in the sand body after the shear. The program was written so that a pair of mappings could be singled out to show a bifurcation that coalesced to a single fault with the same fault surface (see Fig. 4.29, Fig 4.30 and Fig 4.31).

From the observations of the fault surfaces reconstructed in the two above mentioned models, the following conclusions could be drawn about a fault surface in an amorphous solid that is plastically sheared:

1. The fault surface is twisted, wavy and devoid of any systematic pattern.

2. It is both corrugated and bifurcated (torn) into splays that sometimes extend beyond the shear zone.

3. Faults that were widely spread across the shear zone on the surface of the sand body corresponded to faults that coalesced into a single fault at the base of the box.

4. As the fault surface approached the bottom of the sand body, it appeared to straighten in what seemed to be aligning itself with the straight interface of the halves of the bisected experimental box.

CHAPTER 5

DISCUSSION

5.1 INTRODUCTION.

Both the perspex and computer models were studied to determine the shape of the fault surface with the following aims:

1. Investigating the characteristics of the fault surface generated in the sand as a model of an amorphous solid subjected to shear.

2. Observing if there are similarities and differences between the fault surfaces in amorphous solids and in glide planes of crystalline solids.

3. Determining whether the results of a small-scale laboratory experiment in which an amorphous material such as sand is sheared can be extrapolated to crustal faults on a geological scale by correlating features of the latter as described by Sibson (42) with our own observations. If such observations could be shown to be justified, the laboratory experiments could add valuable information to our understanding of fault surface behaviour in plate tectonics, and add to our understanding of the origins of earthquakes.

5.2 MODEL EXAMINING

The fault (slip) surface that was portrayed by both the perspex and the computer models which were described in chapter 4 (see sections 4.4.2 and 4.4.3), is described and examined in this section, with emphasis on analogies to geological faulting.

5.2.1 THE PERSPEX MODEL

1. Comment.

Our models have the weakness inherent in the whole observation procedure that the positions of the fault surfaces are deduced by intrapolation between observed offset points in a relatively coarse grid, so that fault segments comparable in dimensions to grid spacing are lost. Also, each planar perspex sheet meant to represent a marker plane does not have a shape of a lamella after shear, and slight positional inaccuracies arise.

2. Observations

1. Short stepped segments noted on the top surface of the could not be properly represented on the perspex model due to the coarseness of the grid. However, there is clearly one main fault surface which "snakes" along the centre line horizontally on the surface (X-Y plane) and also along the Z-axis from the bottom to the top. This wavy appearance of the fault surface, observed in perspective in three dimensions in this model, was found to be a common feature of all experimental sets per-

formed. Hence, it can be concluded that a fault surface in an amorphous surface is not planar, but is haphazardly corrugated, following no particular pattern as it crosses frequently over the centre line, while oscillating between the boundaries of a fracture zone.

2. The fault surface is observed to be branched into little surface sections called splays. Some splays do not reach the top surface of the sand but end in the sand body. These splays (branches) depart from the main fault surface at different angles and go in different directions, some of them going beyond the borders of the fracture zone.

3. Although the branching segments occur at different levels, all segments coalesce into a common main fault surface as they approach the bottom of the sand body, while at the same becoming more closely aligned with the centre line.

4. Where the fault surface divides (or bifurcates) into, say two branches in the sand, both branches change direction from the original path of alignment with the centre line, and deviate into the fracture zone on both sides of the centre line and away from it, unlike in crystalline solid where surfaces traversed by dislocations are always planar. It thus becomes difficult to determine which segment of the fault surface is analogous to a crystal glide plane traversed by edge dislocation and which segment is analogous to glide plane traversed by screw dislocation.

5.2.2. THE COMPUTER MODEL.

1. Comment.

The computer model was constructed with the aid of a Basic program, using the data accumulated. The program draws the fault surface to scale. The advantage it has is that it can be used to extract a particular portion of the glide surface for examination. Three programs were used. Program A is rather a cumbersome general one that plots all the offset points measured in each marker lamella. Program A was later abridged into Program B. Program C shows an example of an extracted portion where both corrugation and bifurcation were observed. Figs 4.25 to 4.31 are the outcome of these programs.

2. Observations.

On examination, the computer model shows the same features as those observed in perspex model.

5.3 COMMENTS.

Tectonic Faults.

Crustal deformation is revisited in this section to evaluate any similarities between large scale faulting and this behaviour of a model amorphous solid.

Sibson (42), in discussing plate tectonic theory (see section 2.8.2) classified the earth's crust into an upper, brittle region about 15km in depth (the seismogenic régime) and the quasi-plastic régime at greater depths where rock flows in a viscous fashion. This quasi-plastic is in contact with and floating on the liquid magma of the earth's mantle. It is believed that convection currents in the unstable magma in the mantle cause the continuous drifting of the continental plates. When these plates slip past each other, (see section 2.7, Fig 2.13), frictional resistance occurs along the interface of the seismogenic régime. Under increased pressure and temperature a principal slip surface then develops within a fracture zone. This surface is often segmented, curved and twisted, and it oscillates from one margin of the fracture zone to the other. Sibson suggests that such deviations from linearity are responsible for the nucleation of earthquakes. Fig 5.1 shows the process of earthquake nucleation as suggested by Sibson and the formation of the en-echelon segments in such a principal slip surface. Fig 5.1(a), shows how a principal slip surface is continuous at the interface of both the seismogenic and the quasi-plastic regions. As the slip (fault) surface gets higher close to the top surface of earth, it reaches the brittle seismogenic realm, where, if the shear increases, dilational and antidilational jogs form suddenly, namely, D and A jogs respectively (see Fig 5.1(b)). The sudden fractures at these jogs are the foci of the earthquakes where the slip surface ruptures into separate en-echelon faults that will appear as steps on the surface of the earth as seen in Fig 5.1(c) (19,39,42).

Fig 5.2 shows the development of the principal shear surface in the sand model studied here. At the bottom of the body, the surface was almost plane

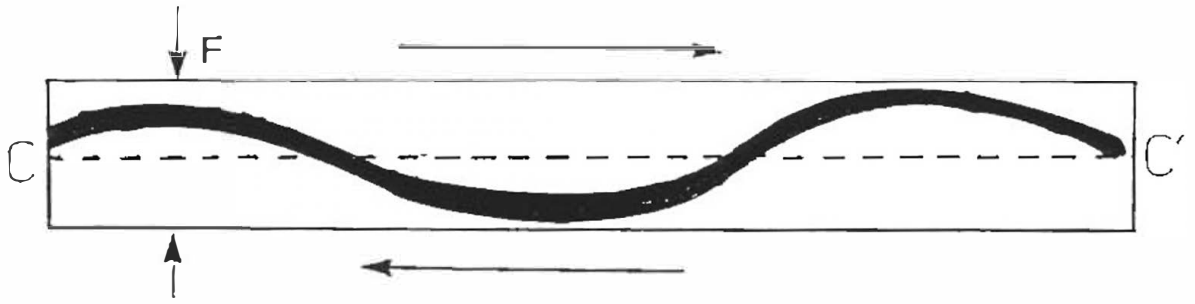

Fig 5.1(a): Principal slip surface, oscillating within F, the width of the fracture (or fault) zone as indicated, at the interface of the seismogenic and quasi-plastic regions.

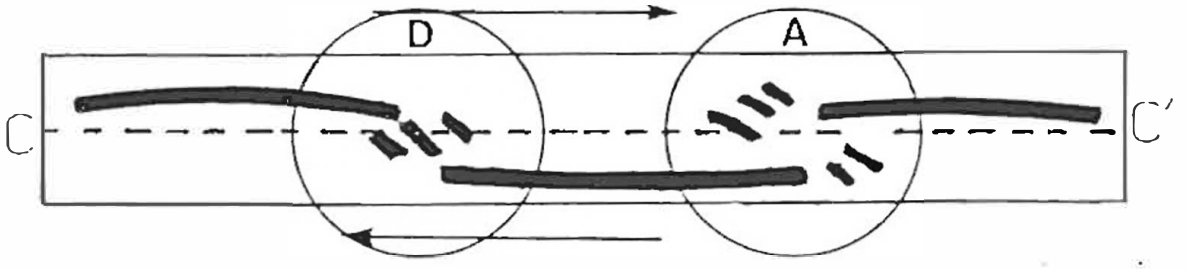

Fig 5.1(b): The principal slip surface in the brittle seismogenic region fracturing into dilational and antidilational jogs, D and A respectively.

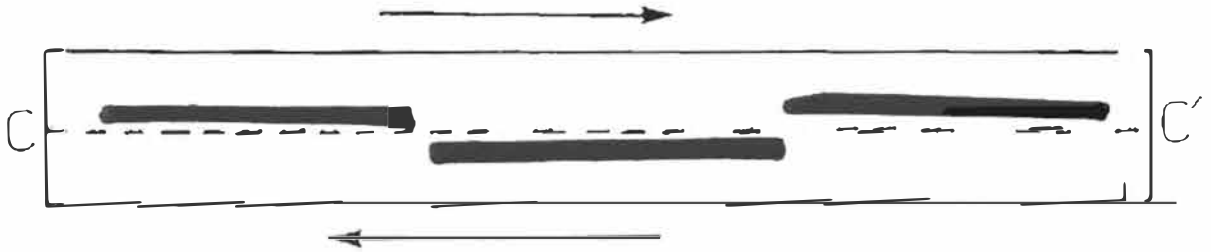

Fig 5.1(c): The principal slip surface at the surface of the earth, showing the steps in the en-echelon form segments.

Fig 5.1: The principal slip surface in crustal deformation, and the possible development of the en-echelon segments as viewed by Segall and Pollard (41), and Sibson (42). F denotes the fracture zone, while CC′ denotes strike-slip center line.

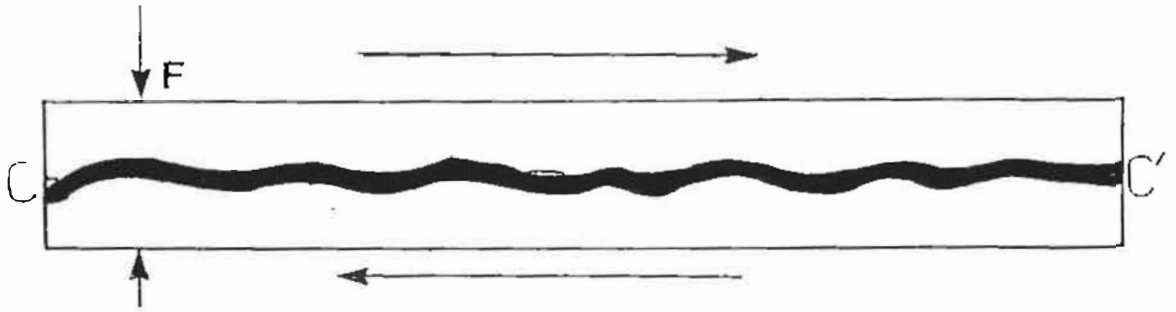

Fig 5.2(a): Fault surface at the bottom of the experimental box, aligning with the center line CC′. F denotes the fault zone.

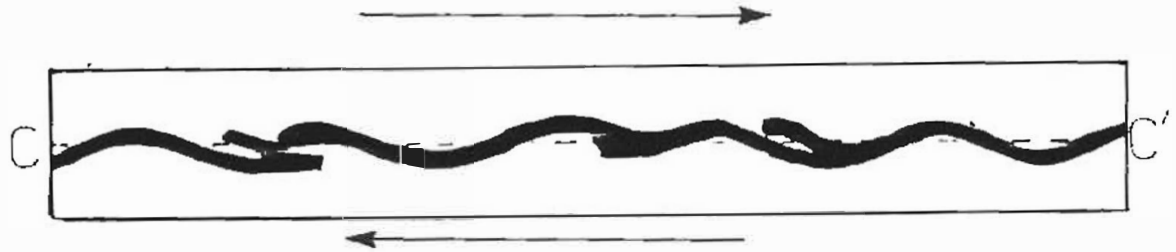

Fig 5.2(b): Fault surface nearer the surface of the sand body, where where it begins to be segmented (about 50mm from the bottom).

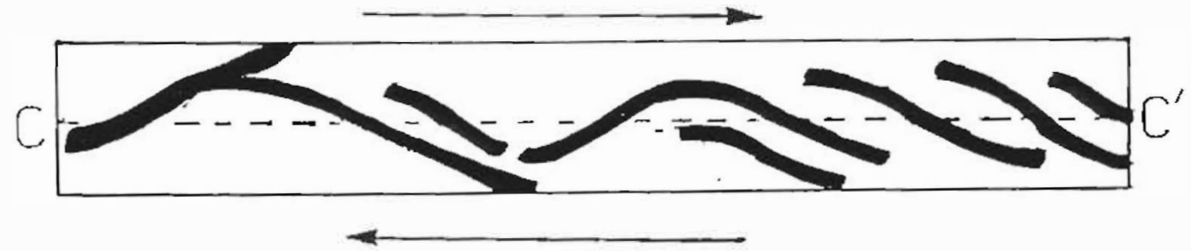

Fig 5.2(c): Fault surface, fragmented and segmented into en-echelon faults at the surface of the sand body.

Fig 5.2: Fault surface schematically viewed developing in sample sand.

and parallel to the center line as shown in Fig.5.2(a). As the fault surface spreads from the bottom of the box upwards into the sand body, the fault surface develops oscillations that extend over the fracture zone of finite thickness. The fracture zone widens towards the surface of the sand body. The fault surface itself consists of complex segments on both sides of the center line (see Fig 5.2b). Figure 5.2(c) shows how the single fault surface near the base of the box becomes a very complex, multiply segmented surface towards and on the top surface of the sand body. The fault surface in some places is divided into two or even three segments across the fracture zone, parallel to the center line. Some segments deviate widely from the center line into parts of the sand body beyond the margins of the heavily fractured region.

5.4 CONCLUSION.

It appears that as in the shear of metals, glide surfaces are bifurcated, split and may be multiply connected. In metals the result of this complex spreading of glide underlies the phenomenon of work hardening.

In metals the formation of a corrugated glide surface is common. This does not impede glide. However the corrugations in general do not run through a metal specimen uninterrupted, but end in the crystal. When corrugations on the glide surface end in the solid, stress concentrations are set up which impede further glide. These stresses have a simple character: they are tensions and compressions in the glide direction (42).

Similar stresses are known in geological faulting as releasing and

restraining jogs along the strike slip faults as already outlined in section 5.3. It is possible that the favoured sites for the origin of the earthquakes are to be found at such jogs (19,24,42). The present observations suggest that the glide surfaces in an amorphous model solid, for example, sand, are quite complex. Further work would be required to fully establish the validity of an analogy between dislocation glide in a metal, as shown in section 2.4, and shear in an amorphous solid.

The present observations have established that glide surfaces in amorphous solids are not planar. Instead, they are multiply connected, twisted, and warped. If geological fault surfaces, in the earth's crust have similar features as those in amorphous solids, these features may be attributed to the tendency of the glide surface to divide and bifurcate.

It is therefore, suggested that a fault surface should not be modelled as a plane as one usually finds done in geology texts. Examples of such models are shown below (see Fig 5.3), where (a) is from Briggs and Smithson (51), (b), (d) and (f) from Billings (16), (e) from Ragan (34), (g) from Gondie (52) and (c) and (h) form Strahler and Strahler (50), where the fault surface of a strike-slip (transform or transcurrent) fault is modelled as planar contrary to the findings of this dissertation.

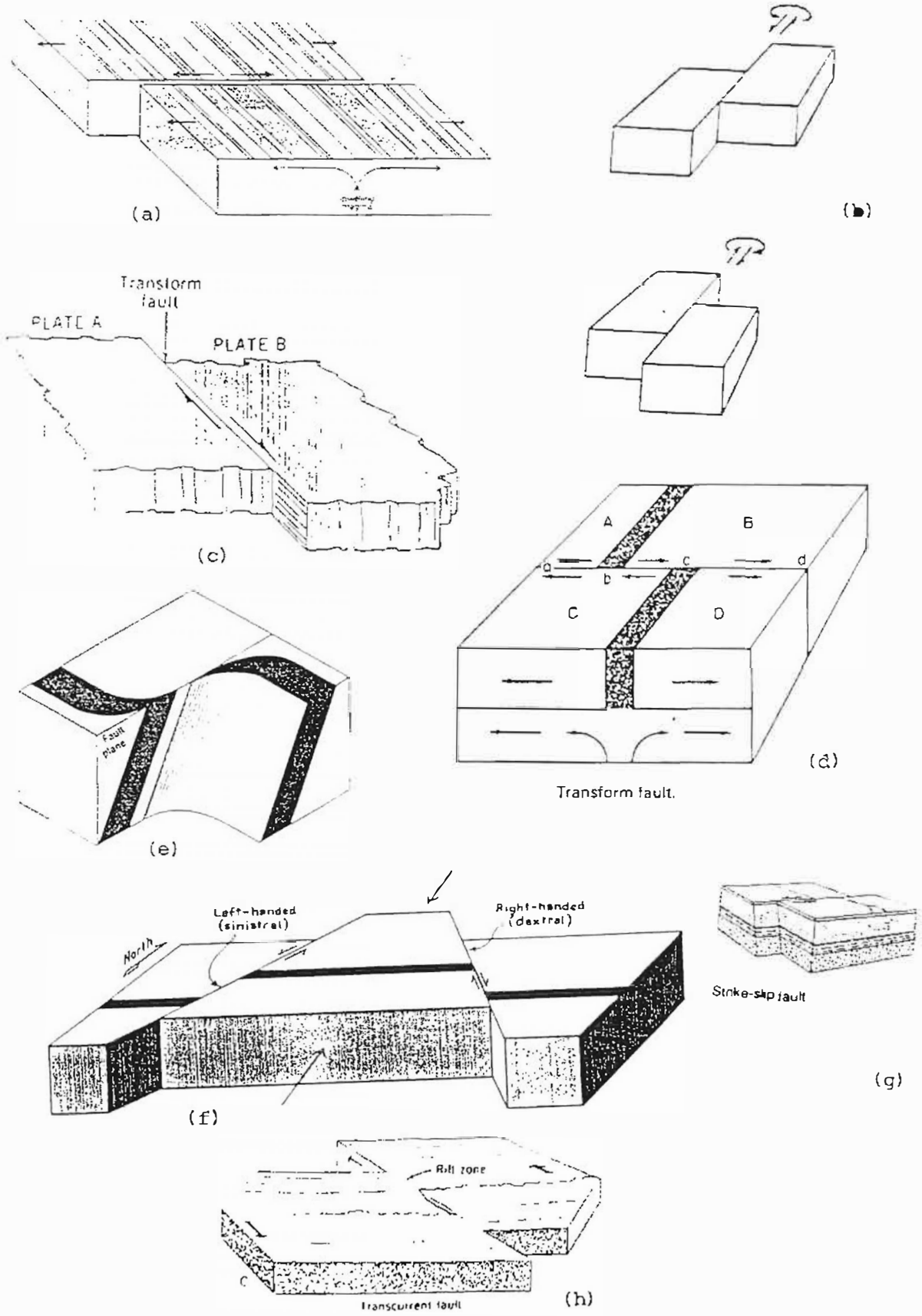

Fig 5.3: Fault surface of the strike-slip fault modelled as a plane by geology texts.

REFERENCE

(1) HULL, D., Introduction to Dislocations, (Second Edition), Pergamon Press, Oxford (1975).

(2) FRIEDEL, J., Dislocations. Pergamon Press Oxford (1967).

(3) FRIEDEL, J., Dislocations - an introduction in F R N Nabarro (ed) Dislocations in solids, vol. 1, North Holland Amsterdam (1970).

(4) COTTRELL, A.H., Theory of Crystal Dislocation, Gordon and Breach Science Publishers Inc., New York (1964).

(5) HONEYCOMBE, R.W.K., The Plastic Deformation of Metals, Edward Arnold, London (1971).

(6) AZAROFF, L.V., Introduction to Solids, Mcgraw-Hill, New York (1986).

(7) KITTEL, C., Introduction to Solid State Physics, John Wiley & Sons, New York (1986).

(8) HENDERSON, B., Defects in Crystalline Solids, Edward Arnold (1978).

(9) LOVELL, M.C., AVERY, A.J. and VERNON, M. W., Physical Properties of Materials, Van Nostrand Reinhold Company, Berkshire (1967).

(10) ROSENBERG, H.M., The Solid State, (Second Edition), Oxford Physics Series, Oxon. (1978).

(11) HALL, H.E., Solid State Physics, John Wiley & Sons, Chichester (1987).

(12) AKRILL, T.B., BENNET, G.A.G. and MILLAR, C.J., Physics, Edward Arnold, London (1989).

(13) BLAKEMORE, J.S., Solid State Physics, Cambridge University Press (1985).

(14) OMAR, M.A., Elementary Solid State Physics, Addison-Wesley Publishing Company (1975).

(15) JAROSZEWSKI, W., Fault and Fold Tectonics, Ellis Horwood Publishers, Chichester (1984).

(16) BILLINGS, M.P., Structural Geology, Prentice-Hall Inc, New Jersey (1972).

(17) WEERTMAN, J. and WEERTMAN, J.R., Elementary Dislocation Theory, Mac-Millan Company, New York (1964).

(18) PATTERSON, M.S., Experimental Deformation and Faulting in Wombeyan Marble, Bull.geol.Soc.Am. 69 (1958) 465-476.

(19) READ, W.T., Dislocations in Crystals, McGraw-Hill Book Company, New York (1953).

(20) WHALLEY, B., Properties of Materials and Geomorphological Explanation, Oxford University Press, Oxford (1976).

(21) NABARRO, F.R.N., Theory of Crystal Dislocations, Oxford University Press, Oxford (1967).

(22) WEERTMAN, J. and WEERTMAN, J.R., Moving Dislocations, in F.R.N. Nabarro (ed) Dislocation in Solids, North Holland, Amsterdam (1980).

(23) JACKSON, P.J., The micromechanics of Plastic Deformation in Crystals: an outline, South Afrian Journal of Science, Vol.81(1985) 439-440.

(24) McCLINTOCK, F.A. and ARGON, A.S., Mechanical Behavior of Materials, Addison-Wesley Publishing Company, Reading, Massachusets (1966).

(25) BASINSKI, Z.S. and BASINSKI, S.J., Philos. Mag., 9 51 (1964).

(26) NEUHAUSER, N., Slip line formation and Collective Dislocation Motion, in F.R.N.Nabarro (ed) Dislocation in Solids, North Holland, Amsterdam (1983).

(27) LIBOVICKÝ, S. and ŠESTÁK, B., Philosophical Magazine, A, Vol. 47 No.1, 63-78.

(28) JACKSON, P.J., The mechanism of Plastic Relaxation in Single Crystal Deformation, Material Science and Engineering, 81 (1986) 169-174.

(29) JACKSON, P.J., DE LANGE, O.L. and NATHANSON, P.D.K., Dislocation Structures produced by Cross slip, in Ashby,M.F.(ed): Dislocation Modelling of Physical System, Pergamon, Oxford (1981) 483.

(30) JACKSON, P.J., DE LANGE, O.L. and YOUNG, C.J., Cross slip and the Stresses of Prismatic Dislocations, Acta Metall 30 (1982) 483.

(31) JACKSON, P.J., Corrugated Glide Surfaces and the Origin of Earthquakes, Proc. 8th Intl.Conf. on Strength of Metals and Alloys, in Kettunen, P.O., et al (ed). Pergamon, Oxford (1988) 217-221.

(32) CHORLEY, R.J., SCHUMM, S.A. and SUGDEN, D.E., Geomorphology, Methuen and Company, London (1984).

(33) HUMBLIN, W.K., The Earth's Dynamic Systems, Burgess Publishing Company, Minneapolis (1978).

(34) RAGAN, D.M., Structural Geology, John Wiley & Sons, London (1973).

(35) SAVAGE, J.C., Dislocation in Seismology, in F.R.N.Nabarro (ed) Dislocations in Solids, Vol.3, North Holland, Amsterdam (1980).

(36) MANDL, G., Mechanics of Tectonic Faulting, Elsevier Science Publishers, Amsterdam (1988).

(37) BOYER, S.E. and ELLIOT, D., Thrust Systems. The American Association of Petrolium Geologists Bulletin, Vol.66 (9) (1982) 1196-1230.

(38) SHARMA, P.V., Geophysical Methods in Geology, Elsevier Science Publishers, New York(1986).

(39) KASAHARA, K., Earthquake Mechanics, Cambridge University Press, Cambridge (1981).

(40) HUMPHREYS, C.J., Imaging of Dislocations, in F.R.N.Nabarro (ed)

Dislocations in Solids, Vol.5, North Holland, Amsterdam (1980).

(41) SEGALL, P. and POLLARD, D.D., Mechanics of Discontinuous Faults, Journal of Geophysical Research, Vol.85, No. B8, (1980) 4337-4350.

(42) SIBSON, R.H., Earthquakes and Lineament Infrastructure, Phil. Trans. R. Soc. London. A 317 (1986) 63-79.

(43) COX, A. and HART, B.R., Plate Tectonics (How it Works), Blackwell Scientific Publications, Palo Alto (1986).

(44) LINDSTROM, M., Steps facing against the Slip Direction: a model, Geol. Mag.111(1) (1974) 71-74.

(45) EMMONS, R.C., Strike Slip Rupture Patterns in Sand Models, Tectonophysics 7 (1) (1969) 71-87.

(46) GROENEWALD, G., Geologist of the Golden Gate Nature Reserve, Golden Gate (1990).

(47) RICHARD, P., BALLARD, F.J., COLLETTA, B. and COBBOLD, P. Fault Initiation and Development above a Basement Strike-Slip Fault, Analogue modelling and Tomography. C.R. Acad. Sci. Paris, t309; serie II.(1989) 2111-2118.

(48) PRESS, F., Earthquake Prediction, Scientific American 232, No.5 (May 1975) 14-23.

(49) FRÖHLICH, C., Deep Earthquakes, Scientific American 260, No.1(Jan.1989) 32-39.

(50) STRAHLER, A.N. and STRAHLER, A.H. Modern Physical Geography, (Second Edition), John Wiley & Sons, New York (1983).

(51) BRIGGS, D. and Smithson P.,Fundamentals of Physical Geography, Hutchison and Co., New York (1985).

(52) GONDIE, A.(ed), The encyclopaedic Dictionary of Physical Geography, Blackwell United, (1985).

APPENDICES

Program A: Plotting the Glide Surface from the data of Table 4.1

```
DF;IM36;OE;
5 GCLEAR
6 DISP "THIS PROGRAM DRAWS A MODEL OF A SHEARED AMORPHOUS SOLID.THE SOLID"
7 DISP "WAS A PURE,HOMOGENOUS RIVER SAND,PRESSED AND SHAKEN TOGETHER TO THE"
8 DISP "MAXIMUM ATTAINABLE DENSITY.THE PICTURE SHOWS HOW THE GLIDE SURFACE"
9 DISP "BIFURCATES AS IT CORRUGATES AROUND AND DEVIATES FROM THE SLIP PLANE"
10 GCLEAR
15 LIMIT 0,250,10,140
16 LOCATE 10,190,10,90
20 SCALE -3.5,28,-10,10
30 XAXIS 0,3.5
40 YAXIS 0,10
50 FOR I=1 TO 2
60 READ X,Y
70 PLOT X,Y
80 NEXT I
90 DATA 0,0,24,-9.5
100 MOVE 3.5,-1.4
110 FOR J=1 TO 2
120 READ X,Y
130 PLOT X,Y
140 NEXT J
150 DATA 3.5,-1.4,3.5,8.6
160 MOVE 7,-2.8
170 FOR K=1 TO 2
180 READ X,Y
190 PLOT X,Y
200 NEXT K
210 DATA 7,-2.8,7,7.2
220 MOVE 10.5,-4.1
230 FOR L=1 TO 2
240 READ X,Y
250 PLOT X,Y
260 NEXT L
270 DATA 10.5,-4.1,10.5,5.9
280 MOVE 14,-5.4
290 FOR M=1 TO 2
300 READ X,Y
310 PLOT X,Y
320 NEXT M
330 DATA 14,-5.4,14,4.6
340 MOVE 17.5,-6.6
350 FOR N=1 TO 2
360 READ X,Y
370 PLOT X,Y
380 NEXT N
390 DATA 17.5,-6.8,17.5,3.2
400 MOVE 21,-8.1
410 FOR P=1 TO 2
420 READ X,Y
430 PLOT X,Y
440 NEXT P
450 DATA 21,-8.1,21,1.9
460 MOVE 24.5,-9.5
470 FOR R=1 TO 2
480 READ X,Y
490 PLOT X,Y
500 NEXT R
510 DATA 24.5,-9.5,24.5,.5
520 MOVE 0,0
530 FOR I1=1 TO 21
540 READ X,Y
550 PLOT X,Y
```

```
560 NEXT I1
570 DATA 0,0,.1,.5,0,1,.3,1.5,.2,2,.2,2.5,.3,3,.4,3.5,.2,4,0,4.5,0,5,0,5.5
575 DATA 0,6,0,6.5,-.2,7,.1,7.5,0,8,.2,8.5,-.1,9,-.6,9.5,-2.5,10
580 MOVE 3.5,-1.4
590 FOR J1=1 TO 21
600 READ X,Y
610 PLOT X,Y
620 NEXT J1
630 DATA 4.3,-1.4,3.6,-.9,3.6,-.4,3.9,.1,4.3,.6,4.2,1.1,4.2,1.6,4.2,2.1,4,2.6
640 DATA 4,3.1,4.4,3.6,4.1,4.1,4.5,4,6,3.9,5.1,4.2,5.6,4.7,6.1,4,6.6,4.1,7.1
650 DATA 4.3,7.6,3.9,8.1,3.5,8.6
670 MOVE 7,-2.6
680 FOR K1=1 TO 21
690 READ X,Y
700 PLOT X,Y
710 NEXT K1
720 DATA 7,-2.8,6.6,-2.3,7,-1.8,7.2,-1.3,7.8,-.8,7.7,-.3,7.8,.2,7.6,.7,7.2,1.2
725 DATA 7.3,1.7,7.6,2.2,7.3,2.7,7.3,3.2,6.8,3.7,6.9,4.2,7,4.7,7,5.2,6.7,6.7
728 DATA 6.3,6.2,6.6,6.7,7,7.2
730 MOVE 10.2,-4.1
740 FOR L1=1 TO 21
750 READ X,Y
760 PLOT X,Y
770 NEXT L1
780 DATA 10.2,-4.1,10.4,-3.6,10.1,-3.1,10.5,-2.6,10.5,-2.1,10.4,-1.6,10.7,-1.1
782 DATA 10.5,-.6,10.5,-.1,11,.4,10.6,.9,11.3,1.4,11,1.9,12.6,2.4,13.3,2.9
785 DATA 10.2,3.3,10.5,3.9,10.7,4.4,10.2,4.9,9.8,5.4,9.5,5.9
790 MOVE 14,-5.4
800 FOR M1=1 TO 21
810 READ X,Y
820 PLOT X,Y
830 NEXT M1
840 DATA 14,-5.4,14,-4.9,13.7,-4.4,14.5,-3.9,14.3,-3.4,14.4,-2.9,14.6,-2.4
842 DATA 14.4,-1.9,14.5,-1.4,15,-.9,15.4,-.4,15.8,.1,16.3,.6,17.4,1.1,14.1,1.6
845 DATA 14.2,2.1,14.8,2.6,15.1,3.1,15.4,3.6,14.6,4.1,12.6,4.6
860 MOVE 17.5,-6.8
870 FOR N1=1 TO 21
880 READ X,Y
890 PLOT X,Y
900 NEXT N1
910 DATA 17.5,-6.8,17.5,-6.3,17.6,-5.8,17.9,-5.3,17.5,-4.8,17.6,-4.3,17.9,-3.8
912 DATA 17.5,-3.2,17,-2.8,17.7,-2.3,17.9,-1.8,17.6,-1.3,17.3,-.8,17.4,-.3
915 DATA 17,.2,16.9,.7,17,1.2,17.5,1.7,17,2.2,17.2,2.7,17.2,3.2
920 MOVE 21.1,-8.1
930 FOR P1=1 TO 21
940 READ X,Y
950 PLOT X,Y
960 NEXT P1
965 DATA
970 DATA 21.1,-8.1,21.6,-7.6,21.2,-7.1,21.6,-6.6,21.2,-6.1,21.3,-5.6,21.7,-5.1
972 DATA 21.2,-4.6,21.3,-4.1,21.6,-3.6,21.1,-3.1,21.1,-2.6,21,-2.1,20.9,-1.6
975 DATA 20.8,-1.1,21,-.6,21,-.1,21.5,.4,20.8,.9,20.6,1.4,20.2,1.9
980 MOVE 24.5,-9.5
990 FOR R1=1 TO 21
1000 READ X,Y
1010 PLOT X,Y
1020 NEXT R1
1030 DATA 24.6,-9.5,24.6,-9,24.6,-8.5,24.6,-8,24.4,-7.5,24.6,-7,24.9,-6.5
1032 DATA 24.6,-6,24.6,-5.5,25.2,-5,25.6,-4.5,25.6,-4,24.9,-3.5,25.1,-3
1035 DATA 25.2,-2.5,25.1,-2,25.3,-1.3,25.2,-1,25,-.5,24.4,0,22.8,.5
1040 MOVE 0,10
1050 FOR A=1 TO 2
1060 READ X,Y
1070 PLOT X,Y
1075 NEXT A
1080 DATA 0,10,24.5,.5
```

```
1085 MOVE 0,10
1090 MOVE 0,10
1100 FOR A1=1 TO 6
1110 READ X,Y
1120 PLOT X,Y
1130 NEXT A1
1140 DATA 0,10,-3.5,10,-3.5,0,3.5,0,3.5,10,0,10
1145 MOVE 3.5,-1.4
1150 MOVE 3.5,-1.4
1160 FOR B1=1 TO 6
1170 READ X,Y
1180 PLOT X,Y
1190 NEXT B1
1200 DATA 3.5,-1.4,0,-1.4,0,8.6,7,8.6,7,-1.4,3.5,-1.4
1210 MOVE 7,-2.8
1220 FOR C1=1 TO 6
1230 READ X,Y
1240 PLOT X,Y
1250 NEXT C1
1260 DATA 7,-2.8,3.5,-2.8,3.5,7.2,10.5,7.2,10.5,-2.8,7,-2.8
1270 MOVE 10.5,-4.1
1280 FOR D1=1 TO 6
1290 READ X,Y
1300 PLOT X,Y
1310 NEXT D1
1320 DATA 10.5,-4.1,7,-4.1,7,5.9,14,5.9,14,-4.1,10.5,-4.1
1330 MOVE 14,-5.4
1340 FOR E1=1 TO 6
1350 READ X,Y
1360 PLOT X,Y
1370 NEXT E1
1380 DATA 14,-5.4,10.5,-5.4,10.5,4.6,17.5,4.6,17.5,-5.4,14,-5.4
1390 MOVE 17.5,-6.8
1400 FOR F1=1 TO 6
1410 READ X,Y
1420 PLOT X,Y
1430 NEXT F1
1440 DATA 17.5,-6.8,14,-6.8,14,3.2,21,3.2,21,-6.8,17.5,-6.8
1450 MOVE 21,-8.1
1460 FOR G1=1 TO 6
1470 READ X,Y
1480 PLOT X,Y
1490 NEXT G1
1500 DATA 21,-8.1,17.5,-8.1,17.5,1.9,24.5,1.9,24.5,-8.1,21,-8.1
1510 MOVE 24.5,-9.5
1520 FOR H1=1 TO 6
1530 READ X,Y
1540 PLOT X,Y
1550 NEXT H1
1560 DATA 24.5,-9.5,21,-9.5,21,.5,28,.5,28,-9.5,24.5,-9.5
1570 MOVE -3.5,0
1580 FOR V=1 TO 8
1590 READ X,Y
1600 PLOT X,Y
1610 NEXT V
1620 DATA -3.5,0,21,-9.5,21,.5,-3.5,10,3.5,10,28,.5,28,-9.5,3.5,0
1624 PEN 2
1630 MOVE 0,0
1640 FOR S1=1 TO 8
1650 READ X,Y
1660 PLOT X,Y
1670 NEXT S1
1680 DATA 0,0,4.3,-1.4,7,-2.8,10.2,-4.1,14,-5.4,17.5,-6.8,21.1,-8.1,24.6,-9.5
1690 MOVE .1,.5
1700 FOR S2=1 TO 8
1710 READ X,Y
```

```
1720 PLOT X,Y
1730 NEXT S2
1740 DATA .1,.5,3.6,-.9,5.6,-2.3,10.4,-3.6,14,-4.9,17.5,-6.3,21.6,-7.6,24.6,-9
1750 MOVE 0,1
1760 FOR S3=1 TO 8
1770 READ X,Y
1780 PLOT X,Y
1790 NEXT S3
1800 DATA 0,1,3.6,-.4,7,-1.8,10.1,-3.1,13.7,-4.4,17.6,-5.8,21.2,-7.1,24.6,-8.5
1810 MOVE .3,1.5
1820 FOR S4=1 TO 8
1830 READ X,Y
1840 PLOT X,Y
1850 NEXT S4
1860 DATA .3,1.5,3.9,-.1,7.2,-1.3,10.5,-2.6,14.5,-3.9,17.9,-5.3,21.6,-6.6
1862 DATA 24.6,-8
1870 MOVE .2,2
1880 FOR S5=1 TO 8
1890 READ X,Y
1900 PLOT X,Y
1910 NEXT S5
1920 DATA .2,2 4.3,.6,7.8,-.8,10.5,-2.1,14.3,-3.4,17.5,-4.8,21.2,-6.1,24.4,-7.5
1930 MOVE .2,2.5
1940 FOR S6=1 TO 8
1950 READ X,Y
1960 PLOT X,Y
1970 NEXT S6
1980 DATA .2,2.5,4.2,1.1,7.7,-.3,10.4,-1.6,14.4,-2.9,17.6,-4.3,21.3,-5.6199
1982 DATA 24.6,-7
1990 MOVE .3,3
2000 FOR S7=1 TO 8
2010 READ X,Y
2020 PLOT X,Y
2030 NEXT S7
2040 DATA .3,3,4.2,1.6,7.8,.2,10.7,-1.1,14.6,-2.4,17.9,-3.8,21.7,-5.1,24.9,-6.5
2050 MOVE .4,3.5
2060 FOR S8=1 TO 8
2070 READ X,Y
2080 PLOT X,Y
2090 NEXT S8
2100 DATA .4,3.5,4.2,2.1,7.6,.7,10.5,-.6,14.4,-1.9,17.5,-3.2,21.2,-4.6,24.6,-6
2110 MOVE .2,4
2120 FOR S9=1 TO 8
2130 READ X,Y
2140 PLOT X,Y
2150 NEXT S9
2160 DATA .2,4,4,2.6,7.2,1.2,10.5,-.1,14.5,-1.4,17,-2.8,21.3,-4.1,24.6,-5.5
2170 MOVE 0,4.5
2180 FOR SS=1 TO 8
2190 READ X,Y
2200 PLOT X,Y
2210 NEXT SS
2220 DATA 0,4.5,4,3.1,7.3,1.7,11,.4,15,-.9,17.7,-2.3,21.6,-3.6,25.2,-5
2230 MOVE 0,5
2240 FOR SZ=1 TO 8
2250 READ X,Y
2260 PLOT X,Y
2270 NEXT SZ
2280 DATA 0,5,4.4,3.6,7.6,2.2,10.6,.9,15.4,-.4,17.9,-1.8,21.1,-3.1,25.6,-4.5
2290 MOVE 0,5.5
2300 FOR T1=1 TO 8
2310 READ X,Y
2320 PLOT X,Y
2330 NEXT T1
2340 DATA 0,5.5,4.1,4.1,7.3,2.7,11.3,1.4,15.8,.1,17.6,-1.3,21.1,-2.6,25.6,-4
2350 MOVE 0,6
```

```
2360 FOR T2=1 TO 8
2370 READ X,Y
2380 PLOT X,Y
2390 NEXT T2
2400 DATA 0,6,4.5,4.6,7,3.2,11,1.9,16.3,.6,17.3,-.8,21,-2.1,24.9,-3.5
2410 MOVE 0,6.5
2420 FOR T3=1 TO 8
2430 READ X,Y
2440 PLOT X,Y
2450 NEXT T3
2460 DATA 0,6.5,3.9,5.1,6.8,3.7,12.6,2.4,17.4,1.1,17.4,-.3,20.9,-1.6,25.1,-3
2470 MOVE -.2,7
2480 FOR T4=1 TO 8
2490 READ X,Y
2500 PLOT X,Y
2510 NEXT T4
2520 DATA -.2,7,4.2,5.6,6.9,4.2,13.3,2.9,14.1,1.6,17,.2,20.8,-1.1,25.2,-2.5
2530 MOVE .1,7.5
2540 FOR T5=1 TO 8
2550 READ X,Y
2560 PLOT X,Y
2570 NEXT T5
2580 DATA .1,7.5,4.7,6.1,7,4.7,10.2,3.4,14.2,2.1,16.9,.7,21,-.6,25.1,-2
2590 MOVE 0,8
2600 FOR T6=1 TO 8
2610 READ X,Y
2620 PLOT X,Y
2630 NEXT T6
2640 DATA 0,8,4,6.6,7,5.2,10.5,3.9,14.8,2.6,17.5,1.2,21,-.1,25.3,-1.5
2650 MOVE ,2,8.5
2660 FOR T7=1 TO 8
2670 READ X,Y
2680 PLOT X,Y
2690 NEXT T7
2700 DATA .2,8.5,4.1,7.1,6.7,5.7,10.7,4.4,15.1,3.1,17.5,1.7,21.5,.4,25.2,-1
2710 MOVE -.1,9
2720 FOR T8=1 TO 8
2730 READ X,Y
2740 PLOT X,Y
2750 NEXT T8
2760 DATA -.1,9,4.3,7.6,6.3,6.2,10.2,4.9,15.4,3.6,17,2.2,20.8,.9,25,-.5
2770 MOVE -.6,9.5
2780 FOR T9=1 TO 8
2790 READ X,Y
2800 PLOT X,Y
2810 NEXT T9
2820 DATA -.6,9.5,3.9,8.1,6.6,5.7,9.8,5.4,14.6,4.1,17.2,2.7,20.6,1.4,24.4,0
2830 MOVE -2.5,10
2840 FOR T=1 TO 8
2850 READ X,Y
2860 PLOT X,Y
2870 NEXT T
2880 DATA -2.5,10,3.5,8.6,7,7.2,9.5,5.9,12.6,4.6,17.2,3.2,20.2,1.9,22.8,.5
2890 PEN #
2990 END
```

Program B: The edited version of Program A.

```
10 GCLEAR
11 DISP "THIS PROGRAM DRAWS A MODEL OF A SHEARED AMORPHOUS SOLID. THE SOLID"
12 DISP "WAS A PURE, HOMOGENOUS RIVER SAND, PRESSED AND SHAKEN TOGETHER TO THE"
13 DISP "MAXIMUM ATTAINABLE DENSITY. THE PICTURE SHOWS HOW THE GLIDE SURFACE"
14 DISP "BIFURCATES AS IT CORRUGATES AROUND AND DEVIATES FROM THE SLIP PLANE."
20 LIMIT 0,250,10,140
30 LOCATE 10,130,10,90
40 SCALE -3.5,28,-10,10
50 XAXIS 0,3.5
60 YAXIS 0,10
70 MOVE -3.5,0
80 FOR I1=1 TO 29
90 READ X,Y
110 PLOT X,Y
120 NEXT I1
130 DATA 0,0,-3.5,0,-3.5,10,3.5,10,3.5,0,0,0,0,0,.1,.5,0,1,.3,1.5,.2,2,.2,2.5
140 DATA .3,3,.4,3.5,.2,4,0,4.5,0,5,0,5.5,0,6,0,6.5,-.2,7,.1,7.5,0,8,.2,8.5
150 DATA -.1,9,-.6,9.5,-2.5,10,0,10,0,0
160 MOVE 3.5,-1.4
170 DIM I2(2,30)
180 FOR I2=1 TO 30
190 READ X,Y
210 PLOT X,Y
220 NEXT I2
230 DATA 3.5,-1.4,0,-1.4,0,8.6,7,8.6,7,-1.4,3.5,-1.4,4.3,-1.4,3.6,-.9,3.6,-.4
240 DATA 3.9,.1,4.3,.6,4.2,1.1,4.2,1.6,4.2,2.1,4,2.6,4,3.1,4.4,3.6,4.1,4.1
250 DATA 4.5,4.6,3.9,5.1,4.2,5.6,4.7,6.1,4,5.6,4.1,7.1,4.3,7.6,3.9,8.1,3.5,8.6
260 DATA 3.5,-1.4,0,-1.4,3.5,-1.4
270 MOVE 7,-2.8
280 FOR I3=1 TO 28
290 READ X,Y
310 PLOT X,Y
320 NEXT I3
330 DATA 7,-2.8,3.5,-2.8,3.5,7.2,10.5,7.2,10.5,-2.8,7,-2.8,7,-2.8,6.6,-2.5
340 DATA 7,-1.8,7.2,-1.3,7.8,-.8,7.7,-.3,7.8,.2,7.6,.7,7.2,1.2,7.3,1.7,7.6,2.2
350 DATA 7.3,2.7,7,3.2,6.8,3.7,6.9,4.2,7,4.7,7,5.2,6.7,5.7,6.3,6.2,6.6,6.7
360 DATA 7,7.2,7,-2.8
370 MOVE 10.5,-4.1
380 FOR I4=1 TO 29
390 READ X,Y
410 PLOT X,Y
420 NEXT I4
430 DATA 10.5,-4.1,7,-4.1,7,5.9,14,5.9,14,-4.1,10.5,-4.1,10.2,-4.1,10.4,-3.6
440 DATA 10.1,-3.1,10.5,-2.8,10.9,-2.1,10.4,-1.6,10.7,-1.1,10.9,-.6,10.5,-.1
450 DATA 11,.4,10.6,.9,11.3,1.4,11,1.9,12.6,2.4,13.3,2.9,10.2,3.4,10.5,3.9
460 DATA 10.7,4.4,10.2,4.9,9.8,5.4,9.5,5.9,10.5,5.9,10.5,-4.1
470 MOVE 14,-5.4
480 FOR I5=1 TO 29
490 READ X,Y
510 PLOT X,Y
520 NEXT I5
530 DATA 14,-5.4,10.5,-5.4,10.5,6.6,17.5,6.6,17.5,-5.4,14,-5.4,14,-5.4,14,-4.9
540 DATA 13.7,-4.4,10.5,-3.9,14.3,-3.4,14.4,-2.9,14.6,-2.4,14.4,-1.9,14.5,-1.4
550 DATA 15,-.9,15.4,-.4,15.8,.1,16.3,.6,17.4,1.1,14.1,1.6,14.2,2.1,14.8,2.6
560 DATA 15.1,3.1,15.4,3.6,14.6,4.1,12.6,4.6,14,4.6,14,-5.4
570 MOVE 17.5,-6.8
580 FOR I6=1 TO 29
590 READ X,Y
610 PLOT X,Y
620 NEXT I6
630 DATA 17.5,-6.8,14,-6.8,14,3.2,21,3.2,21,-6.8,17.5,-6.8,17.5,-6.8,17.5,-6.5
640 DATA 17.6,-5.8,17.9,-5.3,17.5,-4.8,17.6,-4.3,17.9,-3.8,17.5,-3.3,17,-2.8
650 DATA 17.7,-2.3,17.9,-1.8,17.6,-1.3,17.3,-.8,17.4,-.3,17,.2,16.9,.7,17,1.2
660 DATA 17.5,1.7,17,2.2,17.2,2.7,17.2,3.2,17.5,3.2,17.5,-6.8
670 MOVE 21,-8.1
680 FOR I7=1 TO 29
```

```
690 READ X,Y
710 PLOT X,Y
720 NEXT I7
730 DATA 21,-8.1,17.5,-8.1,17.5,1.9,24.5,1.9,24.5,-8.1,21,-8.1,21.1,-8.1
740 DATA 21.5,-7.6,21.2,-7.1,21.6,-6.5,21.2,-6.1,21.3,-5.5,21.7,-5.1,21.2,-4.6
750 DATA 21.3,-4.1,21.6,-3.6,21.1,-3.1,21.1,-2.6,21,-2.1,20.9,-1.6,20.8,-1.1
760 DATA 21,-.6,21,-.1,21.5,.4,20.8,.9,20.6,1.4,20.2,1.9,21,1.9,21,-8.1
770 MOVE 24.5,-9.5
780 FOR I8=1 TO 29
790 READ X,Y
810 PLOT X,Y
820 NEXT I8
830 DATA 24.5,-9.5,21,-9.5,21,.5,28,.5,28,-9.5,24.5,-9.5,24.6,-9.5,24.6,-9
840 DATA 24.6,-8.5,24.6,-8,24.4,-7.5,24.6,-7,24.9,-6.5,24.6,-6,24.6,-5.5
850 DATA 25.2,-5,25.6,-4.5,25.6,-4,24.9,-3.5,25.1,-3,25.2,-2.5,25.1,-2
860 DATA 25.3,-1.5,25.2,-1,25,-.5,24.4,0,22.8,.5,24.5,.5,24.5,-9.5
870 MOVE 0,-3.5
880 FOR Z=1 TO 12
890 READ X,Y
910 PLOT X,Y
920 NEXT Z
930 DATA -3.5,0,21,-9.5,21,.5,-3.5,10,0,10,24.5,.5,24.5,-9.5,0,0,3.5,0
940 DATA 28,-9.5,28,.5,3.5,10
945 PEN 2
950 MOVE 0,0
960 FOR A=1 TO 8
970 READ X,Y
980 PLOT X,Y
990 NEXT A
1000 DATA 0,0,4.3,-1.4,7,-2.8,10.2,-4.1,14,-5.4,17.5,-6.8,21.1,-8.1,24.6,-9.5
1010 MOVE .1,.5
1020 FOR B=1 TO 16
1030 READ X,Y
1040 PLOT X,Y
1050 NEXT B
1060 DATA .1,.5,3.6,-.9,6.6,-2.3,10.4,-3.6,14,-4.9,17.5,-6.3,21.6,-7.6,24.6,-9
1070 DATA 24.6,-9,21.6,-7.6,17.5,-6.3,14,-4.9,10.4,-3.6,7.5,-2.3,3.9,-.9,.1,.5
1080 MOVE 0,1
1090 FOR C=1 TO 8
1100 READ X,Y
1110 PLOT X,Y
1120 NEXT C
1130 DATA 0,1,3.6,-.4,7,-1.8,10.1,-3.1,13.7,-4.4,17.6,-5.8,21.2,-7.1,24.6,-8.5
1140 MOVE .3,1.5
1150 FOR D1=1 TO 8
1160 READ X,Y
1170 PLOT X,Y
1180 NEXT D1
1190 DATA .3,1.5,3.9,.1,7.2,-1.3,10.5,-2.6,14.5,-3.9,17.9,-5.3,21.6,-6.112
1200 DATA 24.6,-8
1202 MOVE .9,1.5
1203 FOR D2=1 TO 8
1204 READ X,Y
1205 PLOT X,Y
1206 NEXT D2
1207 DATA .9,1.5,3.9,.1,7.8,-1.3,10.5,-2.6,14.5,-3.9,18.5,-5.3,22.3,-6.1
1208 DATA 25.6,-8
1210 DATA 3.9,.1,.9,1.5
1220 MOVE .2,2
1230 FOR E=1 TO 16
1240 READ X,Y
1250 PLOT X,Y
1260 NEXT E
1270 DATA .2,2,4.3,.6,7.8,-.8,10.5,-2.1,14.3,-3.4,17.5,-4.8,21.2,-6.1,24.4,-7.5
1280 DATA 24.4,-7.5,21.2,-6.1,18.7,-4.8,14.3,-3.4,10.5,-2.1,8.8,-.8,4.3,-.6
1290 DATA 1.2,2
```

```
1300 MOVE .2,2.5
1310 FOR F=1 TO 16
1320 READ X,Y
1330 PLOT X,Y
1340 NEXT F
1360 DATA 24.6,-7,24.6,-7,21.3,-5.6,17.6,-4.3,14.4,-2.9,10.6,-1.6,8.5,-.3
1370 DATA 4.2,1.1,1.4,2.5
1380 MOVE .3,3
1390 FOR G=1 TO 8
1400 READ X,Y
1410 PLOT X,Y
1420 NEXT G
1430 DATA .3,3,4.2,1.6,7.8,.2,10.7,-1.1,14.6,-2.4,17.9,-3.8,21.7,-5.1,24.9,-6.5
1440 MOVE 25.2,-6.5
1441 FOR G1=1 TO 16
1442 READ X,Y
1443 PLOT X,Y
1444 NEXT G1
1450 DATA 25.2,-6.5,21.7,-5.1,17.9,-3.8,14.6,-2.4,10.7,-1.1,8.8,.2,4.2,1.6
1460 MOVE 4,3.5
1470 FOR H=1 TO 8
1480 READ X,Y
1490 PLOT X,Y
1500 DATA .4,3.5,4.2,2.1,7.6,.7,10.5,-.6,14.4,-1.9,17.5,-3.2,21.2,-4.6,24.6,-6
1510 DATA 24.6,-6,21.2,-4.6,17.5,-3.2,14.4,-1.9,12.3,-.6,9.1,.7,4.2,2.1,1.6,3.5
1520 MOVE .2,4
1530 FOR J=1 TO 16
1540 READ X,Y
1550 PLOT X,Y
1560 NEXT J
1570 DATA .2,4,4,2.6,7.2,1.2,10.5,-.1,14.5,-1.4,17.5,-2.8,21.3,-4.1,24.6,-5.5
1580 DATA 24.6,-5.5,21.3,-4.1,18.5,-2.8,14.5,-1.4,12.1,-.1,8.9,1.2,4,2.6,1.5,4
1590 MOVE 0,4.5
1600 FOR K=1 TO 16
1610 READ X,Y
1620 PLOT X,Y
1630 NEXT K
1640 DATA 0,4.5,4,3.1,7.3,1.7,11,.4,15,-.9,17.7,-2.3,21.6,-3.6,25.2,-5,25.2,-5
1650 DATA 21.6,-3.6,17.7,-2.3,15,-.9,11,.4,8.1,1.7,4,3.1,1.3,4.5
1660 MOVE 25.6,-4.5
1670 FOR L=1 TO 16
1680 READ X,Y
1690 PLOT X,Y
1700 NEXT L
1710 DATA 25.6,-4.5,21.1,-3.1,17.9,-1.8,15.4,-.4,10.6,.9,7.6,2.2,4.4,3.6,0,5
1720 DATA 0,5,4.4,3.6,9,2.2,10.6,.9,15.4,-.4,17.9,-1.8,22,-3.1,24.5,-4.5
1730 MOVE 25.6,-4
1740 FOR M=1 TO 16
1750 READ X,Y
1760 PLOT X,Y
1770 NEXT M
1780 DATA 25.6,-4,21.1,-2.6,17.6,-1.3,15.8,.1,11.3,1.4,7.3,2.7,4.1,4.1,0,5.5
1790 DATA 0,5.5,4.1,4.1,8.6,2.7,11.3,1.4,15.8,.1,17.6,-1.3,21.1,-2.6,24.5,-4
1800 MOVE 24.8,-3.5
1810 FOR N=1 TO 16
1820 READ X,Y
1830 PLOT X,Y
1840 NEXT N
1850 DATA 24.8,-3.5,21,-2.1,17.3,-.8,14,.6,11,1.9,7,3.2,4.5,4,6,0,6
1860 DATA 0,6,4.6,4.6,8.7,3.2,11,1.9,16.3,.6,17.3,-.8,21,-2.1,24.2,-3.5
1870 MOVE 0,6.5
1880 FOR P=1 TO 16
1890 READ X,Y
1900 PLOT X,Y
1902 NEXT P
1910 DATA 0,6.5,3.9,5.1,6.8,3.7,12.6,2.4,17.4,1.1,17.4,-.3,20.9,-1.6,25,-3
```

```
1920 DATA 25,-3,20.9,-1.6,17.4,-.3,17.4,1.1,12.6,2.4,9.3,3.7,3.3,5.1,0,6.5
1930 MOVE 25.2,-2.5
1940 FOR R=1 TO 16
1950 READ X,Y
1960 PLOT X,Y
1970 NEXT R
1980 DATA 25.2,-2.5,20.8,-1.1,17,.2,14.1,1.6,13.3,2.9,6.9,4.2,4.2,5.6,-.2,7
1990 DATA -.2,7,4.2,5.6,8.8,4.2,13.3,2.9,14.1,1.6,17,.2,20.8,-1.1,25.1,-2.5
2000 MOVE 25.1,-2
2010 FOR S=1 TO 16
2020 READ X,Y
2030 PLOT X,Y
2040 NEXT S
2050 DATA 25.1,-2,21,-.6,16.9,.7,14.2,2.1,10.2,3.4,7,4.7,4.7,6.1,.1,7.5
2060 DATA .1,7.5,4.6,6.1,9.3,4.7,10.2,3.4,14.2,2.1,16.9,.7,21,-.6,25,-2
2070 MOVE 25.3,-1.5
2080 FOR T=1 TO 16
2090 READ X,Y
2100 PLOT X,Y
2110 NEXT T
2120 DATA 25.3,-1.5,21,-.1,17,1.2,14.8,2.6,10.5,3.9,7,5.2,4,6.6,0,8
2130 DATA 0,8,4.8,6.6,9.9,5.2,10.5,3.9,14.8,2.6,17,1.2,21,-.1,25.3,-1.5
2140 MOVE 25.1,-1
2150 FOR U=1 TO 16
2160 READ X,Y
2170 PLOT X,Y
2180 NEXT U
2190 DATA 25.1,-1,21.5,.4,17.5,1.7,15.1,3.1,10.7,4.4,6.7,5.7,4.1,7.1,.2,8.5
2200 DATA -.2,8.5,6,7.1,10.5,7,10.7,4.4,15.1,3.1,17.5,1.7,21.5,.4,25.6,-1
2210 MOVE 25,-.5
2220 FOR V=1 TO 16
2230 READ X,Y
2240 PLOT X,Y
2250 NEXT V
2260 DATA 25,-.5,20.8,.9,17,2.2,15.4,3.6,10.2,4.9,6.3,6.2,4.3,7.6,-.1,9
2270 DATA -.1,9,6.3,7.6,9.5,6.2,10.2,4.9,15.4,3.6,17,2.2,20.8,.9,25,-.5
2280 MOVE -.6,9.5
2290 FOR W=1 TO 8
2300 READ X,Y
2310 PLOT X,Y
2320 NEXT W
2330 DATA -.6,9.5,3.9,8.1,6.6,6.7,9.8,5.4,14.6,4.1,17.2,2.7,20.6,1.4,24.4,0
2340 MOVE -2.5,10
2350 FOR Y=1 TO 8
2360 READ X,Y
2370 PLOT X,Y
2380 NEXT Y
2390 DATA -2.5,10,3.5,8.6,7,7.2,9.5,5.9,12.6,4.6,17.2,3.2,20.2,1.9,22.8,.5
2400 END
```

Program C; To single out Vertical Colour Maps between which the corrugation and bifurcation can be demonstrated.

```
10 GCLEAR
20 LIMIT 0,250,10,180
30 LOCATE 10,190,10,90
40 SCALE -3.5,28,-10,10
50 XAXIS 0,3.5
60 YAXIS 0,10
70 MOVE 10.5,-4.1
80 FOR I4=1 TO 44
90 READ X,Y
100 PLOT X,Y
110 NEXT I4
120  DATA 10.5,-4.1,7,-4.1,7,5.9,14,5.9,14,-4.1,10.5,-4.1,10.2,-4.1,10.4,-3.6
130  DATA 10.1,-3.1,10.5,-2.6,10.5,-2.1,10.4,-1.6,10.7,-1.1,10.5,-.6,10.5,-.1
140  DATA 11,.4,10.6,.9,11.3,1.4,11,1.9,10.7,2.4,10.2,2.9,10.2,3.4,10.5,3.9
150  DATA 10.7,4.4,10.2,4.9,9.8,5.4,9.5,5.9,10.5,5.9,10.5,-4.1,10.2,-4.1
160  DATA 10.4,-3.6,10.1,-3.1,10.5,-2.6,10.5,-2.1,10.4,-1.6,10.7,-1.1,10.5,-.6
170  DATA 10.5,-.1,11,.4,10.6,.9,11.3,1.4,12,1.9,12.6,2.4,13.3,2.9
180 MOVE 14,-5.4
190 FOR I5=1 TO 43
200 READ X,Y
210 PLOT X,Y
220 NEXT I5
230 DATA 14,-5.4,10.5,-5.4,10.5,4.6,17.5,4.6,17.5,-5.4,14,-5.4,14,-5.4,14,-4.9
240 DATA 13.7,-4.4,14.5,-3.9,14.3,-3.4,14.4,-2.9,14.6,-2.4,14.4,-1.9,14.5,-1.4
250 DATA 15,-.9,14.8,-.4,14.5,.1,14,.6,14,1.1,14.1,1.6,14.2,2.1,14.8,2.6
260 DATA 15.1,3.1,15.4,3.6,14.6,4.1,12.6,4.6,14,4.6,14,-5.4,14,-5.4,14,-4.9
270 DATA 13.7,-4.4,14.5,-3.9,14.3,-3.4,14.4,-2.9,14.6,-2.4,14.4,-1.9,14.5,-1.4
280 DATA 15,-.9,15.4,-.4,15.8,.1,16.3,.6,17.4,1.1,17.5,1.6,13.3,2.9
300 MOVE 10.2,-4.1
310 FOR L1=1 TO 42
320 READ X,Y
330 PLOT X,Y
340 NEXT L1
350 DATA 10.2,-4.1,14,-5.4,14,-4.9,10.4,-3.6,10.1,-3.1,13.7,-4.4,14.5,-3.9
352 DATA 10.5,-2.6,10.5,-2.1,14.3,-3.4,14.4,-2.9,10.4,-1.6,10.7,-1.1,14.6,-2.4
355 DATA 14.4,-1.9,10.5,-.6,10.5,-.1,14.5,-1.4,15,-.9,11,.4,10.6,.9,14.8,-.4
356 DATA 14.5,.1,11.3,1.4,11,1.9,14,.6,14,1.1,10.7,2.4,10.2,2.9,14.1,1.6
357 DATA 14.2,2.1,10.2,3.4,10.5,3.9,14.6,2.6,15.1,3.1,10.7,4.4,10.2,4.9
358 DATA 15.4,3.6,14.6,4.1,9.8,5.4,9.5,5.9,12.6,4.6
360 PEN 2
370 MOVE 10.2,-4.1
380 FOR L2=1 TO 30
390 READ X,Y
400 PLOT X,Y
410 NEXT L2
420 DATA 10.2,-4.1,14,-5.4,14,-4.9,10.4,-3.6,10.1,-3.1,13.7,-4.4,14.5,-3.9
422 DATA 10.5,-2.6,10.5,-2.1,14.3,-3.4,14.4,-2.9,10.4,-1.6,10.7,-1.1,14.6,-2.4
425 DATA 14.4,-1.9,10.5,-.6,10.5,-.1,14.5,-1.4,15,-.9,11,.4,10.6,.9,15.4,-.4
426 DATA 15.8,.1,11.3,1.4,12,1.9,16.3,.6,17.4,1.1,12.6,2.4,13.3,2.9
430 END
```